Endosymbiotic Interaction Between Hydra and Green Algae, and its Evolutionary Significance

Masakazu Ishikawa

DOCTOR OF PHILOSOPHY

Department of Genetics

School of Life Science

The Graduate University for Advanced Studies

ABSTRACT

Endosymbiosis is defined as a phenomenon in which one organism lives inside the cells of another organism. Clearly, endosymbiosis has played a monumental role in the evolution of organisms, such as the generation of mitochondria and chloroplasts. Therefore, it is quite important to understand how endosymbiotic interactions are established.

Hydra is a freshwater cnidarian animal that has been used as a model organism for 300 years. In genus *Hydra*, two groups of species (*H. vulgaris* and *H. viridissima* groups) show endosymbiosis with green algae. In culture collection of *Hydra* at the National Institute of Genetics, all of the six *H. viridissima* strains show endosymbiosis, and the endosymbiosis has been considered as a key characteristic of this species. In *H. vulgaris* group, on the other hand, only two of twenty-five strains show endosymbiosis. These two *Hydra* groups with different endosymbiotic status could be useful to understand evolutionary process of endosymbiotic interaction. However, the evolution of the endosymbiosis is not fully understood. A previous study suggested that the endosymbiosis in *H. viridissima* group occurred in the ancestor of *H. viridissima* group strains, but it remains obscure about evolution of the endosymbiosis in *H. vulgaris* group. It is possible that the twenty-three non-symbiotic *H. vulgaris* group strains are also able to harbor the algae, therefore *H. vulgaris* group may have acquired the potential for harboring algae before or during radiation of *H. vulgaris* group strains. In order to understand evolution of endosymbiosis in *H. vulgaris* group, I examined the endosymbiotic potential of the *H. vulgaris* group strains by artificially introducing the algae. As a result, twelve of the twenty-three non-symbiotic *H. vulgaris* group strains were also able to harbor the algae. Moreover, my phylogenetic analysis by sequencing these mitochondrial genomes of the twenty-five *H. vulgaris* group strains showed that the strains with endosymbiotic potential were grouped into one of the three clusters. These results suggest that the endosymbiotic potential obtained once during radiation of the *H. vulgaris* group strains, but most of *H. vulgaris* group strains remains non-

symbiotic. This implies that the endosymbiosis in *H. vulgaris* group is not stable compared with that in *H. viridissima*. Therefore, I next examined whether the endosymbiotic interaction with algae is different between the two *Hydra* species or not.

As typical cases for investigating the endosymbiotic interaction, I compared survival rates between symbiotic polyps and aposymbiotic polyps in which algae were removed. The result showed that symbiotic *H. viridissima* group was more tolerant to starvation than aposymbiotic polyp, whereas symbiotic *H. vulgaris* group was less tolerant than aposymbiotic polyp, which is in contrast to *H. viridissima* group. To understand the interaction at molecular level, I compared gene expression profiles between symbiotic and aposymbiotic polyps by using RNA-seq method. The analysis showed that the differential gene expression pattern in *H. viridissima* group was extensively different from that in *H. vulgaris* group, even though the differential gene expression pattern in *H. viridissima* group is similar to that in other endosymbiotic organisms such as *Paramecium bursaria* and *Ciona varians*. Considering oxidative stress response, *H. viridissima* group seems to have the mechanisms to manage the oxidative stress, such as down-regulation of the respiratory chain genes and up-regulation of calcium ion binding genes, whereas these mechanisms seem unlikely to exist in *H. vulgaris* group. These results suggest that *H. viridissima* group has already established stable endosymbiotic relationships with green algae, whereas the mechanisms of stable endosymbiosis in *H. vulgaris* group still seem to be immature.

Through the present studies, I found that although both hydra groups (*H. vulgaris* and *H. viridissima*) show endosymbiosis with algae, the interaction with algae was substantially different between the two *Hydra* groups. *H. viridissima* group showed a mutualistic relationship with the algae, whereas *H. vulgaris* group did not show. These results suggest that the endosymbiosis in *H. vulgaris* group is still in the course of an evolutionary process toward stable endosymbiosis compared with *H. viridissima* group. The endosymbiosis of hydras with different

stages of evolution will therefore provide deeper insight into the evolutionary process of endosymbiosis, from non-symbiotic to stable endosymbiosis.

1 Chapter 1

General introduction

1.1 Endosymbiosis

Symbiosis is defined as a long-term, intimate physical association between differently named organisms (Margulis and Sagan, 2002). In the case of endosymbiosis, one of the organisms lives inside the cells of the other organism (Kovacevic, 2012). The idea that several organelles, such as mitochondria and chloroplasts evolved from free-living bacteria via endosymbiosis within a eukaryotic host cell was first proposed by Schimper (1883), and revived by Lynn Margulis (1971), who published an influential book "Origin of Eukaryotic Cells". Over the past several decades, numerous reviews have documented in detail the biochemical, molecular and cell biological data bearing on the endosymbiotic hypothesis of organelle origins (Bhattacharya et al., 2003; Bullerwell and Gray, 2004; McFadden, 2001; Timmis et al., 2004). Nowadays, there is no doubt that mitochondria and chloroplasts were obtained by the endosymbiosis. These endosymbiotic events enabled the eukaryotes to utilize oxygen as an electron receptor and to generate carbohydrates from water and carbon-dioxide.

Endosymbiosis also contributes to the genome modification of both hosts and symbionts. For example, the endosymbiotic bacterial symbiont, *Buchnera* lacks genes for the biosynthesis of cell-surface components and the genome size of *Buchnera* is only one-seventh of that of *Escherichia coli*, which is a close relative (Shigenobu et al., 2000). It is suggested that this odd gene repertoire of the *Buchnera* genome is specialized to the endosymbiotic life. Moreover, at least 22 expressed genes of the mealybug, *Planococcus citri*, are known to be transferred from multiple endosymbiotic bacteria. Thus, endosymbiosis can be considered as an enormous impact on evolution of organisms.

1.2 Endosymbiotic relationships between cnidarians and algae

It is widely known that many cnidarian species show endosymbiosis with algae (Hofmann and Kremer, 1981; Meyer and Weis, 2012; Muscatine and Lenhoff, 1963). One of the most popular cases is the endosymbiosis between stony corals and dinoflagellates. Coral reefs are among the richest and most diverse ecosystems on Earth, and are founded by the calcium carbonate secreted by corals (Odum HT and Odum EP, 1955). Corals show endosymbiosis with photosynthetic dinoflagellates (genus *Symbiodinium*) in a relationship centered around nutrient exchange, whereby the dinoflagellates provide high amounts of photosynthetic products in return for CO_2 and NH_4^+ (Muller-Parker and D'Elia, 1997; also see Figure 1.1). Globally, coral reefs are facing to an increasing amount of environmental stress, especially from global warming, which has resulted in widespread bleaching of corals (Weis, 2008). The coral bleaching greatly decreases the carbon available for translocation to the host and is becoming increasingly significant cause of the mortality and degradation of coral reefs on a global scale. Therefore, the disruption of the endosymbiotic relationships could also induce the disruption of oceanic ecosystems on a global scale.

The endosymbiosis affects not only the survival of cnidarians host but also their lifecycles. Evidence from both the laboratory and the field studies suggest that transitions between developmental stages within an cnidarian individual, so called checkpoints, were controlled by specific factors (Hofmann et al., 1996). *Cassiopea andromeda* is a jellyfish which lives upside-down on the bottom, and this jellyfish also harbors *Symbiodinium* (Hofmann and Kremer, 1981). Surprisingly, this jellyfish can never strobilate without harboring the algae (Rahat and Adar, 1980, see also Figure 1.2). This means that the endosymbiosis with algae is a key factor of the development of the jellyfish. Thus, the endosymbiosis has had a massive impact on the survival and lifecycle of cnidarian hosts.

Although the endosymbiosis is quite important to cnidarian animals, it is still unclear how the stable endosymbiotic relationships have evolved. For understanding the evolutionary process of endosymbiotic relationships, endosymbioses in cnidarians such as corals, sea anemone, and jellyfish face several major limitations. For example, (i) it is difficult or impossible to maintain and culture these animals in the laboratory condition, (ii) it is almost impossible to keep the animals alive while they are rendered fully aposymbiotic, (iii) it is difficult to focus on the endosymbiosis in the early stage, because the stable endosymbiotic relationships have already been established.

1.3 Hydra and its endosymbiosis

Genus *Hydra* is a fresh water cnidarian animal that has no medusa stage and usually reproduces by budding asexually (Chapman et al., 2010). It is organized along a single oral-aboral axis that is divided into three parts: the foot region, the body column corresponding to the gastric cavity, and the apical head region with the mouth opening surrounded by a ring of tentacles (Amimoto et al., 2006). Because of the simplicity of its composition and structure (Campbell and Bode, 1983), its remarkable powers of regeneration (Holstein et al., 2003; Hemmrich et al., 2007), and its accessibility to a variety of experimental manipulations (Lenhoff, 1983), *Hydra* has widely been used as a model organism for 300 years. The molecular phylogenetic analysis has shown that genus *Hydra* comprises four species groups, *H. vulgaris* group, *H. oligactis* group, *H. braueri* group, and *H. viridissima* group (Kawaida et al., 2010; Martínez et al., 2010; also see the phylogenetic tree of genus *Hydra* in Figure 1.3).

Among the four species group of genus *Hydra*, two groups (*H. viridissima* and *H. vulgaris*) show endosymbiotic associations with algae. The algae harbored by *H. viridissima* group is defined as *Chlorella* sp., whereas the algae harbored by the *H. vulgaris* group is defined as

Chlorococcum sp. (Kawaida et al., 2013). The endosymbiotic algae were located in the endodermal epithelial cells (Figure 1.4), enclosed within a membrane structure called "symbiosome" (Kovacević et al., 2005). In a hydra's endodermal epithelial cell, several dozens of algal cells exist (Figure 1.5). Endosymbiotic algae are stably transmitted over generations. In asexual conditions of reproduction (budding), algae are transferred through buds from generation to generation (Figure 1.6). During sexual development, algae are incorporated in the oocyte (Kawaida et al., 2013). In addition, both endosymbiotic *Hydra* species also can expel them and continue surviving without endosymbionts (Figure 1.7). Such *Hydra* is named "aposymbiotic".

The National Institute of Genetics (NIG, Mishima, Japan) maintains the world's largest collection of hydra strains that were collected from all over the world (http://www.nig.ac.jp/labs/OntoGen/keitou.html). In the NIG collection, all six of the *H. viridissima* group strains show endosymbiosis. In fact, the endosymbiosis has been considered to be a key characteristic of this species. On the other hand, among twenty-five *H. vulgaris* group strains maintained in NIG, only two *H. vulgaris* group strains (J7 and J10) show endosymbiosis with green algae. In addition to the simplicity of maintenance and control of Hydra's endosymbiosis, therefore, these two kinds of the endosymbiotic *Hydra* species with apparently different status of the endosymbiosis would be useful to understand the endosymbiosis.

Despite the importance of the endosymbiosis in *Hydra*, little is known about the relationships between the two endosymbiosis in terms of evolutionary and physiological aspects. Kawaida et al. (2013) conducted phylogenetic analysis among *H. viridissima* group strains and suggested that *H. viridissima* group obtained the endosymbiotic algae before the radiation of the *H. viridissima* group strains (Figure 1.8). On the other hand, it remains obscure about the evolution of the endosymbiosis in *H. vulgaris* group. Although only two among twenty-five *H. vulgaris* group strains currently show endosymbiosis with algae, it is possible that the other aposymbiotic *H. vulgaris* group strains have the potential to harbor the algae, and therefore the

evolution of the endosymbiotic potential for harboring endosymbiotic *Chlorococcum* may have occurred earlier than we expect based on only phenotypic observation.

Moreover, it is also unknown whether the interaction with algae is different between the two *Hydra* species or not. It is suggested that the endosymbiosis between *H. viridissima* group and the algae is mutualistic (Muscatine and Lenhoff, 1963), but the effect of the endosymbiosis on the survival of *H. vulgaris* group is so far completely unknown. Furthermore, the molecular mechanisms to respond to or control the endosymbiotic algae in both *Hydra* species are also unknown. Habetha and Bosch (2005) conducted cDNA representational difference analysis of *H. viridissima* group by suppressive subtractive hybridization, but they found only a few genes which were differentially expressed between symbiotic and aposymbiotic states. It is suggested the few of the differentially expressed genes are mainly because of the technical limitation. Because only portion of the animal is symbiotic, profile of the transcriptome of an entire animal becomes very low signal-to-noise ratio. (Meyer and Weis, 2012). As *Hydra* is an excellent organism in which to study endosymbiosis, it is important to understand its endosymbiosis on a physiological and evolutionary basis.

1.4 The aim of the study

As mentioned above, the interaction and evolution of endosymbiosis between hydra and algae are still poorly understood. In the doctoral thesis, I therefore aim to gain a comprehensive insight into the evolution and interaction of the endosymbiotic relationship between hydra and algae.

In Chapter 2 of this thesis, in order to understand the evolution of the endosymbiosis between *H. vulgaris* group and algae, I first examined the endosymbiotic potential of the *H. vulgaris* group strains maintained in the NIG culture collection. Next, I conducted phylogenetic

analysis of the *H. vulgaris* group strains by sequencing the mitochondrial genomes of the *H. vulgaris* group strains. I then discuss the evolution of the endosymbiosis between *H. vulgaris* group and algae.

In Chapter 3, in order to understand the endosymbiotic interaction with algae, I examined the interaction of the endosymbiosis on the survival of the two *Hydra* species. I then compared the differential gene expression pattern of the two hydra species. The recent development of RNA sequencing (RNA-seq) could help to overcome the limitations of a low signal-to-noise ratio that exist in the conventional methods. Thus, I conducted the differential gene expression analysis between aposymbiotic and symbiotic states of polyps by using an RNA-seq method. I then discussed possible molecular mechanisms of hydra-algae relationships.

In Chapter 4, I summarized the results of the Chapters 2 and 3 and made several conclusions.

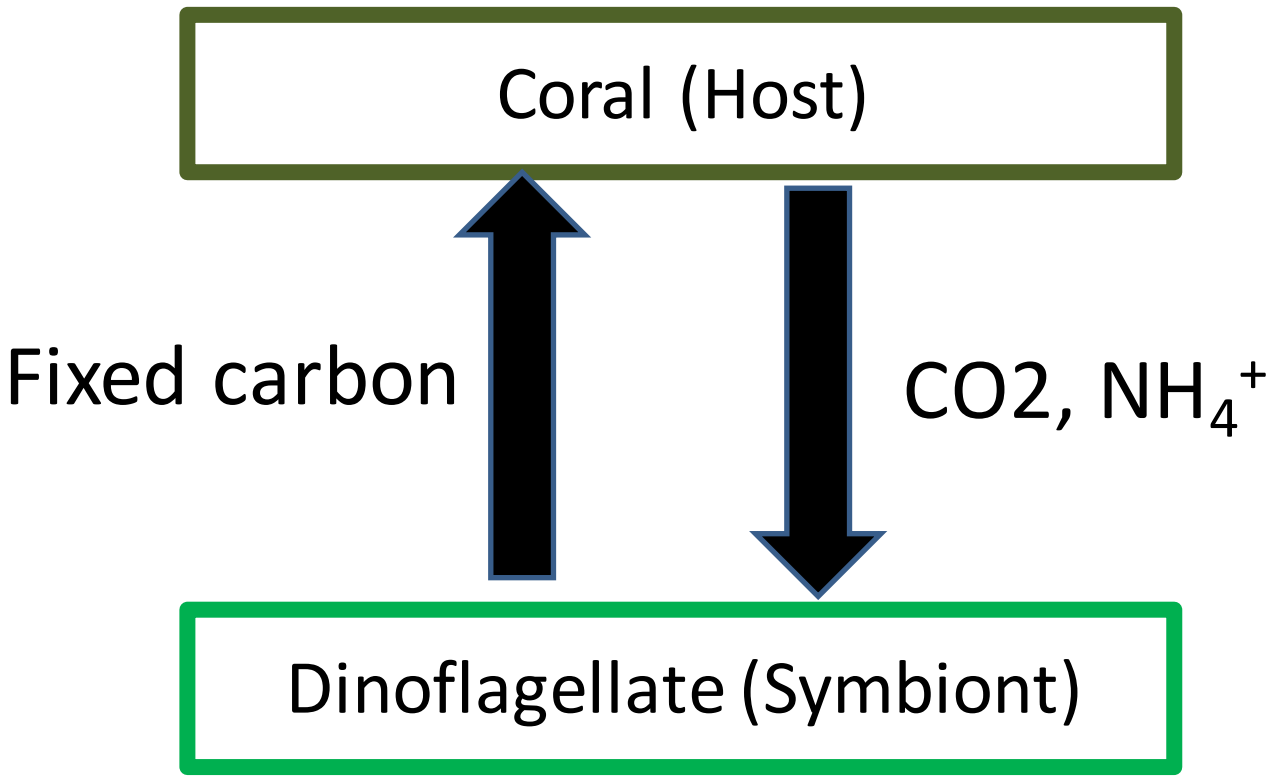

Figure 1.1. Endosymbiotic relationship between coral and dinoflagellate.

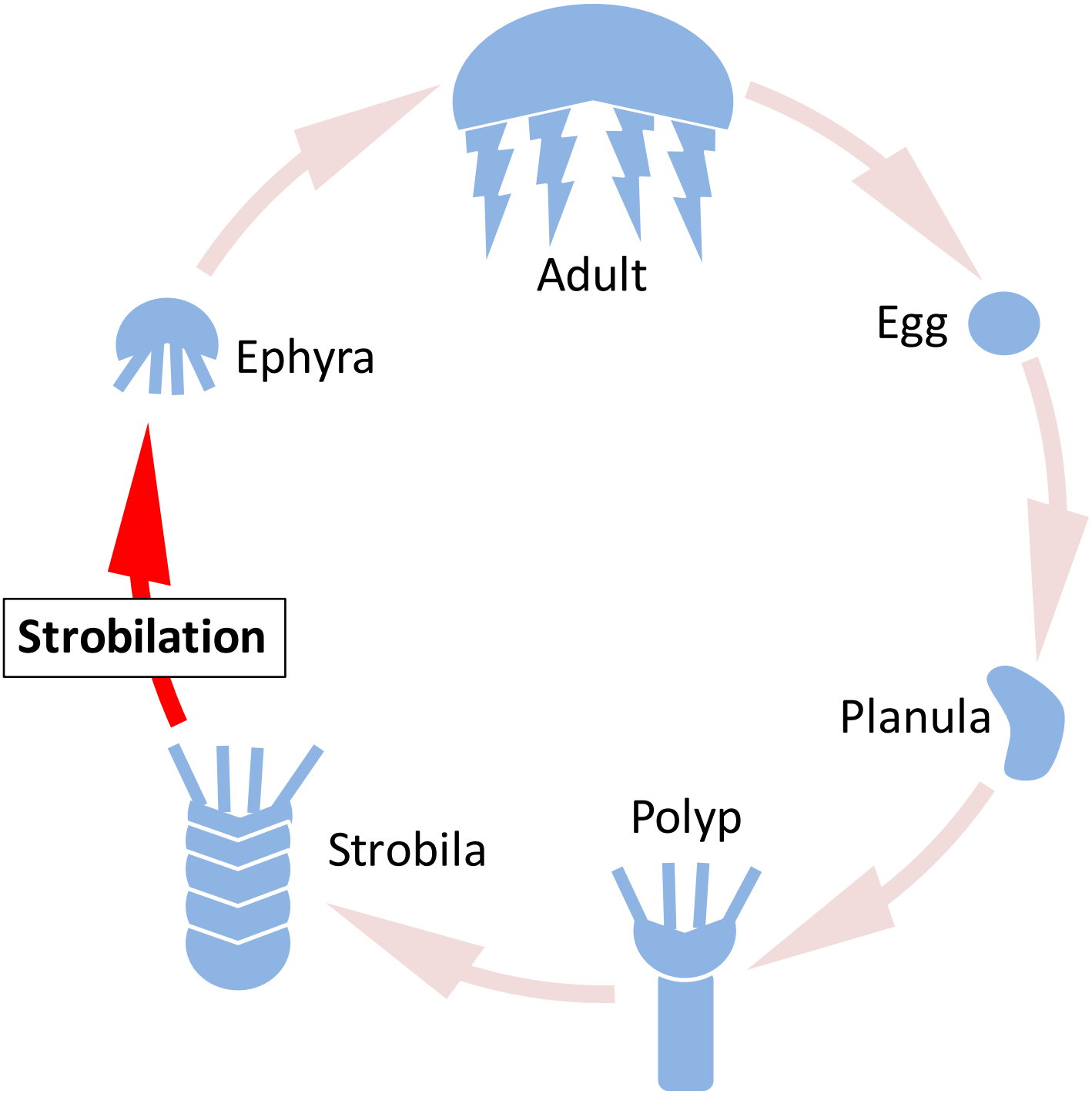

Figure 1.2. Lifecycle of a jellyfish. *Cassiopea andromeda,* which lives upside-down on the bottom, can never strobilate without harboring the endosymbiotic dinoflagellate (Rahat and Adar, 1980).

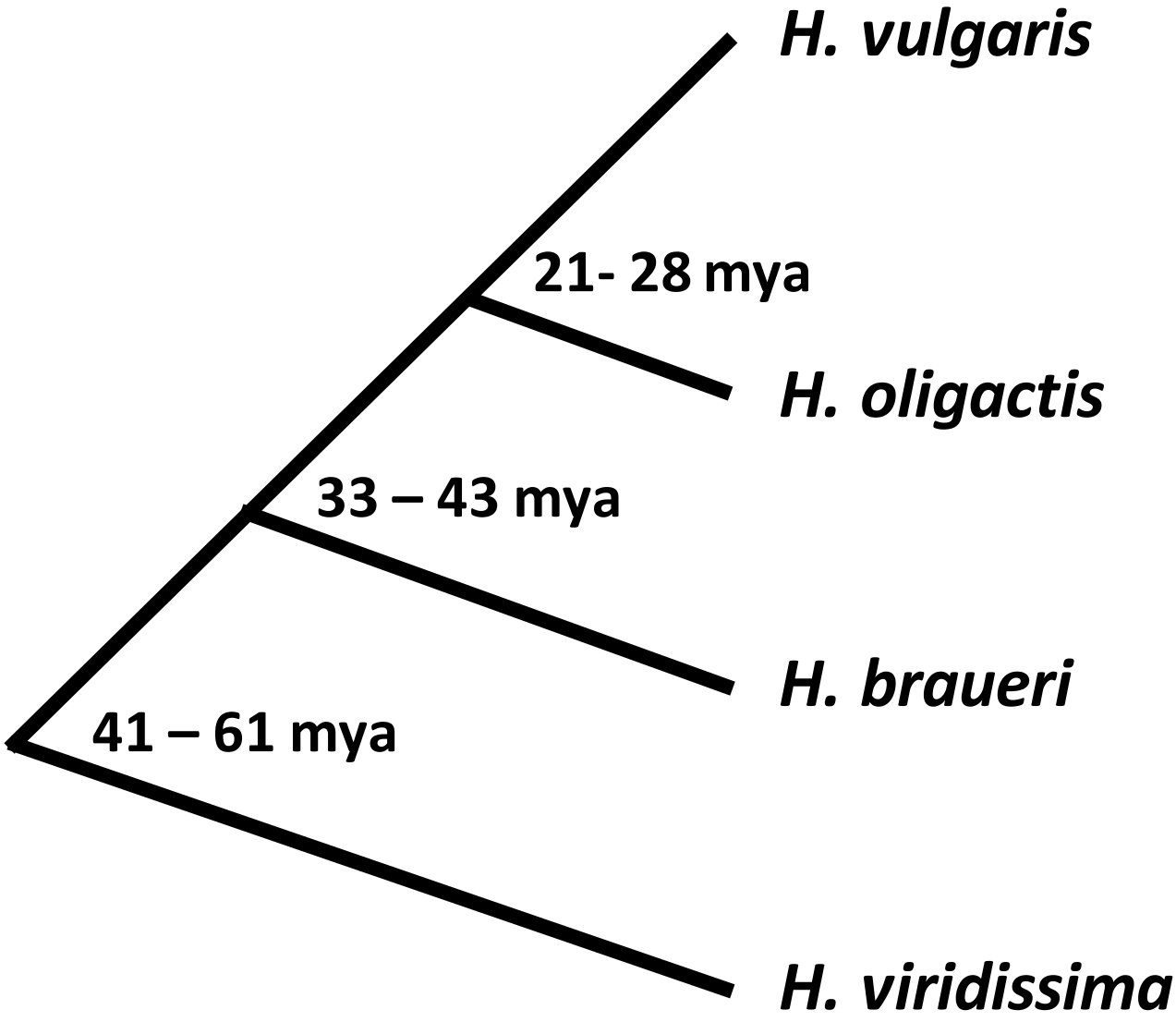

Figure 1.3. Phylogenetic tree of the genus *Hydra*. Estimated times by Martinez et al. (2010) in millions of years ago (mya) for the divergences of the various clades are indicated.

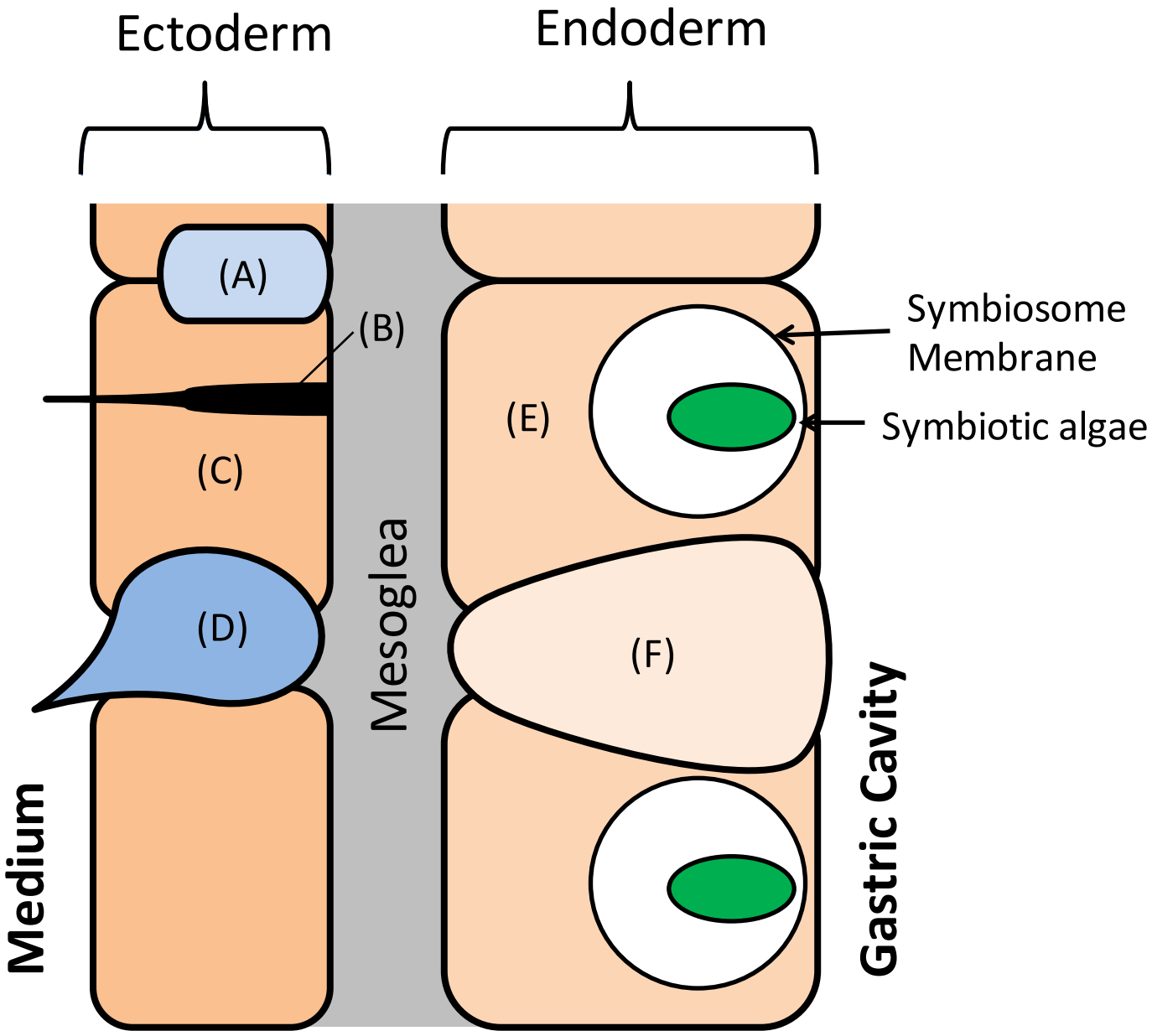

Figure 1.4. A simplified schematic diagram of a section of hydra body wall. Hydra has a bilayered cellular organization. Ectoderm and endoderm are separated by a cellular matrix called the mesogrea. Hydra consists of 6 type of cells, and each cell is represented by different colors. (A) interstitial stem cell, (B) nerve cell, (C) ectodrmal epithelial cell, (D) nematocyte, (E) endodermal epithelial cell, (F) grand cell. The endosymbiotic algae exist in the endodermal epithelial cells enclosed in called symbiosome membrane.

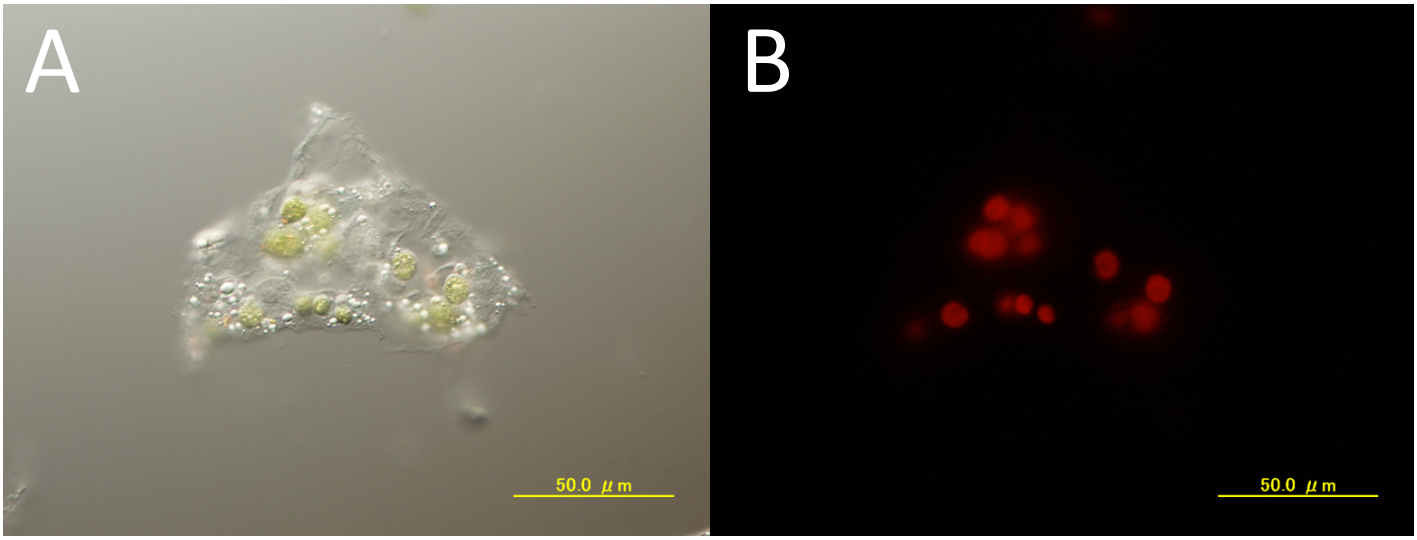

Figure 1.5. Photograpshs of one hydra's cell. (A) Light microscope, (B) fluorescent microscope. Red dots in Figure 3B represent endosymbiotic algae.

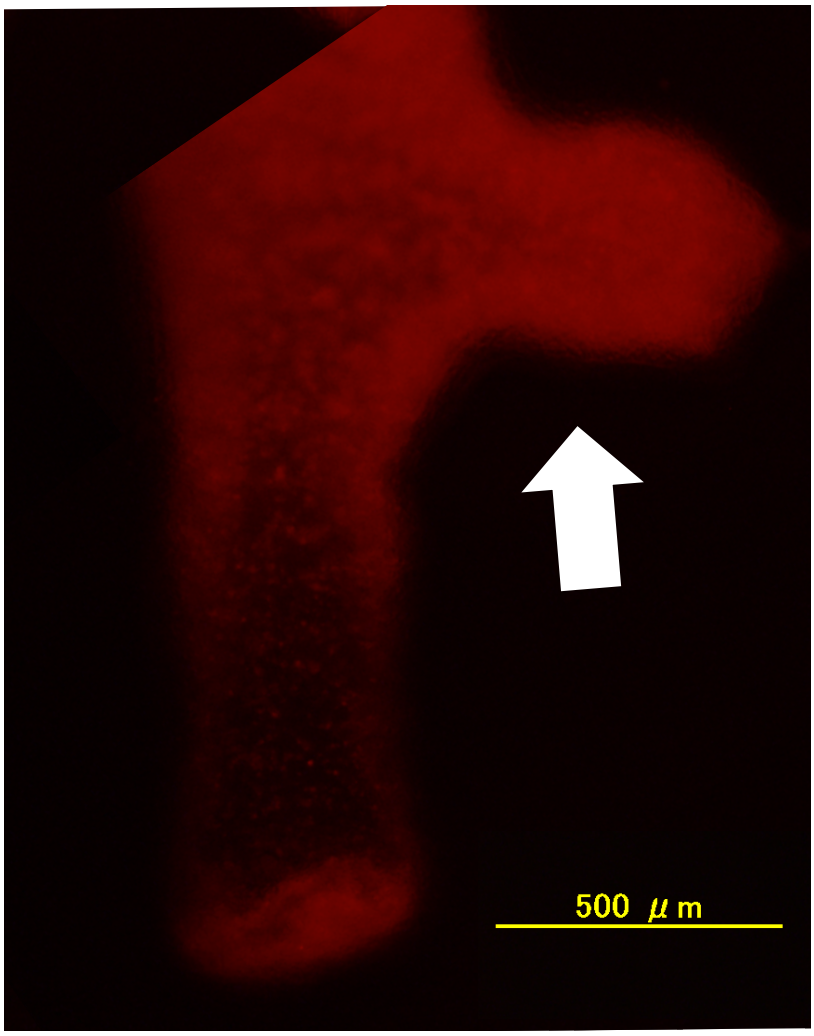

Figure 1.6. Photograph of basal part hydra polyp using fluorescent microscope. The budding offspring is indicated by an arrow.

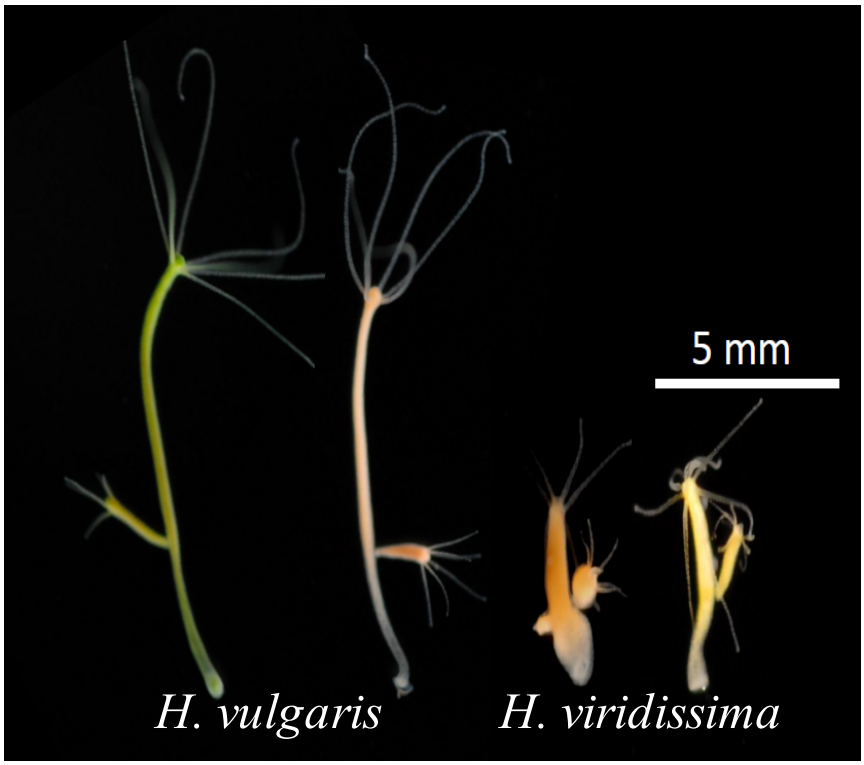

Figure 1.7. Photograph of *H. vulgaris* and *H. viridissima* groups. Left side of each species are symbiotic state, and right side is aposymbiotic state.

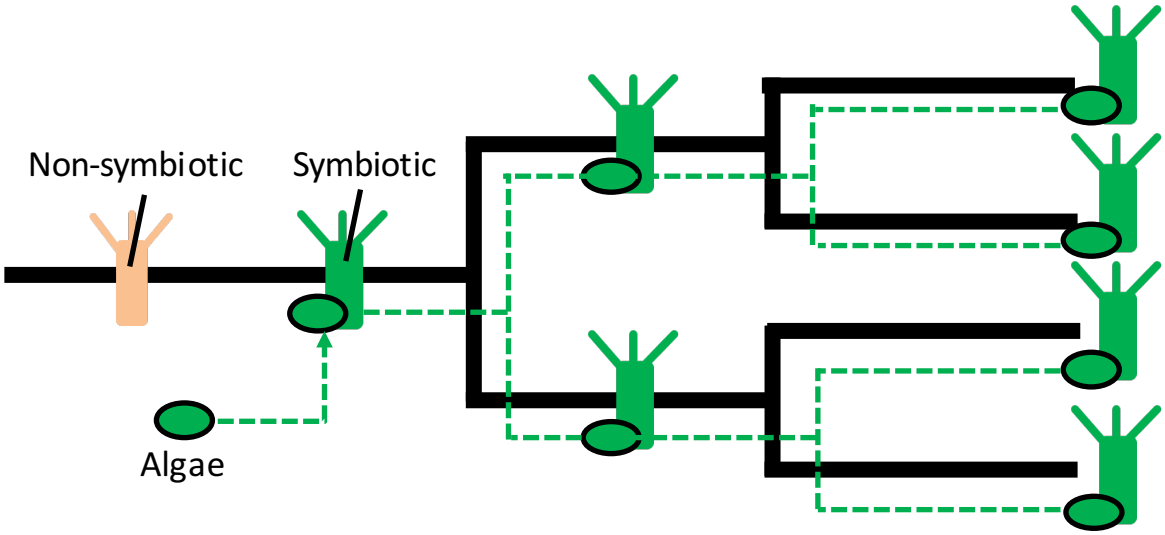

Figure 1.8. A plausible model of the history of symbiosis between *H. viridissima* group and the symbiont. The idea is based on Kawaida et al., 2013. The authors showed that the topology of the phylogenetic tree between *H. vulgaris* group strains and their symbionts was congruent, therefore the authors suggested that the ancestor of the *H. viridissima* group obtained the symbiont, and the hydra and symbiont then cospeciate.

2 Chapter 2

Evolutionary process of endosymbiosis between hydra and algae

2.1 Introduction

It is widely known that many cnidarian animals show endosymbiosis with algae, and the endosymbioses play important roles for growth and life cycles of the cnidarian hosts (Hofmann et al., 1996; Muscatine and Lenhoff, 1963; Muscatine and Porter, 1977, see also Figure 1.1 and 1.2). Despite the importance of the endosymbiosis, little is known about how these endosymbiotic relationships have evolved. As these endosymbioses have already been present in ancient time (Holland et al., 2004; Kawaida et al., 2013; Stanley and Swart, 1995), it is difficult to clarify the evolutionary process of the endosymbiotic relationships.

Genus *Hydra* is a freshwater animal which belongs to phylum cnidaria (Chapman et al., 2010). A molecular phylogenetic analysis of the genus *Hydra* showed that the species can be classified into four monophyletic groups, i.e., *H. vulgaris*, *H. oligactis*, *H. braueri*, and *H. viridissima* (Hemmrich et al., 2007; Martínez et al., 2010). Among the four species groups of genus *Hydra*, endosymbiosis is observed in *H. viridissima* and *H. vulgaris* groups (Kawaida et al. 2013). The National Institute of Genetics (Mishima, Japan) maintains the world's largest collection of hydra strains, which are collected worldwide. In this collection, all strains of *H. viridissima* group harbor *Chlorella*, and the previous study suggested that this endosymbiosis occurred before the divergence of the *H. viridissima* group strains, and then the hydra and algae then continued to cospeciate (Figure 1.8).

On the other hand, only two *H. vulgaris* group strains (J7 and J10) harbor green algae, and the alga that resides in J7 was identified as *Chlorococcum* (Kawaida et al., 2012). Other *H. vulgaris* group strains except for J7 and J10 survive without harboring the alga (non-symbiotic) (Kawaida et al., 2010). This implies that the evolution of the endosymbiosis in *H. vulgaris* group occurred more recently than *H. viridissima* group, therefore these two *Hydra* groups would be useful to study the evolutionary process of endosymbiosis establishment. However, it

is unknown whether the other non-symbiotic *H. vulgaris* group strains also have the potential to harbor the algae or not. It is possible that non-symbiotic strains also are able to harbor the endosymbiotic *Chlorococcum*, because even the symbiotic strains are also able to survive and proliferate without harboring the algae. Thus, the evolution of endosymbiotic potential for harboring endosymbiotic *Chlorococcum* may have occurred before or during the radiation of the *H. vulgaris* group strains, which is more ancient than I expect from the phenotypic observation. Alternatively, endosymbiotic potential is present only in the currently endosymbiotic strains, and therefore non-symbiotic lineages can never be endosymbiotic.

Thus, the aim of this chapter is to test these hypotheses and clarify the evolutionary process of the endosymbiosis between *H. vulgaris* group and the endosymbiotic algae. First, I examined whether non-symbiotic strains have the potential for endosymbiosis by introducing endosymbiotic algae into them. Second, to determine the evolutionary timing of the endosymbiotic events, I sequenced the mitochondrial genomes of the twenty-five strains of the *H. vulgaris* group in the NIG collection and conducted phylogenetic analyses based on these sequences. On the basis of these experiments and data analysis, I discuss the evolutionary process of endosymbiosis between *Hydra* and green algae.

2.2 Materials and methods

2.2.1 Hydra strains

Twenty-five strains of *H. vulgaris* group maintained at the National Institute of Genetics were used in the present study (Table 2.1). Polyps were kept in a plastic dish filled with "modified 'M' solution" (1 mM NaCl, 1mM $CaCl_2$, 0.1 mM KCl, 0.1 mM $MgSO_4$, 1mM tris-(hydroxymethyl)-aminomethane; pH7.4, adjusted with HCl) (Takano and Sugiyama, 1988) at 18°C and fed newly hatched *Artemia* nauplii three times a week under 12 hr dark/light condition with 2,500 lux illumination as the light condition.

2.2.2 Introducing endosymbiotic algae into non-symbiotic strains

To examine whether the non-symbiotic strains had endosymbiotic potential or not, the endosymbiotic algae were introduced into each of the strains as follows. First, the hydra polyps with the endosymbiotic algae were disrupted using a crusher (μT-12, TITEC, Saitama, Japan) without beads in the hydra culture solution. The suspension was centrifuged at 10,000 *g* for 5 min and was washed several times with the culture medium. In the process, the algae were compacted and purified at the bottom of the tube. The purified algae were re-suspended in the hydra culture solution and were introduced into the gastric cavity of individual hydra through the mouth opening using a microglass capillary. The increase of the algae in new hydra cells was periodically checked under a fluorescent microscope (Axiophot, Zeiss); the algae inside the hydra cells appeared as red dots (Figure 2.1). The polyps were maintained for more than 2 weeks in each generation. During the 2 weeks, the polyps budded asexually, and the offspring also

budded, which resulted in grand offspring polyps in the 2-week period. When the algae were fully proliferated in the grand offspring polyps (Figure 2.2), I considered that the host hydra strain had the potential for endosymbiosis with the algae.

I also examined the endosymbiotic potential by grafting the symbiotic J7 polyp to an non-symbiotic polyp using an axial transplantation procedure (Kawaida et al., 2013). The half polyps of a symbiotic J7 and an non-symbiotic polyp were axially grafted to each other. After 2 weeks of the graft, the transfer of the symbiotic *Chlorococcum* from the J7 tissue into the non-symbiotic tissue was observed using the fluorescent microscope.

2.2.3 Determining the mitochondrial genome sequences of the *H. vulgaris* group strains

To conduct the phylogenetic analyses of the hydras, I extracted the genomic DNA from a single polyp of each of the *H. vulgaris* group strains using a DNeasy Blood & Tissue Kit (Qiagen). My PCR experiments were designed to cover the entire mitochondrial genome as much as possible. Because the hydra mitochondrial genome consists of two mitochondrial chromosomes, I designed the primers for the ends of each of the mitochondrial chromosomes based on the mitochondrial genome sequence of *H. magnipapillata* (Accession no. NC_011221). For chromosome 1, the primers used were *Hydra*-mt-first-F 5'-TGGCTCATGACCAGAATATAAGGG-3' and *Hydra*-mt-first-R 5'-AAGCTATCTGGAAAGTCTGCA-3'. For chromosome 2, the primers were *Hydra*-mt-second-F 5'-TGGCTCATGACCAGAATATAAGGG-3' and *Hydra*-mt-second-R 5'-AAGCTATCTGGAAAGTCTGCA-3'. The amplified fragments with the expected length were extracted after gel electrophoresis and were purified using a MiniElute Gel Extraction Kit (Qiagen). Using the products obtained as the starting materials, DNA libraries were constructed

with NEBNext Fast DNA Fragmentation & Library Prep Set for Ion Torrent (NEB, Ipswich, MA). The constructed libraries were enriched and loaded onto the Ion 316 chips, and the sequencing was conducted by the Ion PGM system with the Ion Sequencing 200 kit (Life Technologies).

The raw reads from the Ion PGM system were preprocessed using the scripts in the FASTX-Toolkit (http://cancan.cshl.edu/labmembers/gordon/fastx_toolkit/). In each read, the first 30 nucleotides, the nucleotides after the 250 nt position, and the nucleotide tails with quality scores ≤ 20 were discarded. After the trimming, the reads with lengths shorter than 50 nucleotides were also discarded. The remaining reads were mapped onto the complete mitochondrial genome sequence of *H. magnipapillata* using BWA (Li and Durbin, 2010) implemented in the DNA Database Japan pipeline (Kaminuma et al., 2010; Nagasaki et al., 2013). Through these procedures, I obtained the mitochondrial genome sequences of the 25 strains, although some gaps remained.

2.2.4 Determining the 18S rRNA nucleotide sequence from J10 alga

To conduct the phylogenetic analyses of the endosymbiotic alga, I extracted the genomic DNA of the algae in strain J10 using a genomic DNA extraction kit (DNeasy Plant Mini Kit, Qiagen). To selectively obtain the extract of the DNA of the algae, the algae were compacted and purified as described in the previous section. The DNA was then extracted from the collected algae using the DNeasy Plant Kit (Qiagen). Using the extracted DNA as a template, a genomic region of a partial 18S rRNA gene was amplified. We used the primers that were reported previously (Kawaida et al., 2013). The primer sequences were 5'-AACCTGGTTGATCCTGCCAGT-3' and 5'-TTGATCCTTCTGCAGGTTCACCTACG-3'.

The PCR products were sequenced with an ABI 3130 Avant Genetic Analyzer (Applied Biosystems). A BigDye Terminator v3. 1 Cycle Sequencing Kit (Applied Biosystems) was used for the sequencing reactions.

2.2.5 Phylogenetic analysis

The sequences were aligned using the Clustal omega algorithm (Sievers et al., 2011). The sequence alignment was further optimized by manual inspection on the Alignment Explorer in MEGA 6 (Tamura et al., 2013). I used the maximum likelihood (ML) method using RAxML v.8.1.0 (Stamatakis, 2006) and the Bayesian inference (BI) method using MrBayes5D (Ronquist and Huelsenbeck, 2003) (http://www.fifthdimension.jp/products/molphypack/) to infer the phylogenetic relationships. The best-fit substitution models at each nucleotide partition were estimated using Akaike's information criteria for the ML analyses and the Bayesian information criterion for the BI analyses implemented in Kakusan4 (http://www.fifthdimension.jp/products/molphypack/). For the BI, the settings were applied as follows: number of Markov chain Monte Carlo generations, 50 million; sampling frequency, 1,000; and burn-in, 1,001. The support for internal branches was evaluated using bootstrap percentages from 1,000 nonparametric replicates for the ML method and using Bayesian posterior probabilities for the BI. The divergence time between *H. oligactis* and *H. vulgaris* groups (21-28 million years ago, *Mya*) that was estimated by Martínez et al. (2010) was used as the calibration for estimating the divergence time of the clusters. The analysis was conducted using the RelTime method (Tamura et al., 2012).

2.3 Results

2.3.1 More than half of the non-symbiotic strains of *H. vulgaris* group possess the potential to harbor the endosymbiotic algae

To investigate the evolutionary process of the endosymbiosis between the *H. vulgaris* group strains and the algae, I examined the endosymbiotic potential of the *H. vulgaris* group strains by introducing endosymbiotic algae.

The alga that resides in the strain J7 (hereafter J7-alga) is in the genus *Chlorococcum* (Kawaida et al., 2013). However, the alga that resides in the strain J10 (J10-alga) has not been identified. To determine which algae were introduced, I examined the phylogenetic relationships between the algae in the J7 and the J10 strains. I sequenced the 18S rRNA gene from the J10-alga, and the phylogenetic analysis was conducted with sequences from other *Chlorococcum* species and included the J7-alga. The ML tree based on the 18S rRNA gene clearly showed that the J10-alga was genetically closely related to the J7-alga (Figure 2.3), and therefore I used only the J7-alga in this experiment.

To validate the reintroduction experiment, I removed the endosymbiotic algae from strain J7 and reintroduced the endosymbiotic algae into strain J7 by injection into the gastric cavity. If my experiment is reliable, I should be able to remove the endosymbiotic *Chlorococcum* from strain J7 and reestablish the endosymbiotic relationship by injecting the algae into the gastric cavity of J7. As a result, the algae were fully incorporated into the endodermal epithelial cells of the hydra within 2 weeks. Figure 2.4 shows a typical example of spreading of tissue that contains algae in a new host polyp. On the day of the introduction (0 d; Figure 2.4A), the algae were observed in the

body column as a small number of red dots because of auto fluorescence (arrowheads in Figure 2.4A). Four days after the introduction (Figure 2.4B), the red dots were observed throughout the body column in the endodermal epithelium. Moreover, the algae were transmitted into the offspring (arrow, Figure 2.4B - D). Two weeks after the introduction (Figure 2.4D), the red dots of algae in the hydra body column were highly abundant. Therefore, the endosymbiotic relationship was clearly re-established between the artificially introduced algae and strain J7 with algae removed, and the reintroduction experiment was validated.

For the other 23 strains, excluding the endosymbiotic strains, 12 strains (105, A1, B4, B6, B10, B11, D1, D7, J6, L2, K7, and K9) established stable endosymbiosis, and there were no differences in the incorporation of the algae among individuals. In the 11 other strains, the algal cells were completely absent in the body of the hydra, even after the introduction of the algae (Figure 2.5).

In addition to the artificial introduction of *Chlorococcum* cells, I also confirmed the endosymbiotic potential by grafting polyps of the endosymbiotic J7 and some non-symbiotic strains (B12, K5, K7, L4) to continuously migrate the *Chlorococcum* into non-symbiotic tissues. I observed that the algae spread from the symbiotic J7 into non-symbiotic K7, which also harbored the *Chlorococcum* in the artificial introduction (Figure 2.6A). On the other hand, the algae were not observed in the grafted polyps which did not establish the endosymbiosis in the artificial introduction (B12, K5, L4) (Figure 2.6B - D).

Thus, more than half of the strains retain the endosymbiotic potential to harbor the algae, and therefore the absence of the symbiont do not always indicate the lack of endosymbiotic potential.

2.3.2 Strains with the endosymbiotic potential were grouped into a single phylogenetic cluster

Kawaida et al. (2010) sequenced several genes of *Hydra* that include mitochondrial *COI* and nuclear *CnNOS1* genes and constructed the phylogenetic tree of genus *Hydra*. However, these genes are known to evolve at slow rates and their sequence divergence among species were not sufficient to resolve the phylogenetic relationships among the *H. vulgaris* group strains (Kayal et al., 2012). In this study, in order to show clearer phylogenetic relationships among *H. vulgaris* group strains, mitochondrial genomes that generally evolve at a faster rate were sequenced and the molecular phylogenetic tree was constructed. The mitochondrial genome of the *H. vulgaris* group consists of two chromosomes (Voigt et al., 2008). Both chromosomes in each strain were amplified, and the amplified regions were sequenced using the Ion Torrent platform. The raw sequencing reads of the mitochondrial genome are deposited in the DNA Database of Japan Sequence Read Archive (DRA) (accession number DRA003539, https://trace.ddbj.nig.ac.jp/DRASearch/submission?acc=DRA003539). After trimming the generated reads, approximately 40,000-206,000 reads were obtained for each sample (Table 2.2). These reads were aligned to the reference mitochondrial genome of *H. magnipapillata* using the BWA algorithm in the DNA Database of Japan pipeline. As a result, more than 80% of the reads were successfully mapped to the reference genome. The scaffolds of more than 12,000 bp in each strain were obtained. The accession numbers are listed in Table 2.2.

I conducted the phylogenetic analysis of the *H. vulgaris* group strains based on the aligned mitochondrial genome sequences. The maximum likelihood tree based on the mitochondrial genome is shown in Figure 2.7. The sequence of *H. oligactis* (NC_010214) was used as the outgroup. The BI tree showed the topology identical with that of the maximum likelihood tree. Based on my results, I classified the strains of *H. vulgaris* group into three clusters. The first cluster consisted of strains L4, M2, and M5 (cluster α) that were collected in the United States.

The second cluster consisted of strains K5 and K6 (cluster β), with origins in Europe. The strains in the third cluster (cluster γ) were primarily of Japanese origin, although strains B6, K7, K9, and L2 were collected in Europe. I further classified cluster γ into four subclusters (γ-1, γ-2, γ-3, and γ-4) with high bootstrap values. All strains that were identified with endosymbiotic potential in the algal introduction experiment were in cluster γ (indicated by asterisks in Fig. 4). All strains in the subclusters γ-1, γ-2, and γ-3 showed endosymbiosis, whereas only one strain (K7) in cluster γ-4 showed endosymbiosis. These results suggest that the endosymbiotic potential evolved in the common ancestor of the γ-cluster and that the potential was lost in the γ-4 cluster lineage after the divergence from strain K7 under a parsimony principle.

2.3.3 Evolution of the endosymbiotic potential in *H. vulgaris* group occurred more recently than that in *H. viridissima*

Martínez et al. (2010) estimated the divergence time of *H. viridissima* group and other three groups to be 46-61 Mya. Based on their data, the radiation of *H. viridissima* group strains was estimated to be 27-36 Mya. All the *H. viridissima* group strains show endosymbiosis. Therefore, *H. viridissima* group gained endosymbiotic potential at 27-61 Mya. In *H. vulgaris* group, the phylogenetic analysis showed that the *H. vulgaris* group strains were grouped into three clusters, and cluster α diverged first, followed by β and γ. Among the clusters, only cluster γ strains have endosymbiotic potential. It suggests that *H. vulgaris* group gained the endosymbiotic potential after divergence of clusters β and γ; therefore, I estimated the divergence time between clusters β and γ to be 8.2-11.0 Mya (Table 2.3). In addition, the divergence time between γ-1 and γ-2 was estimated to be 1.3-1.7 Mya. These results suggest that *H. vulgaris* group gained endosymbiotic potential between 1.3 and 11 Mya, which is more recent than that of *H. viridissima* group. Moreover, my study also showed that cluster γ-4 strains other than K7 do not have

endosymbiotic potential. It suggests that endosymbiotic potential was lost after divergence of K7 and the other γ-4 strains. The divergence time between strain K7 and other γ-4 strains was estimated to be 0.1-0.2 Mya (Table 2.3). These results suggest that the evolution of endosymbiotic potential to harbor the *Chlorococcum* took place during radiation of the *H. vulgaris* strains between 1.3 and 11 Mya, and the potential was lost more recently than 0.2 Mya. Although the timing of both events was recent, I was able to clearly distinguish these events.

2.4 Discussion

2.4.1 *H. vulgaris* group gained endosymbiotic potential through radiation of *H. vulgaris* group strains

The algal introduction experiment and the phylogenetic study of *H. vulgaris* showed that the *H. vulgaris* group strains are grouped into three clusters, (α, β, and γ), and cluster α diverged first, followed by β and γ. Among these clusters, only the cluster γ strains, which included the endosymbiotic strains, had endosymbiotic potential (strains indicated by asterisks in Figure 4). This suggests the endosymbiotic potential was gained in the γ lineages during divergence of the *H. vulgaris* group strains (indicated by the star in the orange-colored background, Figure 2.8), and the endosymbiotic potential was lost after the divergence of K7 and the other γ-4 strains (indicated by the cross in the orange-colored background, Figure 2.8). Moreover, the phylogenetic relationship between J7 and J10 was relatively distant (indicated by the solid circles in the orange-colored background, Figure 2.8). Parsimoniously, it is reasonable that J7 and J10 obtained the symbiont independently than that the algae were obtained once in the ancestor of γ lineages after that the strains except for J7 and J10 lost the *Chlorococcum* (indicated by the dashed arrows in the orange-colored background, Figure 2.8).

However, I cannot completely deny the possibility that evolution of the endosymbiotic potential was gained before the γ lineages, but the endosymbiotic *Chlorococcum* changed the host specificity, and therefore the current endosymbiotic *Chlorococcum* that resides in J7 may not show endosymbiosis with the α and β lineages. Yet, note that in the case of *H. viridissima* group, a non-symbiotic strain is also able to harbor the symbiont derived from a different strain, even though the divergence time between the strains was estimated to be 27-36 Mya. If this time

scale is applied to *H. vulgaris* group, it is quite unlikely for *H. vulgaris* group to have experienced such changes of the host specificity among strains.

What types of molecular mechanisms were involved in the gain and the loss of endosymbiotic potential in *H. vulgaris* group? Pattern recognition is a possible candidate for a molecular mechanism; when a host encounters microbes in the environment, the host recognizes the microbes using pattern recognition receptors (PRRs) (Crosnier et al., 2011; Fujita et al., 2004; Jimbo et al., 2000; Meyer and Weis, 2012; Weis et al., 1998; Wood-Charlson et al., 2006). For example, lectins are a ubiquitous and diverse group of PRRs that bind glycans, and in parasitic interactions, lectins play an important role in the innate immune response that leads to the destruction of the pathogens (Fujita et al., 2004). Lectin/glycan interactions are also implicated as an interpartner signaling mechanism during the onset of symbiosis in anthozoan/*Symbiodinium* associations (Jimbo et al., 2000). I have not identified the genes for the PRRs in hydra, but similar molecular mechanisms may be used in acquiring endosymbiotic algae. Moreover, this function might have been lost after the divergence of K7 and the other γ-4 strains. In my study, I used strain K7 and the other cluster γ-4 strains that were genetically closely related to one another, and therefore I could compare the genomes of these strains and identify the genetic differences responsible for the endosymbiotic potential.

2.4.2 Most of the strains which have the endosymbiotic potential survive without harboring the algae

I found that most of the *H. vulgaris* group strains with endosymbiotic potential survived without harboring the endosymbiotic algae. This result suggests that the absence of the symbionts does not always indicate the absence of endosymbiotic potential. Although many strains gained endosymbiotic potential, why do only two strains naturally harbor the symbiont at

present? One possible reason why the J7 and J10 strains acquired the algae was that the hydras or algae were transported to the location of the partner. In a previous study, the phylogenetic relationships of several hydra did not match their geographic origins (Martínez et al., 2010), which suggests that hydra are often transported. My phylogenetic analysis demonstrated that strains with Japanese and European origins both were part of cluster γ. This result also provided support for the frequent transport of hydra. Many animals and plants are transported worldwide by humans and migratory birds (Heck et al., 2008; Mack and Lonsdale, 2001), and it is possible that the hydra or the alga attaches to objects and is transported. As another possible explanation, *H. vulgaris* group has not yet adapted to endosymbiosis. Recent studies reveal that evolutionary patterns of mutualism are similar to those of parasitism (Sachs et al., 2011), and Toft and Andersson, (2010) suggest that bacterial mutualism evolves from parasitic lineages. I demonstrated that the evolution of endosymbiotic potential in *H. vulgaris* group was more recent than that in *H. viridissima* group (Figure 2.8). Moreover, *H. viridissima* group use the photosynthetic products from the endosymbiotic algae (Douglas and Smith, 1984) and are more tolerant of starvation (Muscatine and Lenhoff, 1963). Thus, *H. viridissima* group has apparently established a mutualistic endosymbiotic relationship with the algae. Based on this study, however, I found that *H. vulgaris* group gained endosymbiotic potential much more recently than did *H. viridissima* group, and therefore, it is possible that the mechanisms for stable endosymbiosis in *H. vulgaris* group would not be as well established as those in *H. viridissima* group. In the future, to understand the mechanisms of the tolerance for endosymbiosis in *H. vulgaris* group, analyses of the gene expression or the protein profile of endosymbiotic *H. vulgaris* group should be conducted.

2.5 Conclusion

I propose that the endosymbiotic potential was gained during radiation of the *H. vulgaris* group strains, but most of the strains remain non-symbiotic. This feature is in contrast with *H. vidirissima* group, in which all strains harbor symbionts. This difference implies that the endosymbiotic relationship between *H. vulgaris* group and *Chlorococcum* has not well established compared to *H. viridissima* group. As the gain of the endosymbiotic potential in *H. vulgaris* group were more recent than in *H. viridissima* group, the mechanisms for stable endosymbiosis would not be established well in *H. vulgaris* group. The difference between *H. vulgaris* and *H. viridissima* groups about the evolution of endosymbiosis would be useful to understand the evolutionary process of endosymbiosis.

Table 2. 1. List of the analyzed strains of *H. vulgaris*

No.	Strain code	Old species name	Origin of strain	Remarks
1	105	*H. magnipapillata*	Japan	Reference genome determined
2	A1	*H. magnipapillata*	Japan	Lacking holotrichous isorhiza
3	A9	*H. magnipapillata*	Japan	Another code; sf-1
4	B4	*H. magnipapillata*	Tokyo, Japan	
5	B10	*H. japonica*	Fukuoka, Japan	
6	B11	*H. magnipapillata*	Akita, Japan	
7	B12	*H. magnipapillata*	Akita, Japan	
8	D1	*H. magnipapillata*	Japan	Another code; mini-1
9	D7	*H. magnipapillata*	Japan	Another code; maxi-1
10	E4	*H. magnipapillata*	Japan	
11	F2	*H. magnipapillata*	Japan	Another code; Reg16
12	J1	*H. magnipapillata*	Japan	
13	J2	*H. magnipapillata*	Japan	
14	J6	*H. magnipapillata*	Japan	
15	J7	*H. magnipapillata*	Japan	Green algae symbiont
16	J10	*H. magnipapillata*	Japan	Green algae symbiont
17	B6	*H. attenuata*	Basel, Switzerland	
18	K5	*H. attenuata*	Basel, Switzerland	
19	K6	*H. attenuata*	Basel, Switzerland	
20	K9	*H. vulgaris*	Basel, Switzerland	
21	L2	*H. attenuata*	Basel, Switzerland	
22	K7	*H. attenuata*	Basel, Switzerland	
23	L4	*H. carnea*	USA	
24	M2	Not yet determined	CA, USA	
25	M5	*H. vulgaris*	CA, USA	

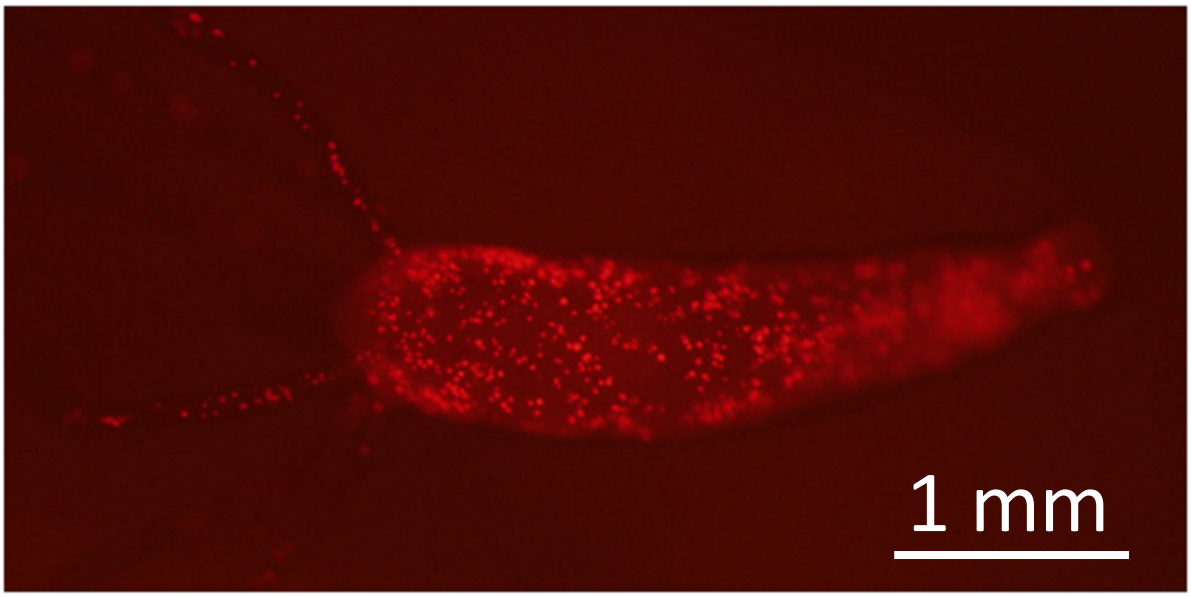

Figure 2.1. Hydra harboring endosymbiotic algae. This photograph was taken under a fluorescent microscope. The small bright red particles inside the hydra body are the endosymbiotic algae.

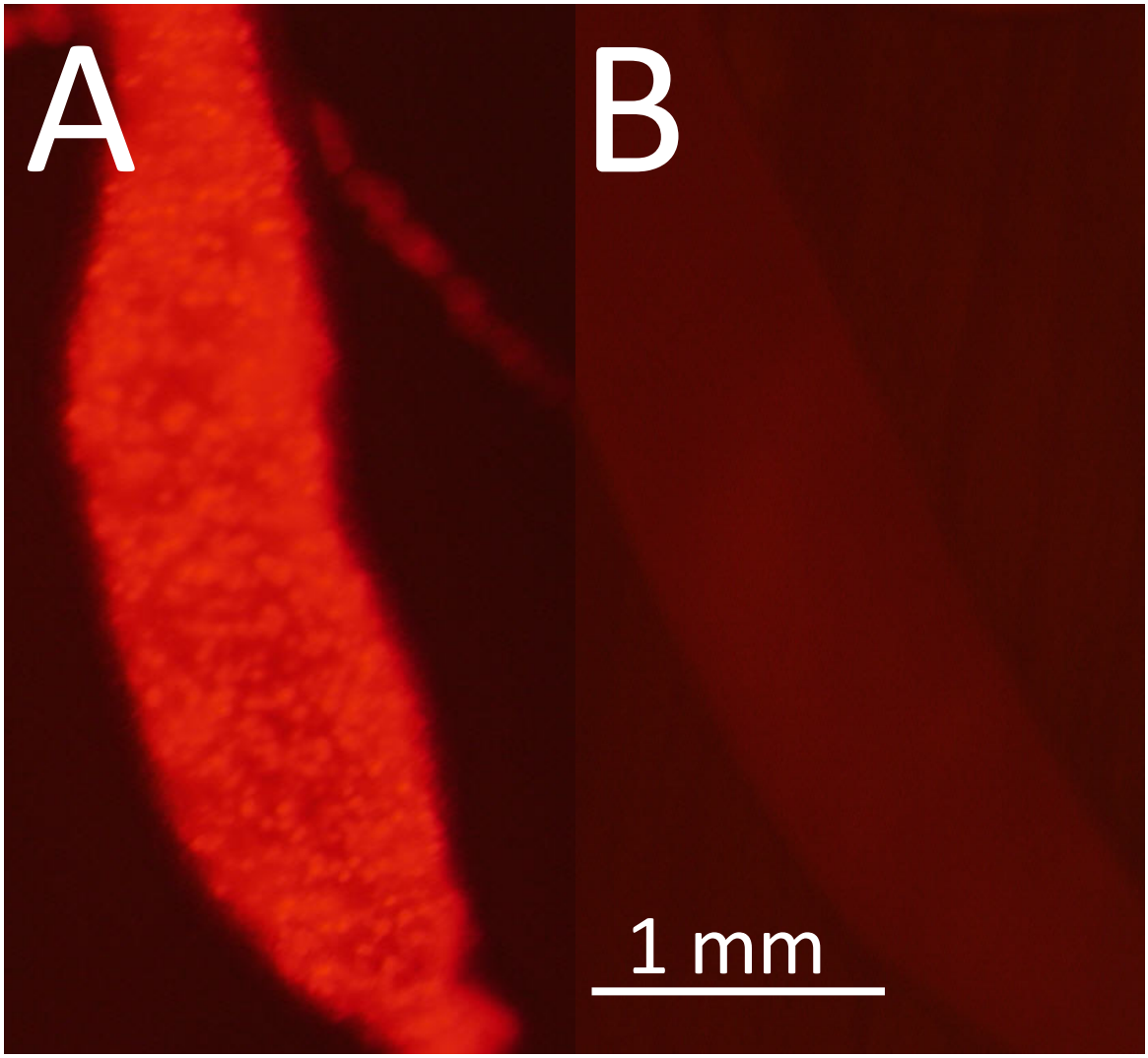

Figure 2.2. Photographs of grand offspring of a polyp in which the algae were introduced. Figure 2.2A is the polyp with endosymbiotic potential, and the algae are fully proliferated in the polyp. Figure 2.2B is the polyp without endosymbiotic potential, and the algae are not seen.

.

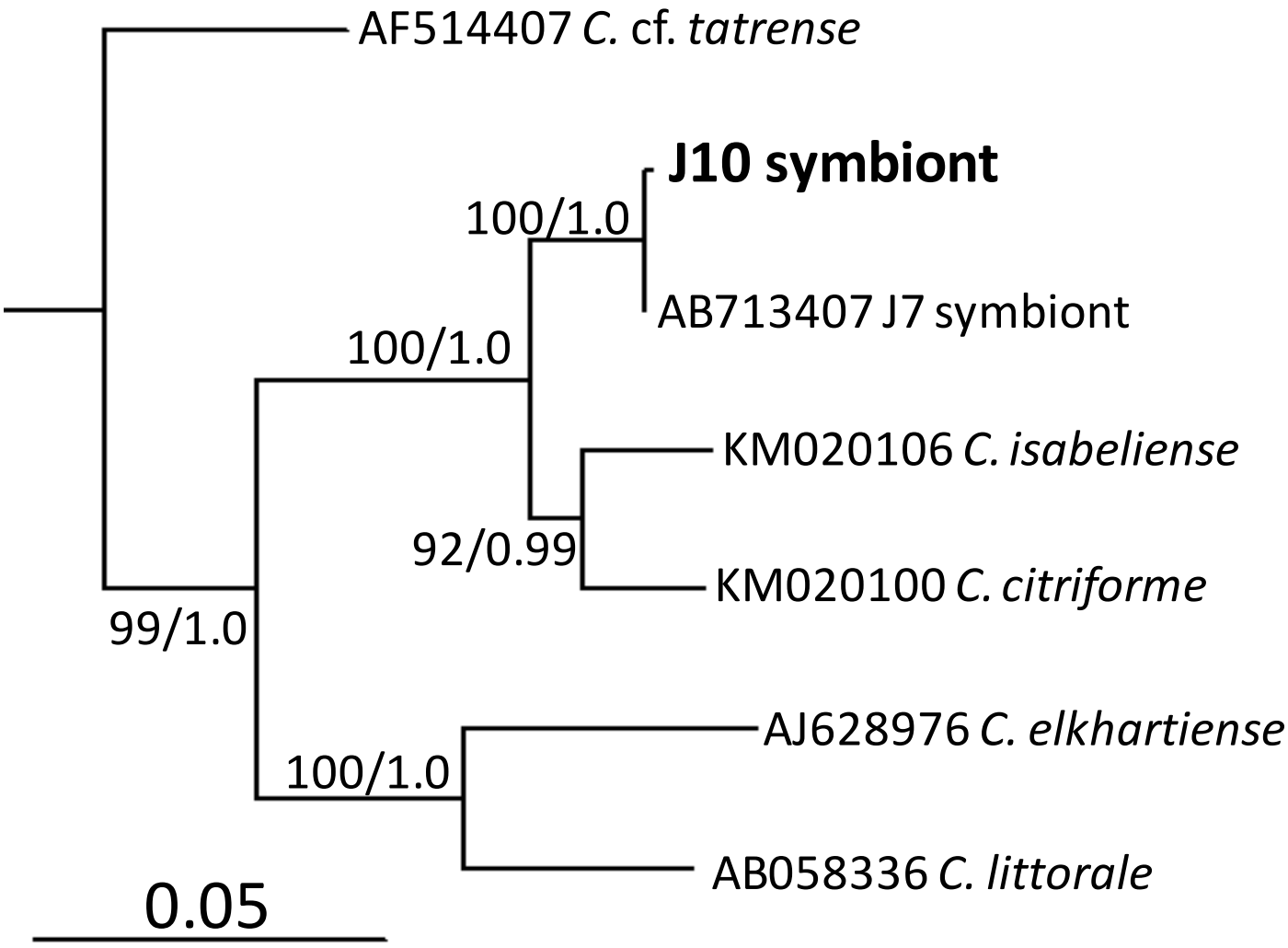

Figure 2.3. Maximum likelihood tree inferred from the nucleotide sequences of the 18S rRNA gene of *Chlorococcum*. The Bayesian tree also showed the topology identical to that of the maximum likelihood tree. The numbers along branches indicate the bootstrap probability (left) and the Bayesian posterior probability (right). The 18S rRNA sequence (X16077) from *Arabidopsis thaliana* was used as the outgroup sequence.

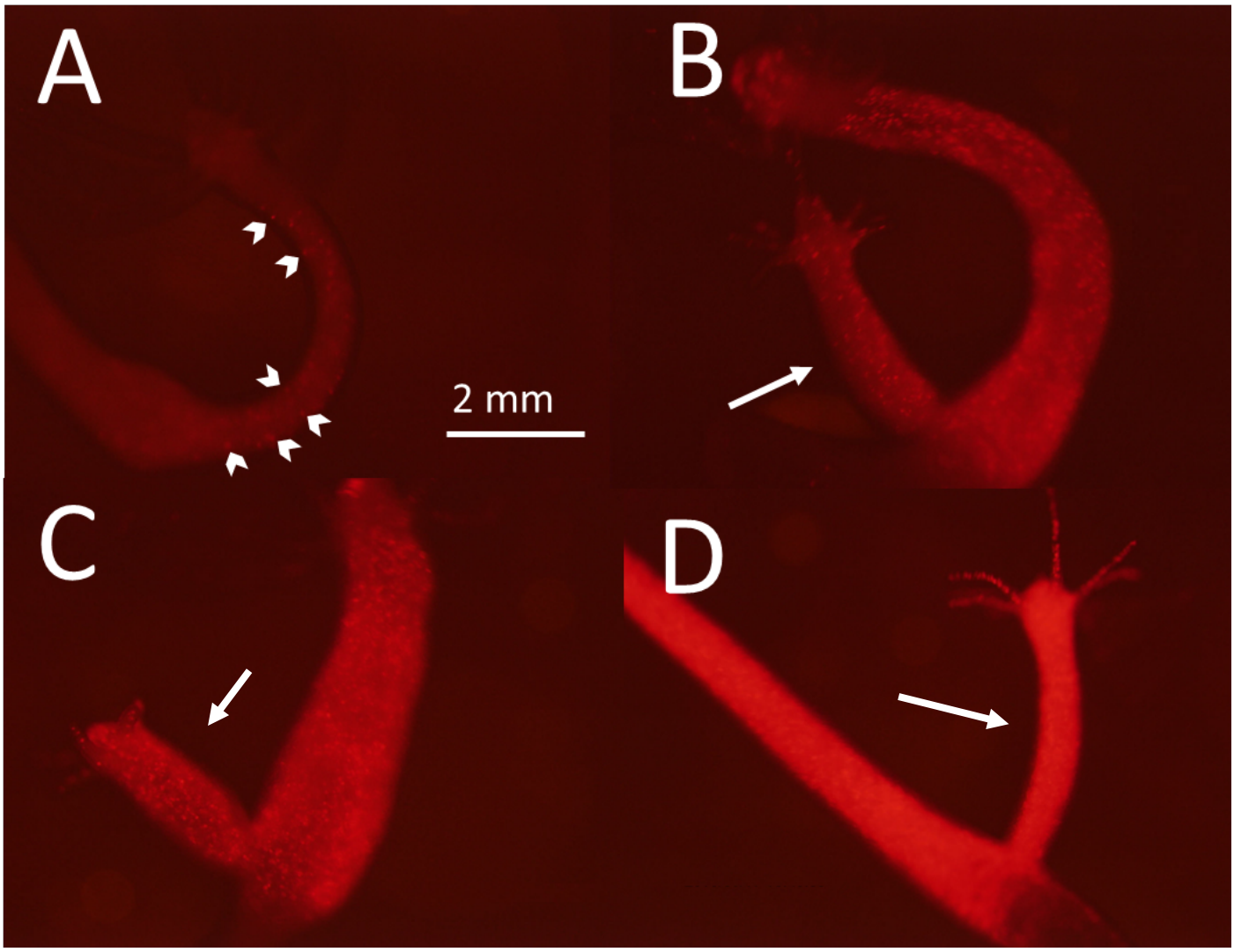

Figure 2.4. Increases in the introduced algae extracted from strain J7 injected into J7 strain polyps after prior algae removal. The pictures show the hydra polyp on day 0 (A), 4 (B), 7 (C), and 14 (D) after the introduction of the algae. Living samples were photographed under a fluorescent microscope. The arrowheads in Figure 2.4A show the endosymbiotic algae as small, bright red small particles in the endodermal epithelium of the polyp. The arrows indicate its offspring.

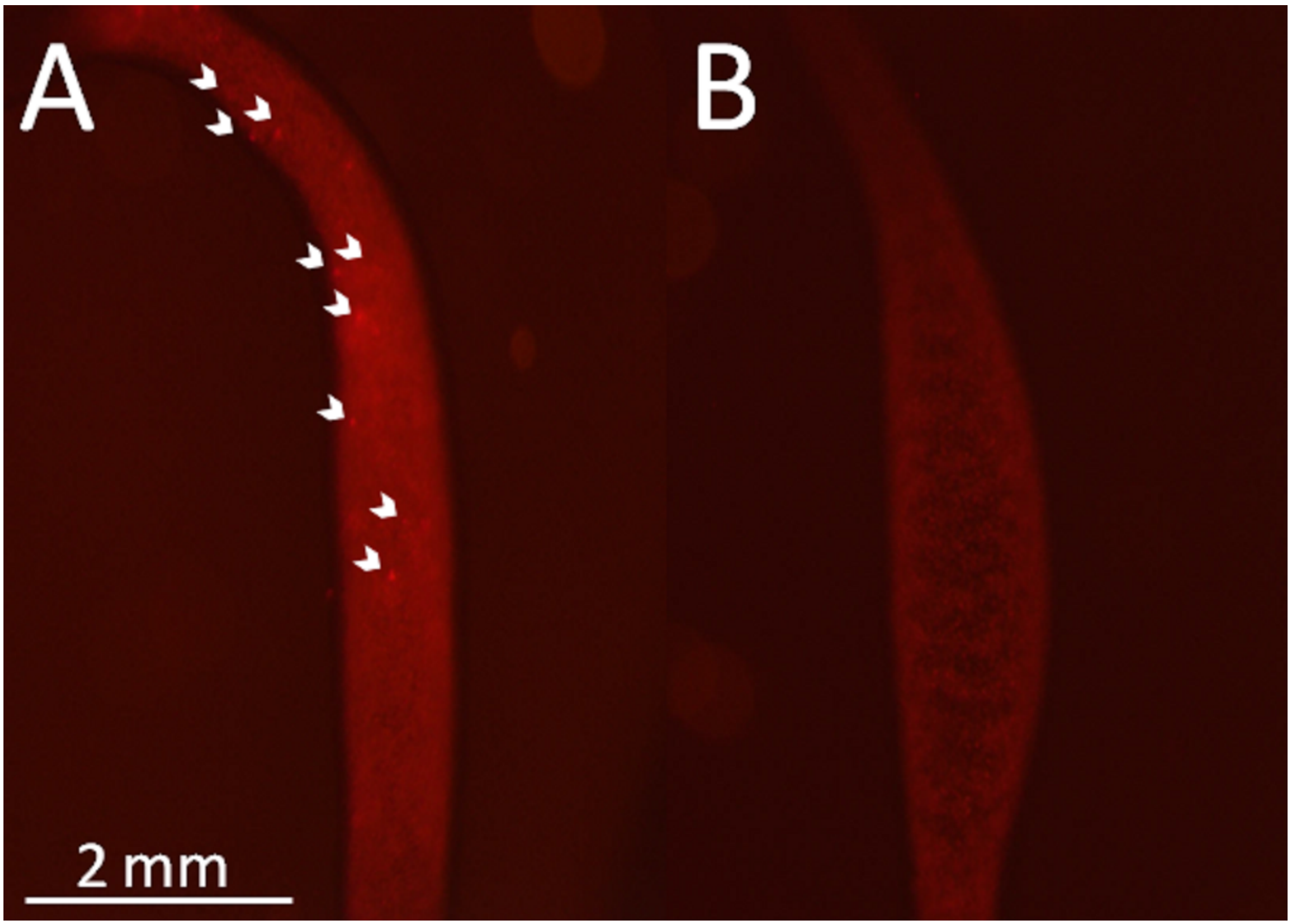

Figure 2.5. Photographs of strain E4 using a fluorescent microscope. Figure 2.5A is an individual 2 hour after the introduction of algae. Figure 2.4B is the same individual 14 day after the introduction, and the algae are absent.

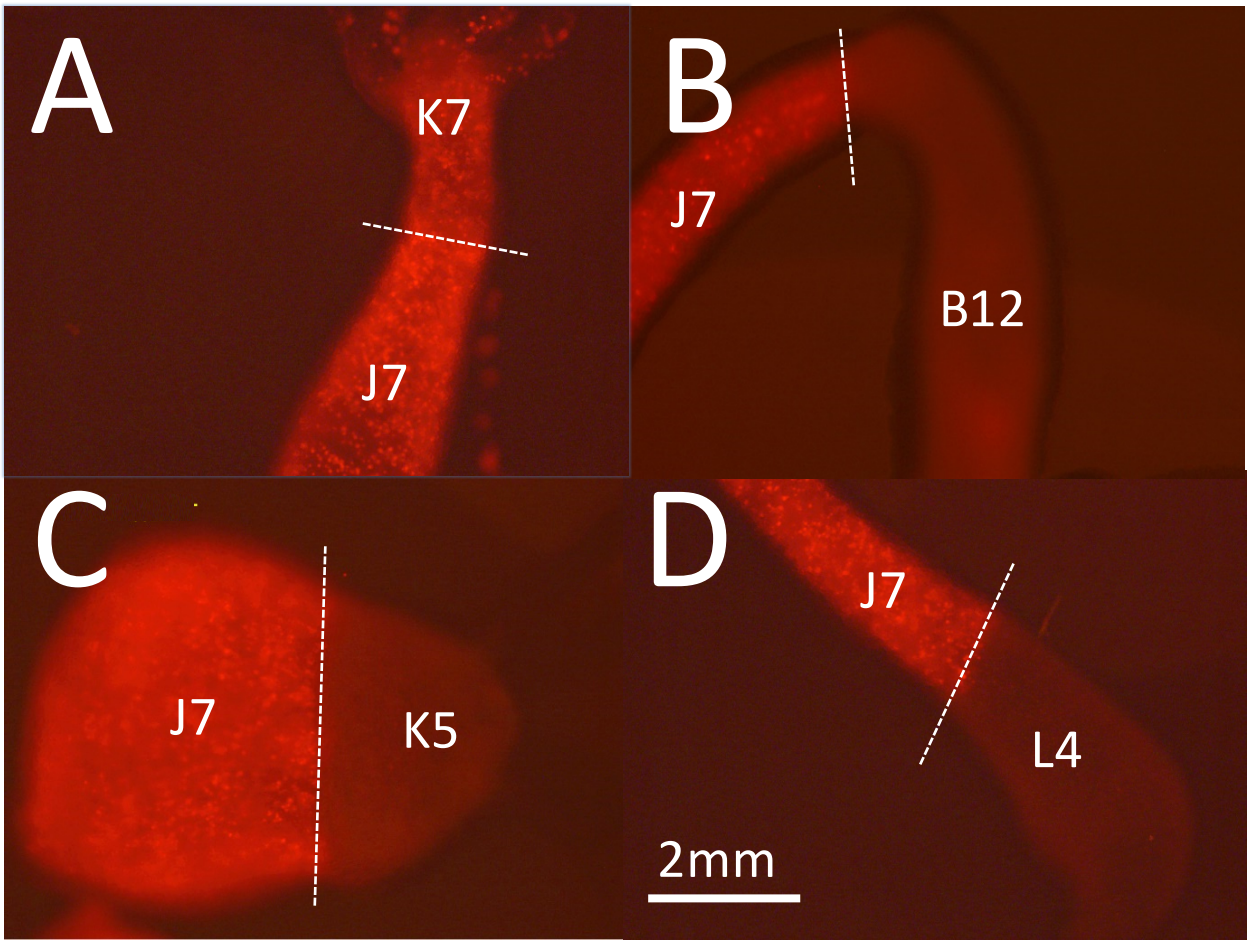

Figure 2.6. Axial graft of a symbiotic J7 and an aposymbiotic polyp. Half of the aposymbiotic polyp was transplanted onto half of the symbiotic J7 polyp. Living samples were photographed under a fluorescent microscope after 2 weeks of the transplantation. Grafted parts were represented as dotted lines.

Table 2.2 Overview of sequence reads.

Strain name	Read number	Map ratio (%)	Total length (bp)	Accession no.	Chromosome 1												
					Length (bp)												
					lsu-rRNA	lsu-rRNA - trnW	trnW	trnW - COX2	COX2	COX2 - ATP8	ATP8	ATP6	COX3	COX3 - ND2	ND2	ND2 - ND5	ND5
105	76,585	95.7	13,438	LC053784	1603	0	69	3	756	1	207	702	786	52	1271	1	1256
A1	81,500	96.0	13,462	LC053785	1603	0	69	3	756	1	207	702	786	52	1304	1	1246
A9	57,871	94.6	13,349	LC053792	1603	0	69	3	756	1	207	702	786	52	1261	1	1246
B4	145,086	96.2	13,445	LC053774	1603	0	69	3	756	1	207	702	786	52	1308	1	1246
B6	81,981	95.3	13,306	LC053779	1604	1	69	3	756	2	208	702	786	52	1250	1	1246
B10	92,193	96.0	13,434	LC053781	1603	0	69	3	756	1	207	702	786	52	1278	1	1246
B11	206,102	96.2	13,466	LC053778	1603	0	69	3	756	1	207	702	786	52	1308	1	1246
B12	99,846	94.9	13,269	LC053776	1602	0	69	3	756	2	207	702	786	52	1271	1	1246
D1	110,362	92.9	13,438	LC053793	1603	0	69	3	756	1	207	702	786	52	1280	1	1246
D7	79,896	95.6	13,462	LC053777	1603	0	69	3	756	1	207	702	786	52	1304	1	1246
E4	58,159	95.4	13,466	LC053786	1603	0	69	3	756	1	207	702	786	52	1308	1	1246
F2	112,223	95.3	13,213	LC053789	1603	0	69	3	756	1	207	702	786	52	1293	1	1246
J1	41,421	95.6	13,437	LC053791	1603	0	69	3	756	1	207	702	786	52	1285	1	1246
J2	47,399	95.7	13,466	LC053790	1603	0	69	3	756	1	207	702	786	52	1308	1	1246
J6	169,919	96.1	13,466	LC053788	1603	0	69	3	756	1	207	702	786	52	1308	1	1246
J7	55,496	96.2	13,408	LC053775	1603	0	69	3	756	1	207	702	786	52	1250	1	1246
K5	53,848	83.7	12,925	LC053797	1600	3	69	3	756	1	207	702	786	65	1106	1	1054
K6	84,544	84.3	13,057	LC053798	1600	3	69	3	756	1	207	702	786	52	1025	1	1208
K7	54,044	96.2	13,466	LC053782	1603	0	69	3	756	1	207	702	786	52	1308	1	1246
K9	107,736	95.0	13,465	LC053787	1603	0	69	3	756	1	207	702	786	52	1308	1	1245
L2	163,839	95.6	13,465	LC053783	1603	0	69	3	756	1	207	702	786	52	1308	1	1245
L4	112,674	84.7	13,429	LC053796	1603	0	69	3	756	1	207	702	786	52	1308	1	1246
M2	60,963	83.0	13,334	LC053794	1603	0	69	3	756	1	207	702	786	52	1308	1	1246
M5	81,325	82.5	13,466	LC053795	1603	0	69	3	756	1	207	702	786	52	1308	1	1246

Table 2.2(continued). Overview of sequence reads .

Strain name	Accession no.	chromosome 2													
		Length (bp)													
		s-rRNA	ND6	ND6 - ND3	ND3	ND3 - ND4L	ND4L	ND4L - ND1	ND1	ND1 -ND4	ND4	ND4 - CYTB	CYTB	CYTB - COX1	COX1
105	LC053809	759	558	-10	348	0	300	0	990	0	1454	0	1149	0	1183
A1	LC053810	759	558	-10	348	0	300	0	990	0	1455	0	1149	0	1183
A9	LC053817	759	558	-10	348	0	300	0	920	0	1455	0	1149	0	1183
B4	LC053801	759	558	-10	348	-1	300	-1	990	-10	1455	-1	1149	-8	1183
B6	LC053818	759	558	-10	348	0	300	0	990	0	1349	0	1149	0	1183
B10	LC053799	759	558	-10	348	0	300	0	988	0	1455	0	1149	0	1183
B11	LC053806	759	558	-10	348	0	300	0	990	0	1455	0	1149	0	1183
B12	LC053803	759	558	-10	348	0	300	0	935	0	1350	0	1149	0	1183
D1	LC053802	759	558	-10	348	0	300	0	990	0	1455	0	1149	0	1183
D7	LC053811	759	558	-10	348	0	300	0	990	0	1455	0	1149	0	1183
E4	LC053814	759	558	-10	348	0	300	0	990	0	1455	0	1149	0	1183
F2	LC053816	759	558	-10	348	0	300	0	909	0	1298	0	1149	0	1183
J1	LC053815	759	558	-10	348	0	300	0	990	0	1449	0	1149	0	1183
J2	LC053800	759	558	-10	348	0	300	0	990	0	1455	0	1149	0	1183
J6	LC053805	759	558	-10	348	0	300	0	990	0	1455	0	1149	0	1183
J7	LC053804	759	558	-10	348	0	300	0	990	0	1455	0	1149	0	1183
K5	LC053822	759	558	-10	348	0	300	0	990	0	1295	0	1149	0	1183
K6	LC053823	759	558	-10	348	0	300	0	990	0	1367	0	1149	0	1183
K7	LC053812	759	558	-10	348	0	300	0	990	0	1455	0	1149	0	1183
K9	LC053808	759	558	-10	348	0	300	0	990	0	1455	0	1149	0	1183
L2	LC053807	759	558	-10	348	0	300	0	990	0	1455	0	1149	0	1183
L4	LC053821	759	558	-10	348	0	300	0	990	0	1418	0	1149	0	1183
M2	LC053819	759	558	-10	348	0	300	0	990	0	1323	0	1149	0	1183
M5	LC053820	759	558	-10	348	0	300	0	990	0	1455	0	1149	0	1183

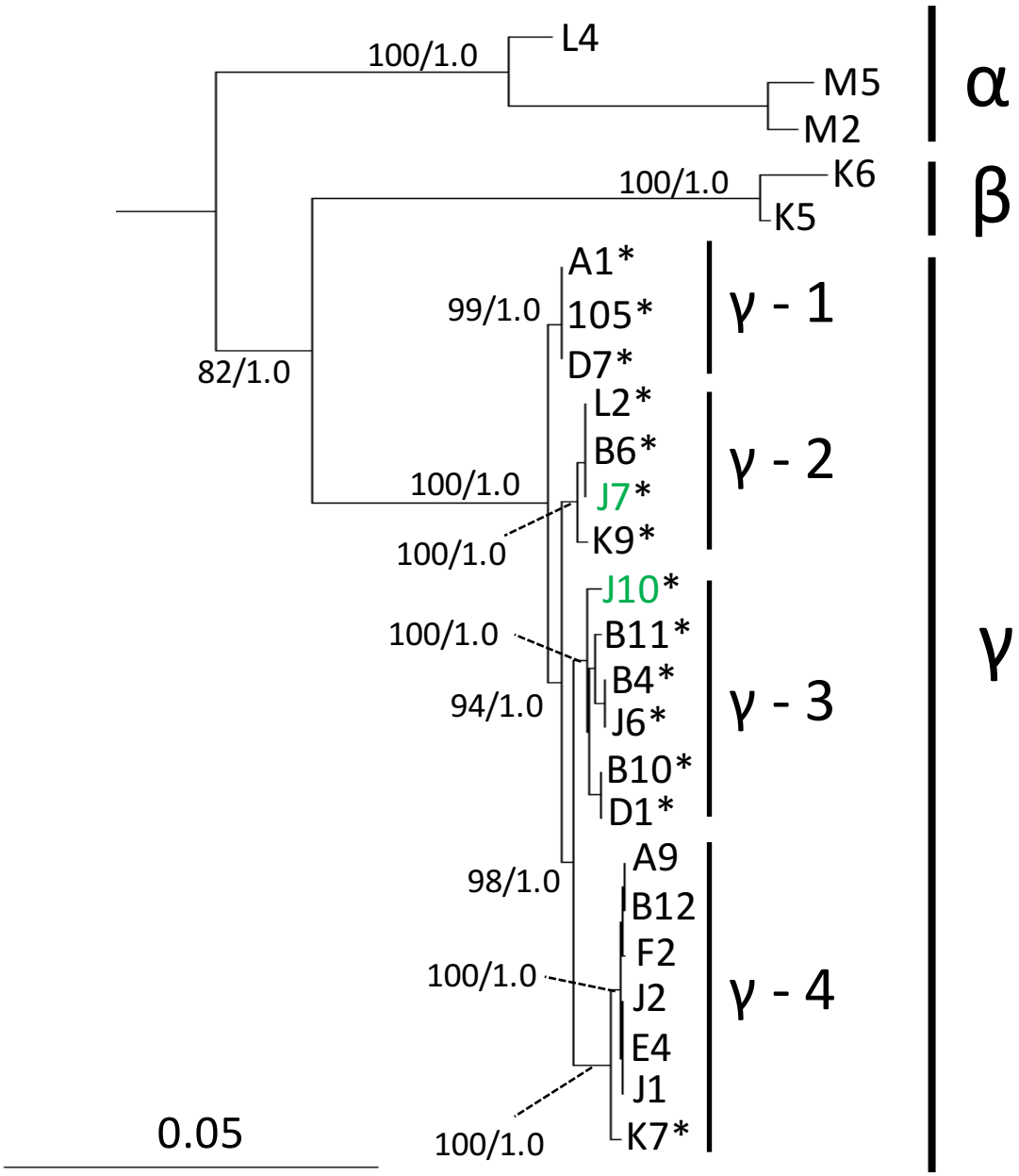

Figure 2.7. Maximum likelihood tree inferred from nucleotide sequences of the mitochondrial genomes of the *H. vulgaris* strains. The Bayesian tree also shows topology identical to that of the maximum likelihood tree. The numbers along branches indicate the bootstrap value (left) and the Bayesian posterior probability (right). The orthologous sequences (NC_010214) from *H. oligactis* were used as the outgroup sequences. The strains that established endosymbiosis with the algae in the introduction experiment are indicated by asterisks.

Table 2.3. Divergence times among the clusters of *H. vulgaris* strains estimated using the RelTime method.

Groups	Time of divergence (Mya)
α and β	10.3-11.3
β and γ	8.2-8.9
γ-1 and γ-2	1.3-1.6
γ-2 and γ-3	0.9-1.5
γ-3 and γ-4	0.7-0.9
K7 and other γ-4 strains	0.1-0.36

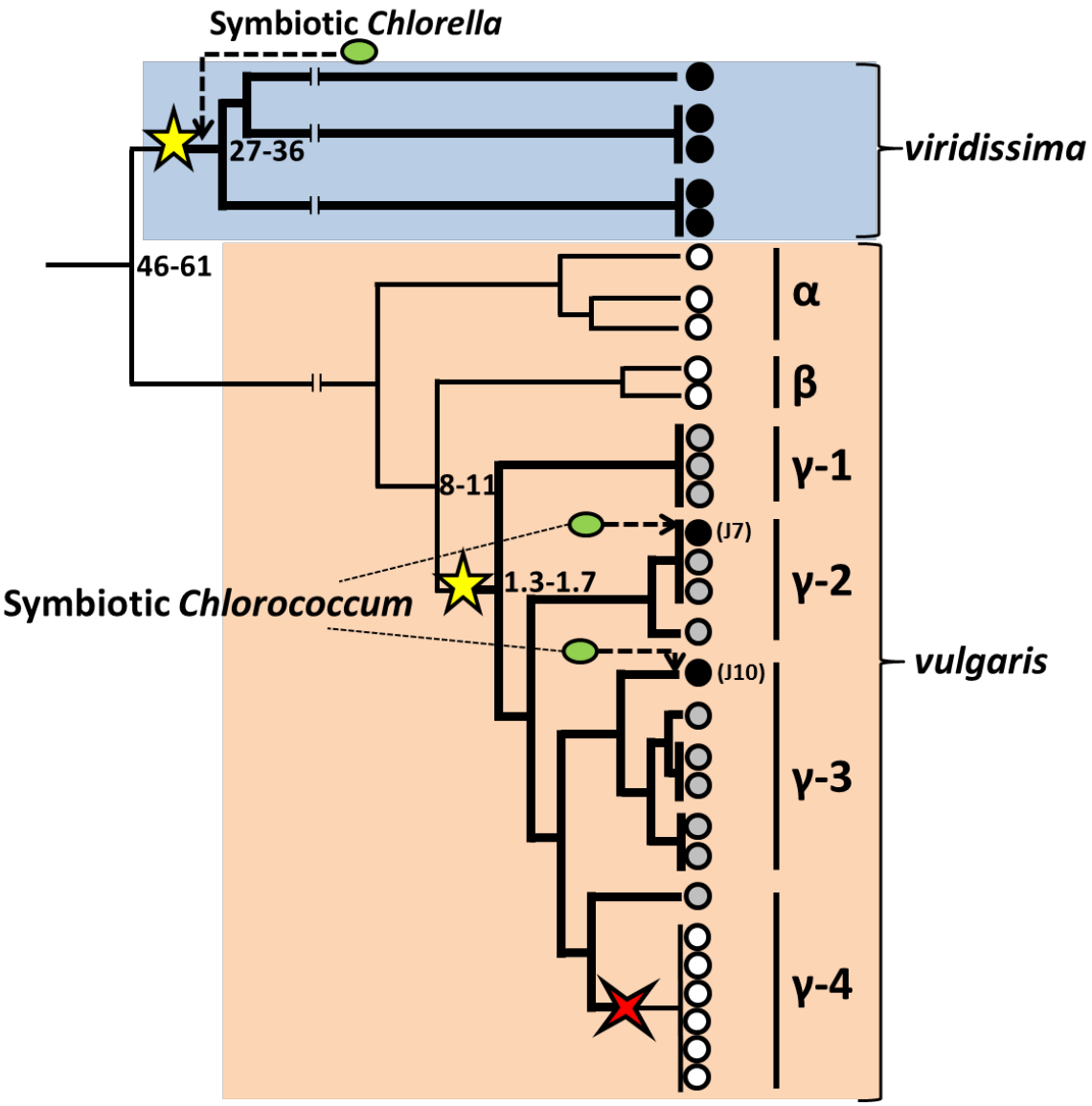

Figure 2.8. A plausible scenario for the origin and evolutionary process of endosymbiosis in *Hydra*s. Gray and open circles represent the strains with and without endosymbiotic potential, respectively. Solid circles indicate the strains that currently harbor the algae. The length of the line is not correlated with the actual divergence time. Numbers of several nodes indicate the divergence times estimated by the RelTime method (Tamura et al., 2012). The bold line shows the divergence of the strains with endosymbiotic potential. The yellow stars show the origins of the endosymbiotic potential in *Hydra*s, whereas the red cross indicates the loss of the potential.

3 Chapter 3

Endosymbiotic interaction between hydra and algae

3.1 Introduction

As endosymbiosis affects the survival and life cycle of cnidarians, elucidating the interactions between cnidarian hosts and symbionts is one of the most popular topics in endosymbiosis studies. However, the establishment of these stable endosymbiotic relationships remain unclear. Because most of the endosymbioses currently known were established at ancient time (Hofmann and Kremer, 1981; Holland et al., 2004; Muscatine and Porter, 1977; Stanley and Swart, 1995), these endosymbioses are not suitable for elucidating the endosymbiotic interaction in the stage of an evolution toward stable endosymbiotic interaction.

Hydra is one of the most suitable taxa for studying the evolutionary process of endosymbiosis. Among the four groups of genus *Hydra*, *H. vulgaris* and *H. viridissima* groups show endosymbiosis with green algae. In chapter 2, I suggest that the evolution of the endosymbiosis in *H. vulgaris* group is much more recent than that in *H. viridissima* group. In addition, I also showed that many *H. vulgaris* group strains survive without harboring the algae although they have the potential to harbor the algae. These imply that the endosymbiosis in *H. vulgaris* group is still in the middle of the stable endosymbiosis, and therefore it can be hypothesized that the interaction with algae is different between the two hydra groups. However, little is known whether interaction with the symbiont is different between the two hydra groups or not. The previous studies showed that the interaction between *H. viridissima* group and the algae was mutualistic (Muscatine and Lenhoff, 1963), but almost nothing is known about the interaction between *H. vulgaris* group and the algae. Moreover, little is known about the molecular mechanisms maintaining the two *Hydra* groups - green algae relationships. Habetha and Bosch (2005) conducted gene expression analysis of symbiotic *H. viridissima* by suppressive subtractive hybridization. However, they were able to find only a few genes that were differentially expressed by endosymbiosis, probably because of technical limitation (Meyer and Weis, 2012). This problem can be overcome by the recent next-generation sequencing (NGS)

techniques. Whole transcriptome shotgun sequencing (RNA-seq) allows to estimate the expression level of almost all genes with an unbiased way (Wang et al., 2009), and this technology offers to discern aspects of host–symbiont interactions while identifying the genes and pathways regulating those relationships (Meyer and Weis, 2012). Therefore, I would be able to find more genes that were differentially expressed by endosymbiosis by RNA-seq method.

Thus, the aim of this chapter is to evaluate the endosymbiotic interactions of the two *Hydra* groups with the algae. As the typical cases for investigating the endosymbiotic interaction, I first compared the growth and tolerance for starvation between aposymbiotic and symbiotic polyps. Next, in order to know the differences of interaction at the molecular level, I compared gene expression levels between aposymbiotic and symbiotic polyps by RNA-seq method. I then discuss possible mechanisms underlying the stable endosymbiosis.

3.2 Materials and methods

3.2.1 *Hydra* strains and estimation of growth and tolerance to starvation in symbiotic and aposymbiotic polyps

Endosymbiotic strains of *H. viridissima* group (strain M9) and *H. vulgaris* group (strain J7), stored in the NIG, were used in this study. Polyps were kept in a plastic container filled with Hydra-culture solution (Kawaida et al., 2013) at 18°C, and growth was estimated by feeding with newly hatched Artemia sp. nauplii three times a week, under a 12 h dark/light cycle (illumination = 2,500 lx). Tolerance to starvation was estimated in non-fed polyps kept in plastic containers; when non-budding polyps were unable to keep their shape, as observed under the stereomicroscope, they were determined to be dead. All polyps were kept under a 12 h dark/light condition (illumination = 2,500 lx) at 18 ˚C, and the solution within each container was changed three times per week in both conditions.

3.2.2 RNA isolation and sequencing

Total RNA was extracted from complete *Hydra* individuals after they were starved for seven days, using a PureLink® RNA Mini Kit (Thermo Fisher Scientific Inc., Madison, USA) and following the manufacturer's instructions. Individuals bearing endosymbiotic alga were disrupted using the μT-12 beads crusher (TAITEC Co., Saitama, Japan). The RNA-integrity number (RIN) of each sample was determined using an Agilent 2100 Bioanalyzer (Agilent Technologies, Santa Clara, USA), and only samples with RIN ≥ 9 were used. Total RNA was processed using the TruSeq RNA Library Prep Kit (Illumina® Inc., San Diego, USA), following the manufacturer's instructions, and including a poly-A^+ selection step. The indexed libraries

produced were then pooled, based on their indices and clustering, and sequenced in an Illumina® HiSeq 2000.

3.2.3 *De novo* assembly, functional annotation, and reciprocal best hit (RBH) analysis

The *de novo* assembly of the resulting 101 bp paired-end reads was performed using Trinity (Haas et al., 2013) as implemented in the DNA Data Bank of Japan (DDBJ) Read Annotation Pipeline (Kaminuma et al., 2010; Nagasaki et al., 2013). After removing the *de novo* assembled contigs shorter than 200 bp, contigs were compared to those deposited in the UniProtKB/Swiss-Prot (ftp://ftp.uniprot.org/pub/databases/uniprot/current_release/knowledgebase/complete/uniprot_sprot.fasta.gz) and in the nonredundant National Centre for Biotechnology (NCBInr, ftp://ftp.ncbi.nlm.nih.gov/blast/db/nr.**.tar.gz) databases, using the basic local alignment search tool (BLAST) with an E-value cutoff equal of 10^{-5}. Gene ontology (GO) terms were then assigned to each contig using the authors' scripts and a UniProt-GOA file (ftp://ftp.ebi.ac.uk/pub/databases/GO/goa/UNIPROT/gene_association.goa_uniprot.gz).

To identify orthologous genes of *H. vulgaris* group, *H. viridissima* group, *Paramecium bursaria*, and *Ciona varians*, RBH analysis (Moreno-Hagelsieb and Latimer, 2008) was conducted using the representative contigs remaining after discarding the low expressed contigs of these organisms. The contigs of *P. bursaria* (accession: DRA000907) and *C. varians* (accession: PRJNA214560) were generated by the method used in this study from the raw reads deposited in the DDBJ database.

3.2.4 Differential gene expression analysis

Raw reads were mapped to the *de novo* assembled transcripts of each species using Bowtie2 (Langmead and Salzberg, 2012). Transcript abundance was estimated using eXpress (Roberts and Pachter, 2013) and eff_count values were used to determine differential expression (DE). Two biological replicates (1 and 2) were used for each *Hydra* species condition (symbiotic and aposymbiotic); normalization and differential gene expression analysis between conditions were performed using the iDEGES/edgeR method comprised in TCC R package ver. 1.0.0 (Sun et al., 2013) and a false discovery rate (FDR) $\leq$ 0.1. Cluster analysis of the organisms was done referenced by Waring et al. (2001). The clustering was performed using R-package pvclust. Fold-changes in gene expression (determined as $\log_2$ (symbiotic) -$\log_2$ (aposymbiotic)) were used as the clustering data. The nearest neighbor method was used in the clustering, and the clustering was hierarchical using correlation as the distance.

3.2.5 Gene Ontology (GO) enrichment analysis

GO enrichment analysis was performed for the *de novo* assembled transcripts of *H. vulgaris* and *H. viridissima* using the Database for Annotation, Visualization, and Integrated Discovery (DAVID) version 6.7 (Dennis et al., 2003). This program performs Fisher's exact tests to determine the GO terms that are significantly enriched among the differentially expressed transcripts compared with the entire transcriptome. Queries were based on the UniProt ID of *de novo* annotated assembled references.

3.2.6 Phylogenetic analysis of ascorbate peroxidase gene in hydra

In my gene expression analysis, ascorbate peroxidase was up-regulated in both symbiotic hydra species, and the previous study suggested that this gene is transferred from plants or algae to hydra (Habetha and Bosch, 2005). In order to validate whether other non-symbiotic hydra species also have this gene, I extracted the genomic DNA of the *H. vulgaris* group strains J7 and M2, *H. oligactis* group strain Q12, and *H. viridissima* group strain M9, which has been maintained in NIG, using a genomic DNA extraction kit (DNeasy Plant Mini Kit, Qiagen). Using the extracted DNA as a template, a genomic region of a partial ascorbate gene was amplified. The primer sequences were 5'-TATTCATTTCGATCATGCGGTT-3' and 5'-AGAGACTTACCGATGATTGCTGG -3'. The PCR products were sequenced with an ABI 3130 Avant Genetic Analyzer (Applied Biosystems). A BigDye Terminator v3. 1 Cycle Sequencing Kit (Applied Biosystems) was used in the sequencing reactions. The sequences and other peroxidase genes were aligned using the ClustalW algorithm on the Alignment Explorer in MEGA 6 (Tamura et al., 2013). I used the maximum likelihood (ML) method to infer the phylogenetic relationships. The support for internal branches was evaluated using bootstrap percentages based on 1,000 nonparametric replicates.

3.2.7 Data Access.

Whole Genome Shotgun projects have been deposited in the DNA Data Bank of Japan (DDBJ)/European Molecular Biology Laboratory (EMBL)/GenBank databases (BioProject Accession; PRJDB4331).

3.3 Results and discussion

3.3.1 Change in growth and tolerance to starvation of the hydras

The comparison of growth rates and tolerance to starvation in symbiotic and aposymbiotic polyps of *H. viridissima* and *H. vulgaris* groups, revealed that the growth rate of symbiotic *H. viridissima* group was significantly higher than that of the aposymbiotic state (Figure 3.1). The number of polyps doubled at approximately four days of incubation in the symbiotic state and at approximately 28 days of incubation in the aposymbiotic state, the number of polyps was 8.3 ± 4.3 in the symbiotic state and 2.2 ± 0.8 in the aposymbiotic state after 27 days of incubation. On the other hand, the growth rates between symbiotic and aposymbiotic *H. vulgaris* group were almost identical (Figure 3.1), with the number of individuals (polyps) in both conditions doubling after approximately 10 days. For the symbiotic state, the number of polyps was 3.8 ± 0.8 after 32 days of incubation, and for the aposymbiotic state, it was 3.5 ± 0.8 after 29 days of incubation.

Considering the tolerance to starvation, symbiotic *H. viridissima* survived for a significantly longer period than aposymbiotic polyps (nearly seven weeks vs. nearly 33 days, Fig. 2, $p < 10^{-6}$ by Student's *t*-test). In *H. vulgaris* group, on the other hand, aposymbiotic *H. vulgaris* group survived for nearly 25 days, whereas symbiotic *H. vulgaris* group survived for a significantly shorter time (nearly two weeks, Fig. 2, $p < 10^{-12}$ by Student's *t*-test). Thus, these results support the idea that the endosymbiosis in *H. vulgaris* group is not as stable as in *H. viridissima* group.

3.3.2 Sequencing, *de novo* assembly, and functional annotation of *Hydra* spp transcriptomes.

The previous result showed that the symbiotic *H. viridissima* group was more tolerant to starvation than aposymbiotic polyp, whereas symbiotic *H. vulgaris* group was less tolerant to starvation. In order to understand the differences of interaction at molecular level, I isolated the RNA of *Hydra* species after 7 days' starvation, and gene expression levels between symbiotic and aposymbiotic states were compared. The total RNA isolated from symbiotic and aposymbiotic polyps and analyzed by RNA-seq yielded a total of ~60.7 million pairs of reads containing ~12.6 Gb of *H. viridissima* group sequences, and a total of ~110 million pairs of reads containing ~20 Gb of *H. vulgaris* group sequences. All reads were assembled using Trinity and yielded over 100,000 contigs for each species (Table 3.1). In order to choose a representative contig for each isoform, the longest transcripts of *H. viridissima* group (72,018 contigs) and *H. vulgaris* group (122,330 contigs) were selected for.

Figure 3.3 shows the distribution of representative contigs within each species; red dots indicate representative contigs annotated as Cnidaria and green dots representative contigs annotated as Chlorophyta. As can be depicted from Figures 3.3A and C, the *de novo* assembled *H. vulgaris* and *H. viridissima* representative contigs also contain endosymbiotic algae contigs. To exclude endosymbiotic algae contigs, only the representative contigs with fragments per kilobase of representative contigs per million mapped fragments of greater than 1 (FPKM $\geq$ 1) were selected resulting in 15,144 and 18,469 *H. viridissima* and *H. vulgaris* contigs, respectively (Table 3.1). As shown in Figures 3*B* and *D*, the representative contigs belonging to the endosymbiotic algae were able to be almost completely eliminated. After discarding low expressed contigs, the map ratio decreased only 1% in the aposymbiotic state, suggesting that most of the hydra contigs were conserved in the process (Table 3.2). Thus, the representative contigs remaining after discarding the low expressed contigs were used as the contig set of

"*Hydra* genes". In addition, the proportion of representative contigs in the symbiotic state decreased about 5%, suggesting that the reads belonging to the endosymbiotic algae were discarded.

The contigs were searched for homology against the NCBI-NR database (non-redundant protein sequences) (Benson, 2004) and the UniProtKB/Swiss-Prot protein database (Magrane and Consortium, 2011) using blastx (Camacho et al., 2009) (E-value cutoff = 10^{-5}) and functionally annotated according to protein sequence similarity. A total of 8,970 (59%) *H. viridissima* reference genes were matched to the annotated sequences in the UniProtKB/Swiss-Prot database and 11,380 (75%) were matched to those in the NCBI-NR database. In the *H. vulgaris*, 9,757 (53%) and 13,467 (73%) reference genes were matched to the annotated protein sequences in the UniProtKB/Swiss-Prot and NCBI-NR databases, respectively (Table 3.1).

3.3.3 Comparison of differential gene expression patterns between the two *Hydra* species

In *H. viridissima* group, 1,890 contigs were up-regulated and 2,261 were down-regulated in the symbiotic state, while *H.vulgaris* group symbiotic state had 1,092 up-regulated and 1,775 down-regulated genes. Based on these differentially expressed genes within each species, and using DAVID to analyze Gene Ontology (GO) enrichment, a total of 97 GO terms in *H. viridissima* group (42 up-regulated and 55 down-regulated) and 28 in *H. vulgaris* group (11 up-regulated and 17 down-regulated) were detected as enriched, according to their false discovery rates (FDR $\leq$ 0.05, Tables 3.3 and 3.4). No enriched GO terms corresponded to up- or down-regulated genes in both species.

The reciprocal best hits (RBH) analysis (Moreno-Hegelsieb and Latimer, 2008) conducted between the *Hydra* genes of the two groups yielded 9,934 contigs (Table 3.5). Fisher's exact test revealed that the up-regulated genes in *H. viridissima* tend to be down-regulated in *H. vulgaris* group rather than up-regulated (p = 8.3e-0.6), and the down-regulated genes in *H. vulgaris* tend to be up-regulated in *H. viridissima* group rather than up-regulated (p = 2.2e-16). These results suggested *H. viridissima* and *H. vulgaris* groups have a distinct molecular interaction with endosymbiotic algae.

3.3.4 Comparison of differential gene expression patterns with other endosymbiotic organisms.

In order to validate whether the differential gene expression patterns between the two *Hydra* spp. reflect a stability of the endosymbiotic relationship, the differential gene expression patterns obtained in this study were also compared with those of *Paramecium bursaria* and *Cliona varians*. Both species show mutualistic relationships with their symbionts (Hill, 1996; Kamako and Imamura, 2006), and gne expression levels between symbiotic and aposymbiotic states obtained from RNA-seq using an Illumina® HiSeq 2000 platform were compared in previous studies (Kodama et al., 2014; Riesgo et al., 2014). Reads assembly and RBH analysis for each of the four organisms resulted in 1,111 orthologous genes. Using the fold change of these orthologous genes, hierarchical cluster analysis of the organisms was done (Figure 3.4): *P. bursaria*, *H. viridissima*, and *C. varians* were grouped into a single cluster. Thus, the differential gene expression patterns observed in symbiotic *H. viridissima* group were similar to those of other endosymbiotic hosts, but different from those observed in *H. vulgaris* group. This result suggests that a similar stable association with their endosymbionts seems to exist in these three organisms, but not in *H. vulgaris* group.

3.3.5 Possible mechanisms of endosymbiosis

3.3.5.1 Response to oxidative stress

During photosynthesis, endosymbionts generate reactive oxygen species (ROS) that cause major cellular damages including membrane oxidation, protein denaturing, and nucleic acids damaging (Lesser, 2006). Therefore, ROS response is one of hosts' major challenges. The RBH genes annotated as ascorbate peroxidase in the present study were up-regulated in the symbiotic state of both species but this gene was more extensively up-regulated in *H. viridissima* group than in *H. vulgaris* group (Figure 3.5). Four enzymes (superoxide dismutase, ascorbate peroxidase, catalase, and glutathione peroxidase) are responsible for ROS scavenging (Apel and Hirt, 2004). Although ascorbate peroxidase only exists in plants (Apel and Hirt, 2004), Habetha and Bosch, (2005) showed that *H. viridissima* has a plant-related ascorbate peroxidase, which was possibly laterally transferred. The presence of an ascorbate peroxidase gene in symbiotic and aposymbiotic *H. vulgaris* revealed in this study (Figure 3.6), suggested that this gene was present in the common ancestor of *Hydra* species. As this gene was more extensively up-regulated in *H. viridissima* group than in *H. vulgaris* group, *H. viridissima* group would scavenge ROS more than *H. vulgaris* group.

In *H. viridissima* down-regulated genes, mitochondrion-related GO terms were enriched (Table 3.4). Furthermore, almost all genes involved in the respiratory chain were down-regulated in symbiotic *H. viridissima* group (Table 3.6). Mitochondria generate ROS during the respiratory process (Lee et al., 2011; Marchi et al., 2012) and the ROS generated by symbiont and mitochondria have been shown to play a central role in host damages causing coral bleaching (Weis, 2008). In addition, it has been demonstrated that hyperthermic stress induces

the degradation of cnidarian hosts mitochondria (Dunn et al., 2012), which might limit cnidarians' capacity to mitigate ROS generation. Therefore, *H. viridissima* group might respond to ROS by inactivating the respiratory chain process.

"Calcium ion binding" GO terms were enriched in down-regulated *H. vulgaris* genes and upregulated *H. viridissima* genes (Tables 3.3 and 3.4). Oxidative stress can disrupt Ca^{2+} homeostasis, resulting elevation in intracellular Ca^{2+} (Desalvo et al., 2008; Orrenius et al., 2003). One of the characteristic genes in this study is polycystin (Table 3.7). Polycystin is known to be an intracellular calcium release channel (Koulen et al., 2002), and a previous study showed that this gene was inhibited by ROS (Montalbetti et al., 2008). In *H. vulgaris* group, the genes related to polycystin tended to be down-regulated in symbiotic state. Therefore, intracellular Ca_2^+ concentration would increase because of oxidative stress in *H. vulgaris* group. On the other hand, *H. viridissima* group would manage to keep intracellular Ca_2^+ homeostasis by up-regulation of the polycystin.

Disruption of Ca_2^+ homeostasis affects cell adhesion (Hirano et al., 1987). In fact, my study showed that "Cell adhesion" GO term was also enriched in down-regulated *H. vulgaris* genes, and upregulated *H. viridissima* genes (Tables 3.3 and 3.4). One of the abundant genes was cadherin (Table 3.8). Cadherin is responsible for adhesion of the cell, and it was protected from proteinase in presence of Ca^+ ion, and the previous genome study suggests that *Hydra* has classic cadherins exhibiting a highly conserved, bilaterian-type cytoplasmic (CCD) domain (Chapman et al., 2010). Steinhusen et al (2001) showed that cytoplasmic cadherin cleavage by caspase 3 and metalloproteinase in apoptotic cell (Steinhusen et al., 2001), and some of the caspase 3 and metalloproteinase genes were up-regulated (Table 3.9) in *H. vulgaris* group, therefore, the endosymbiosis would cause cell death in *H. vulgaris* group. Although some of the caspase 3 and metalloproteinase were also up-regulated in *H. viridissima* group (Table 3.9), *H. viridissima* group would prevent cell death by up-regulation of cadherin genes.

3.3.5.2 Metabolic interaction

Carbonic anhydrase and carbonate co-transporter were up-regulated in symbiotic *H. viridissima* group but not in *H. vulgaris* group (Table 3.10). Several -omics studies have reported carbonic anhydrase up-regulation (Grasso et al., 2008; Weis et al., 1989, 1996). Symbionts generally uptake inorganic carbon for photosynthesis, and carbonic anhydrase and carbonate cotransporter have been suggested to be involved in inorganic carbon uptake from water and supply to the symbiont (Furla et al., 2000). Therefore, the results obtained here suggest that *H. viridissima* group might uptake CO_2 from water and provide it to the symbiont using a chloroplast-like system, but *H. vulgaris* group is unable to do so.

The GO term "ATP binding" was enriched in up-regulated *H. viridissima* group genes suggesting that symbiotic *H. viridissima* group use more ATP than aposymbiotic *H. viridissima* group. As mentioned above, however, the genes related to the respiratory chain were downregulated in symbiotic *H. viridissima* group. Therefore, ATP synthesis seems to be less active in symbiotic than in aposymbiotic *H. viridissima* group albeit the higher ATP usage in symbiotic than in aposymbiotic polyps. This difference might be due to *H. viridissima* group directly utilizing the ATP or sugar-phosphate produced by the endosymbiont.

In *H. vulgaris* group, GO terms related to endopeptidase were enriched in up-regulated genes (Table 3.3). One of the characteristic genes was cathepsin (Table 3.11). Cathepsins are lysosomal acidic proteases ubiquitously found in animals and other organisms (Chwieralski et al., 2006), and most of the cathepsin genes were up-regulated in *H. vulgaris* genes, but not in *H. viriddisima* (Table 3.11). Futahashi et al., (2013) conducted transcriptome analysis of Stink bug (*Riptortus pedestris*), and showed that many cathepsin related genes were upregulated by symbiosis with extracellular symbionts of the genus *Burkholderia*. In addition, Byeon et al.,

(2015) showed that cathepsin-L protease has antibacterial activity against host gut symbiont, suggesting that cathepsin-L protease regulates the gut symbiont. In my study, as cathepsin related genes were up-reguted in *H. vulgaris* group, *H. vulgaris* group might have anti-algal activity by up-regulating cathepsin.

These evidences suggest that *H. viridissima* group has already established the mechanisms for stable endosymbiotic relationship with algae; *H. viridissima* group responds to the oxidative stress from the endosymbiotic algae, and provide the symbiont with CO_2 from outside. On the other hand, *H. vulgaris* group seems to have damaged by the oxidative stress, resulting the *Hydra*'s cell death (Figure 3.9).

3.4 Conclusion

My study showed that endosymbiotic interaction with algae was significantly different between *H. viridissima* and *H. vulgaris* groups. This difference was evidenced at the physiological and molecular levels: whereas endosymbiosis seems to be advantageous for the survival of *H. viridissima* group, and its mechanisms are well established, in *H. vulgaris* group endosymbiosis seems to be disadvantageous and polyps might in fact be death of the hydra's cell through apoptosis. These results support that the endosymbiosis between *H. vulgaris* group and the algae is still in the middle of the stable endosymbiosis establishment, and it therefore lacks the mechanisms for stable endosymbiosis. Recent studies revealed that mutualism and parasitism have similar evolutionary patterns (Steinhusen et al., 2001) and that bacterial mutualism evolved from parasitic lineages (Sachs et al., 2011). As the evolution of the endosymbiosis in *H. vulgaris* group was more recent than in *H. viridissima* group, the endosymbiotic interaction between *H. vulgaris* group and its algae may still be immature given its recent evolution. Thus, understanding the immature endosymbiotic relationship between *H. vulgaris* group and the algae will provide a significant insight into the evolutionary process of endosymbiotic relationships establishment.

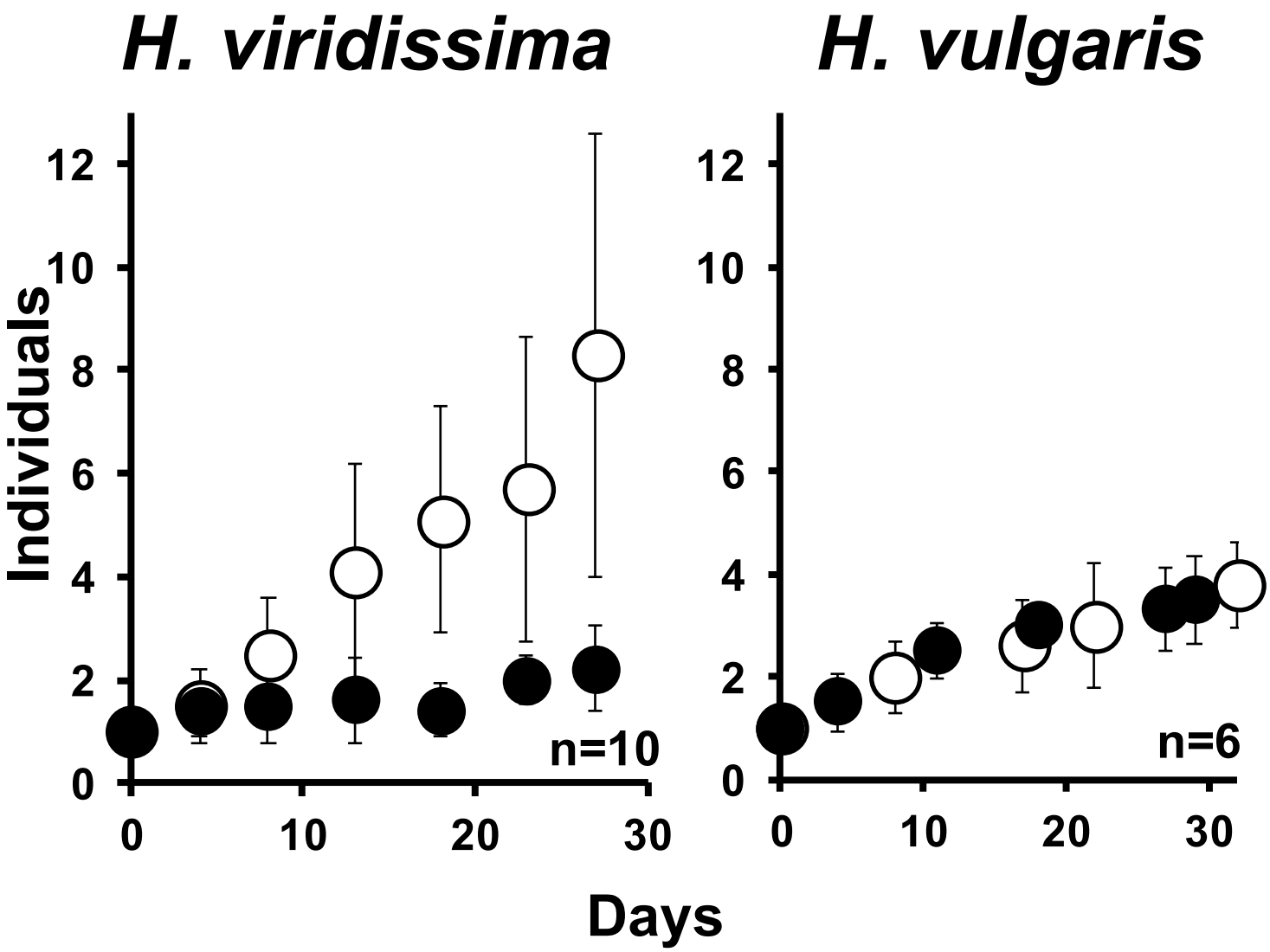

Figure 3.1. Population growth rate of *H. viridissima* and *H. vulgaris*. The hydras were fed three times a week. Open circles correspond to the symbiotic state, and closed circles to the aposymbiotic state. The bars represent standard deviation.

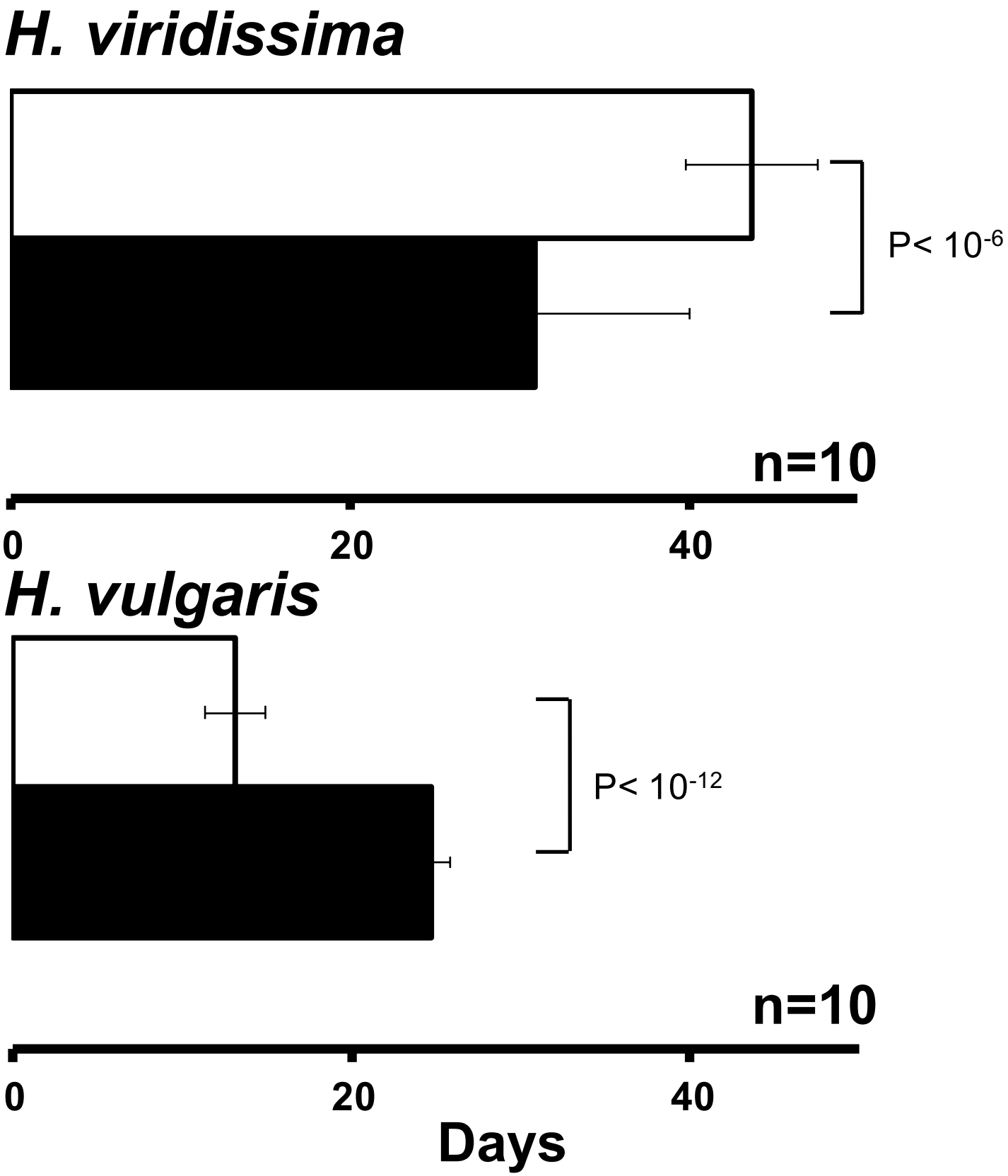

Figure 3.2. *H. viridissima* and *H. vulgaris* survival under starvation. The white column represents the symbiotic state and the black column the aposymbiotic state; the bar indicates the standard deviation.

Table 3.1. Distributions and annotation summary of the *de novo* assembled contigs

Organism	Contig set type	No. of contigs	N50	Average GC content (%)	Contigs aligned to (E-value ≤ 1e-5)	
					UniprotKB	NCBI-NR
Hydra viridissima	Whole	104,912	1,621	41	38,109 (36.3%)	58,368 (55.6%)
	Representative	72,018	1,120	43	22,933 (31.8%)	34,083 (47.3%)
	Hydra	15,114	2,166	34	8,970 (59.3%)	11,380 (75.3%)
Hydra vulgaris	Whole	175,342	1,718	40	42,937 (24.5%)	78,938 (45.0%)
	Representative	122,330	1,102	40	23,657 (19.3%)	42,625 (34.8%)
	Hydra	18,469	2,210	31	9,757 (52.8%)	13,467 (72.9%)

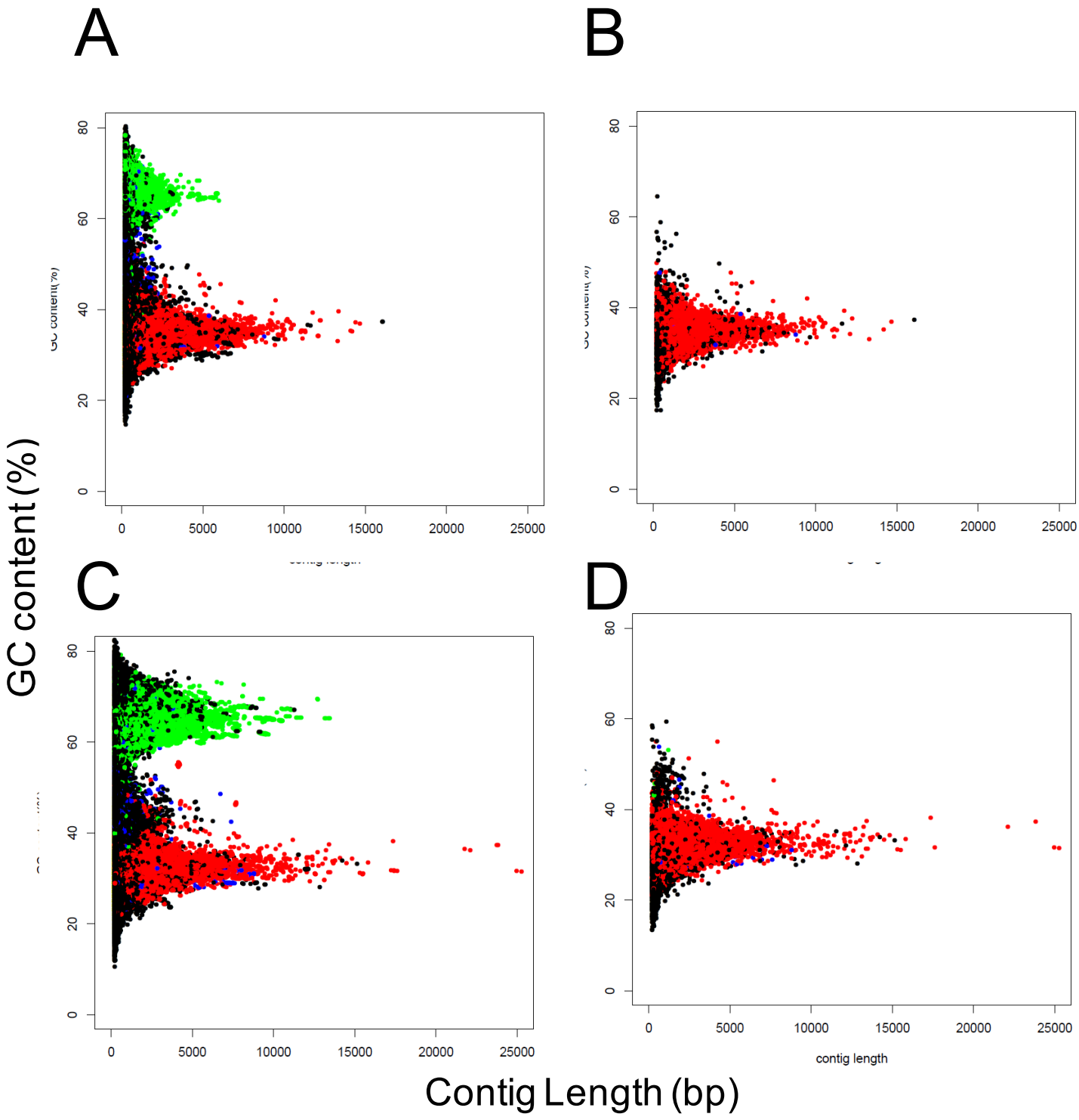

Figure 3.3. Contigs distribution in (*A*) representative contigs of *H. viridissima*, (*B*) *H. viridissima* reference genes, (*C*) representative contigs of *H. vulgaris*, (*D*) *H. vulgaris* reference genes. Cnidaria are represented in red, Chlorophyta in green, Prokaryote in blue, and other organisms in black.

Table 3.2. Reads proportion obtained in symbiotic and aposymbiotic *Hydra* species.

Contig set type	*H. viridissima*				*H. vulgaris*			
	symbiotic		aposymbiotic		symbiotic		aposymbiotic	
	1	2	1	2	1	2	1	2
Whole	92.15	92.47	92.93	93.44	94.76	94.66	94.68	95.18
Unigenes	86.97	87.45	88.46	89.07	88.95	88.7	88.69	89.29
Hydra	83.96	82.71	87.7	88.27	82.58	81.62	87.69	88.59

Table 3.3. Enrichment of GO terms in *H. viridissima* genes (FDR ≤ 0.05).

	GO term	GO id	*P-value*	FDR
	Upregulation			
MF	GTPase regulator activity	GO:0030695	3.10E-14	4.78E-11
MF	nucleoside-triphosphatase regulator activity	GO:0060589	9.08E-14	1.40E-10
CC	plasma membrane	GO:0005886	2.69E-13	3.84E-10
BP	regulation of small GTPase mediated signal transduction	GO:0051056	1.11E-12	1.99E-09
MF	small GTPase regulator activity	GO:0005083	1.21E-12	1.86E-09
BP	protein amino acid phosphorylation	GO:0006468	8.94E-12	1.60E-08
MF	motor activity	GO:0003774	2.02E-11	3.11E-08
MF	microtubule motor activity	GO:0003777	6.47E-11	9.98E-08
MF	ATP binding	GO:0005524	7.27E-11	1.12E-07
MF	adenyl ribonucleotide binding	GO:0032559	1.37E-10	2.11E-07
MF	protein kinase activity	GO:0004672	2.58E-10	3.98E-07
BP	regulation of Ras protein signal transduction	GO:0046578	2.77E-10	4.95E-07
CC	cytoskeleton	GO:0005856	4.14E-10	5.93E-07
CC	cytoskeletal part	GO:0044430	1.25E-09	1.79E-06
MF	adenyl nucleotide binding	GO:0030554	3.53E-09	5.44E-06
MF	purine nucleoside binding	GO:0001883	4.41E-09	6.81E-06
BP	phosphate metabolic process	GO:0006796	4.73E-09	8.44E-06
MF	nucleoside binding	GO:0001882	4.86E-09	7.49E-06
BP	phosphorus metabolic process	GO:0006793	5.47E-09	9.77E-06
CC	plasma membrane part	GO:0044459	1.38E-08	1.97E-05
BP	biological adhesion	GO:0022610	1.96E-08	3.50E-05
BP	cell adhesion	GO:0007155	1.96E-08	3.50E-05
BP	Phosphorylation	GO:0016310	1.97E-08	3.51E-05
BP	microtubule-based movement	GO:0007018	2.07E-08	3.70E-05
MF	guanyl-nucleotide exchange factor activity	GO:0005085	3.90E-08	6.02E-05
MF	GTPase activator activity	GO:0005096	9.13E-08	1.41E-04
MF	purine ribonucleotide binding	GO:0032555	5.52E-07	8.51E-04
MF	ribonucleotide binding	GO:0032553	5.52E-07	8.51E-04
MF	Rho guanyl-nucleotide exchange factor activity	GO:0005089	5.59E-07	8.62E-04
MF	protein serine/threonine kinase activity	GO:0004674	6.59E-07	1.02E-03
BP	regulation of Rho protein signal transduction	GO:0035023	1.34E-06	2.40E-03
MF	enzyme activator activity	GO:0008047	1.88E-06	2.90E-03
MF	Ras guanyl-nucleotide exchange factor activity	GO:0005088	2.02E-06	3.12E-03
CC	cell junction	GO:0030054	2.50E-06	3.58E-03
MF	purine nucleotide binding	GO:0017076	4.05E-06	6.25E-03
MF	calcium ion binding	GO:0005509	1.00E-05	1.54E-02
CC	microtubule cytoskeleton	GO:0015630	1.05E-05	1.50E-02
BP	homophilic cell adhesion	GO:0007156	1.58E-05	2.83E-02
MF	RNA-directed DNA polymerase activity	GO:0003964	2.00E-05	3.08E-02
CC	synapse	GO:0045202	2.40E-05	3.44E-02
BP	Transposition	GO:0032196	2.53E-05	4.51E-02
CC	microtubule	GO:0005874	2.57E-05	3.68E-02

Table 3.3 (continued). Enrichment of GO terms in *H. viridissima* genes (FDR ≤ 0.05).

	GO term	GO id	*P-value*	FDR
	Downregulation			
MF	structural constituent of ribosome	GO:0003735	3.18E-82	4.80E-79
CC	ribosome	GO:0005840	9.07E-75	1.27E-71
BP	translation	GO:0006412	6.20E-64	1.06E-60
MF	structural molecule activity	GO:0005198	8.46E-57	1.27E-53
CC	ribonucleoprotein complex	GO:0030529	1.24E-50	1.73E-47
CC	ribosomal subunit	GO:0033279	1.42E-41	1.98E-38
CC	large ribosomal subunit	GO:0015934	1.59E-23	2.22E-20
CC	mitochondrion	GO:0005739	2.41E-22	3.37E-19
CC	cytosolic ribosome	GO:0022626	6.00E-19	8.37E-16
BP	translational elongation	GO:0006414	1.93E-18	3.31E-15
CC	small ribosomal subunit	GO:0015935	2.99E-18	4.17E-15
BP	generation of precursor metabolites and energy	GO:0006091	4.11E-18	7.03E-15
CC	mitochondrial inner membrane	GO:0005743	2.83E-16	4.66E-13
CC	organelle inner membrane	GO:0019866	3.58E-16	4.66E-13
BP	electron transport chain	GO:0022900	7.43E-16	1.33E-12
CC	mitochondrial part	GO:0044429	7.67E-16	1.09E-12
CC	respiratory chain	GO:0070469	4.11E-15	5.73E-12
CC	cytosolic part	GO:0044445	2.05E-13	2.85E-10
CC	mitochondrial envelope	GO:0005740	4.56E-13	6.37E-10
CC	mitochondrial membrane	GO:0031966	5.87E-13	8.20E-10
BP	oxidative phosphorylation	GO:0006119	2.60E-12	4.44E-09
MF	monovalent inorganic cation transmembrane transporter activity	GO:0015077	2.69E-12	4.06E-09
MF	hydrogen ion transmembrane transporter activity	GO:0015078	1.08E-11	1.63E-08
CC	cytosolic large ribosomal subunit	GO:0022625	1.49E-10	2.09E-07
CC	cytosolic small ribosomal subunit	GO:0022627	4.92E-10	6.86E-07
CC	envelope	GO:0031975	1.06E-09	1.49E-06
CC	mitochondrial ribosome	GO:0005761	1.45E-09	2.02E-06
CC	organellar ribosome	GO:0000313	1.45E-09	2.02E-06
MF	rRNA binding	GO:0019843	1.70E-09	2.56E-06
CC	organelle envelope	GO:0031967	2.09E-09	2.92E-06
MF	inorganic cation transmembrane transporter activity	GO:0022890	8.44E-09	1.27E-05
BP	oxidation reduction	GO:0055114	8.78E-09	1.50E-05
CC	mitochondrial large ribosomal subunit	GO:0005762	4.54E-08	6.33E-05
CC	organellar large ribosomal subunit	GO:0000315	4.54E-08	6.33E-05
CC	non-membrane-bounded organelle	GO:0043228	1.15E-07	1.61E-04
CC	intracellular non-membrane-bounded organelle	GO:0043232	1.15E-07	1.61E-04
CC	mitochondrial membrane part	GO:0044455	2.33E-07	3.25E-04
BP	energy coupled proton transport, down electrochemical gradient	GO:0015985	3.15E-07	5.38E-04
BP	ATP synthesis coupled proton transport	GO:0015986	3.15E-07	5.38E-04
CC	proton-transporting ATP synthase complex	GO:0045259	4.57E-07	6.38E-04
BP	ion transmembrane transport	GO:0034220	1.30E-06	2.22E-03
CC	proton-transporting two-sector ATPase complex	GO:0016469	1.54E-06	2.15E-03
CC	lipid particle	GO:0005811	2.14E-06	2.99E-03
BP	nucleoside triphosphate biosynthetic process	GO:0009142	2.32E-06	3.96E-03
BP	spindle elongation	GO:0051231	5.18E-06	8.86E-03
BP	mitotic spindle elongation	GO:0000022	5.18E-06	8.86E-03
BP	purine ribonucleoside triphosphate biosynthetic process	GO:0009206	6.88E-06	1.18E-02
BP	purine nucleoside triphosphate biosynthetic process	GO:0009145	6.88E-06	1.18E-02
BP	ribonucleoside triphosphate biosynthetic process	GO:0009201	6.88E-06	1.18E-02
MF	ubiquinol-cytochrome-c reductase activity	GO:0008121	8.45E-06	1.27E-02
MF	oxidoreductase activity, acting on diphenols and related substances as donors, cytochrome as acceptor	GO:0016681	8.45E-06	1.27E-02
BP	mitotic spindle organization	GO:0007052	9.40E-06	1.61E-02
CC	mitochondrial proton-transporting ATP synthase complex	GO:0005753	9.97E-06	1.39E-02
BP	proton transport	GO:0015992	1.29E-05	2.20E-02
BP	hydrogen transport	GO:0006818	2.10E-05	3.60E-02

FDR, false discovery rate; MF, molecular function; CC, cellular component; BP, biological process

Table 3.4. Enrichment of GO terms in *H. vulgaris* genes (FDR ≤ 0.05).

	GO term	GO id	*P-value*	FDR
	Up-regulation			
MF	peptidase activity, acting on L-amino acid peptides	GO:0070011	1.20E-10	1.76E-07
MF	peptidase activity	GO:0008233	1.69E-10	2.49E-07
MF	endopeptidase activity	GO:0004175	1.43E-09	2.09E-06
CC	lysosome	GO:0005764	4.15E-08	5.66E-05
MF	cysteine-type endopeptidase activity	GO:0004197	4.52E-08	6.64E-05
CC	vacuole	GO:0005773	4.84E-08	6.60E-05
CC	lytic vacuole	GO:0000323	7.50E-08	1.02E-04
CC	extracellular region	GO:0005576	3.08E-07	4.19E-04
MF	aspartic-type endopeptidase activity	GO:0004190	9.09E-06	1.34E-02
MF	aspartic-type peptidase activity	GO:0070001	9.09E-06	1.34E-02
CC	cytosol	GO:0005829	3.18E-05	4.34E-02
	Down-regulation			
CC	extracellular region	GO:0005576	3.03E-18	4.32E-15
BP	cell adhesion	GO:0007155	2.90E-11	5.11E-08
BP	biological adhesion	GO:0022610	2.90E-11	5.11E-08
MF	calcium ion binding	GO:0005509	1.05E-09	1.59E-06
CC	extracellular matrix	GO:0031012	1.50E-09	2.13E-06
CC	extracellular region part	GO:0044421	3.28E-09	4.68E-06
CC	proteinaceous extracellular matrix	GO:0005578	4.62E-09	6.59E-06
MF	carbohydrate binding	GO:0030246	5.04E-09	7.63E-06
CC	extracellular matrix part	GO:0044420	1.64E-07	2.33E-04
CC	actin cytoskeleton	GO:0015629	6.72E-07	9.57E-04
MF	sugar binding	GO:0005529	8.25E-07	1.25E-03
MF	extracellular matrix structural constituent	GO:0005201	2.51E-06	3.79E-03
MF	ion binding	GO:0043167	5.24E-06	7.92E-03
BP	neurological system process	GO:0050877	9.89E-06	1.74E-02
MF	cation binding	GO:0043169	1.14E-05	1.72E-02
CC	plasma membrane	GO:0005886	2.16E-05	3.08E-02
MF	metal ion binding	GO:0046872	2.47E-05	3.73E-02

FDR, false discovery rate; MF, molecular function; CC, cellular component; BP, biological process

Table 3.5. Number of orthologous genes found between *Hydra viridissima* and *Hydra vulgaris* and their regulation in symbiotic polyps relative to aposymbiotic polyps

Total number of orthologous genes	*H. viridissima*		*H. vulgaris*	
	Regulation[*,†]	Number of genes	Regulation	Number of genes
9,934	Up	1,553	Up	65
			Non	1,124
			Down	364
	Non	6,993	Up	390
			Non	5,935
			Down	668
	Down	1,388	Up	126
			Non	1,150
			Down	112

*In all cases, differential gene expression was significant at a false discovery rate (FDR) ≤ 0.1.

†"Up," significantly upregulated in the symbiotic state; "Non," not significantly up- or downregulated in the symbiotic state; "Down," significantly downregulated in the symbiotic state

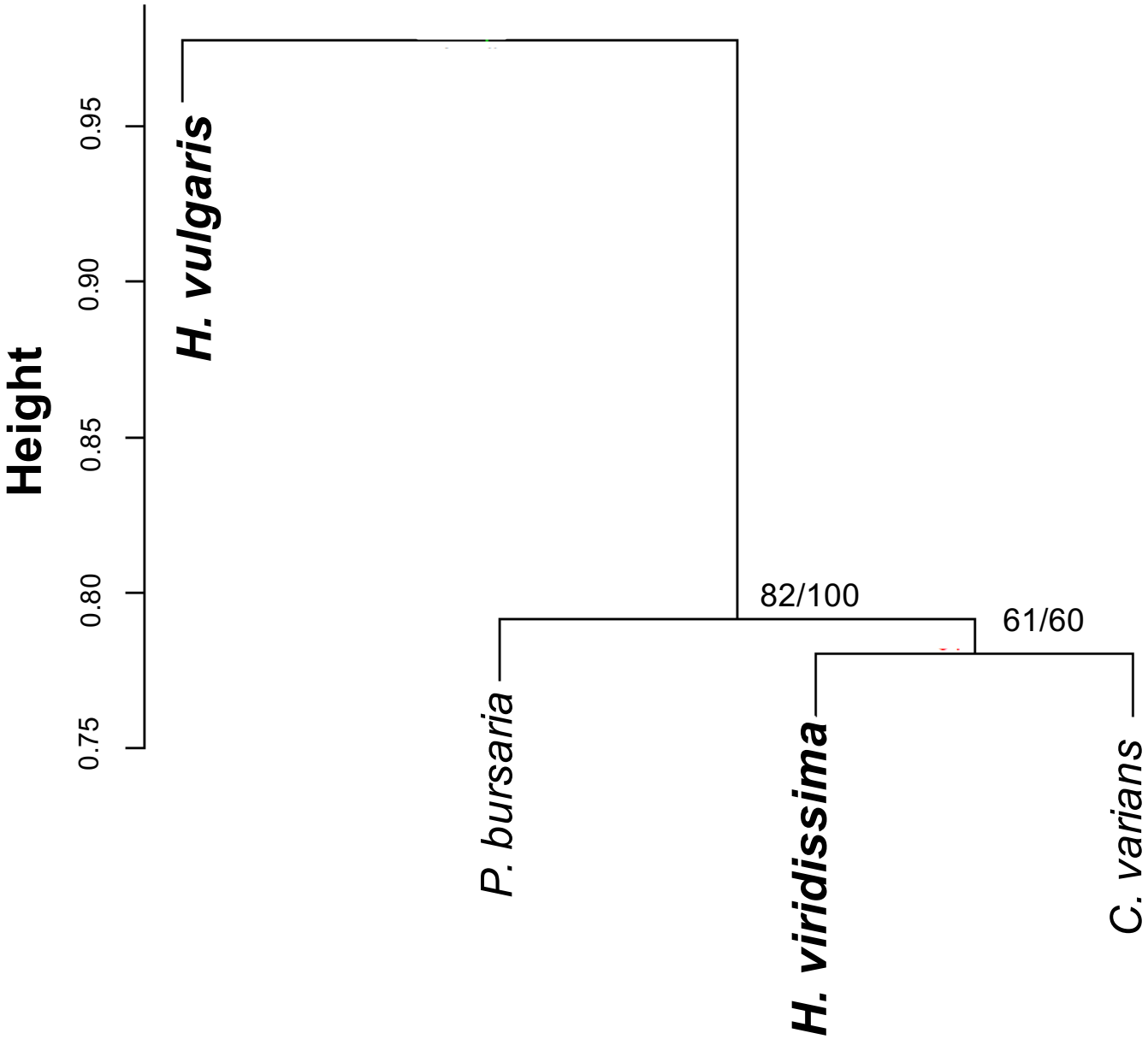

Figure 3.4. Dendrogram evidencing endosymbiotic hosts clustering. The analysis was conducted in the R package "pvclust" using the nearest neighbor as the agglomerative method and correlations as the distance measure. Numbers along branches indicate the AU (Approximately Unbiased) p-value (left) and the bootstrap probability.

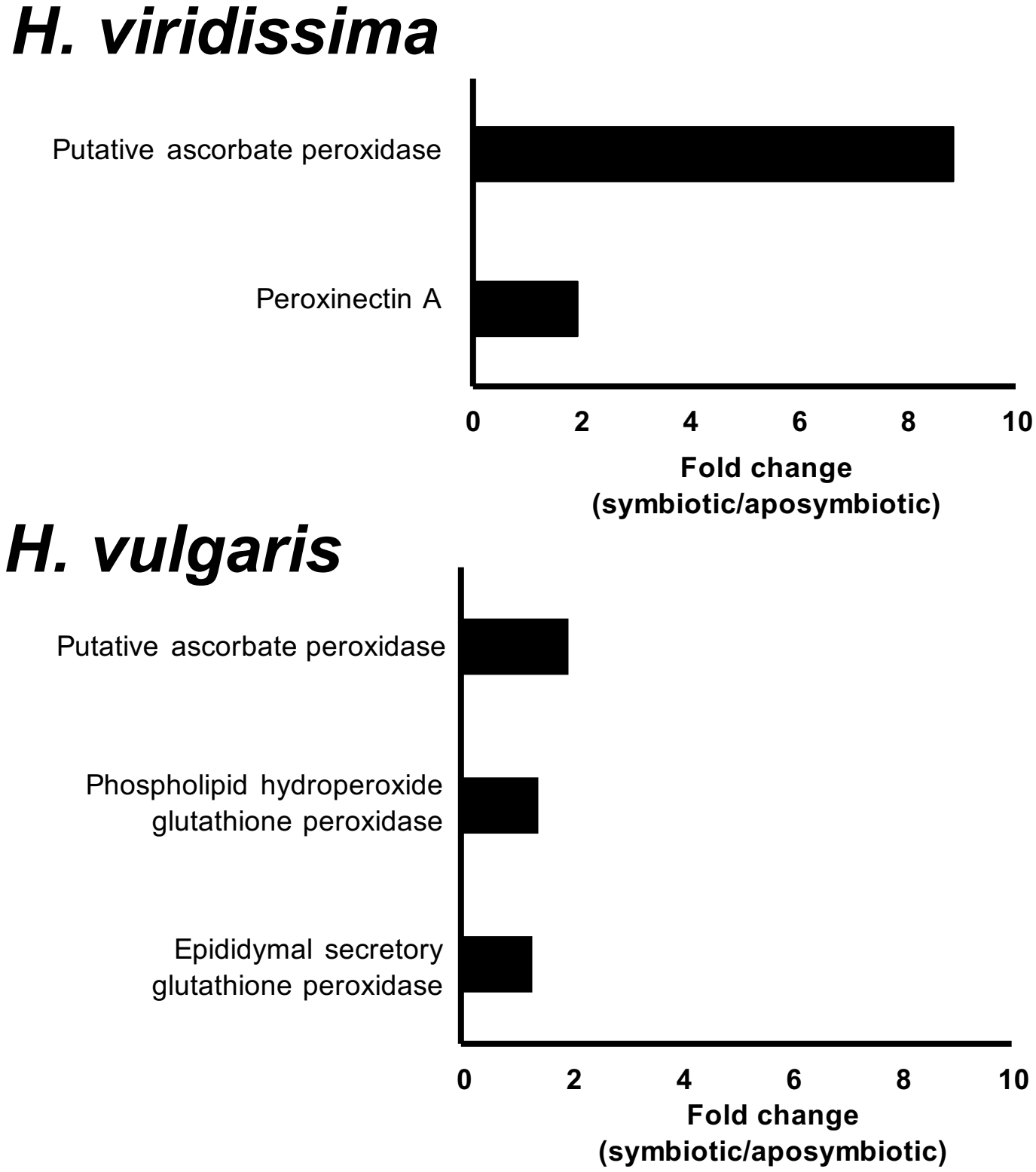

Fig. 3.5. Peroxidase activity (GO:0004601) related genes significantly upregulated in *H. vulgaris* and *H. viridissima* symbiotic states.

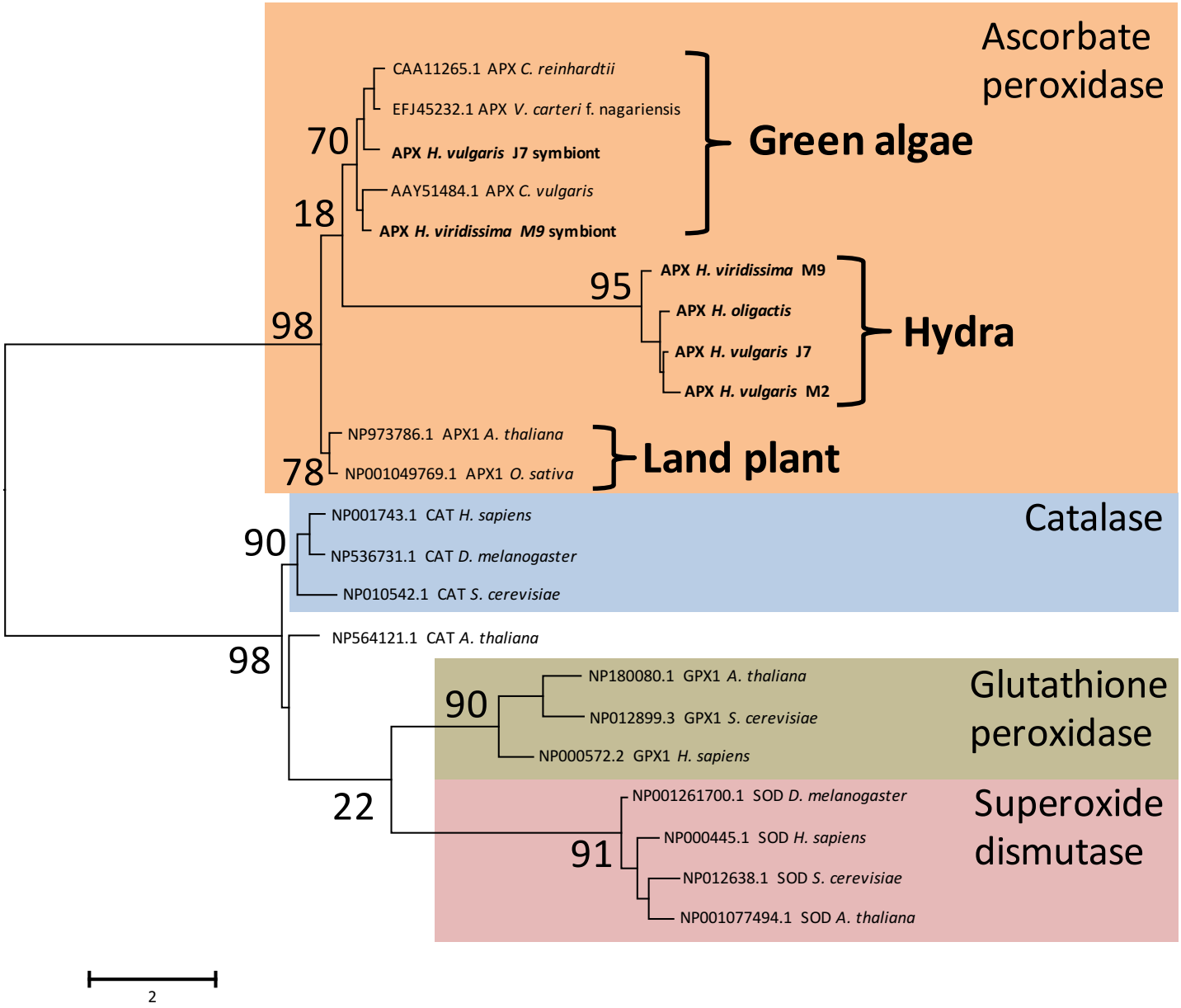

Figure 3.8. Maximum likelihood tree inferred from nucleotide sequences of the peroxidase genes. *Hydras* and symbionts of hydras were indicated as bold type.

Table 3.6. Respiratory chain contigs in *H. viridissima*.

Respiratory chain complex	Contig ID	fold change	Uniprot			NCBI-NR		
		(log2 sym/apo)	ID	Name	E-value	ID	Name	E-value
Complex I	ENTRYcomp9430_c0_seq2	-1.10	P56556	NADH dehydrogenase [ubiquinone] 1 alpha subcomplex subunit 6	2.00E-43	gi|449671533|ref|XP_002161890.2|	PREDICTED: NADH dehydrogenase ubiquinone 1 alpha subcomplex subunit 6-like	3.00E-79
	ENTRYcomp26828_c0_seq1	-1.00	Q8K3J1	NADH dehydrogenase [ubiquinone] iron-sulfur protein 8, mitochondrial	3.00E-98	gi|449665790|ref|XP_002155312.2|	PREDICTED: NADH dehydrogenase ubiquinone iron-sulfur protein 8, mitochondrial-like	3.00E-124
	ENTRYcomp8420_c0_seq1	-1.00	Q62425	NADH dehydrogenase [ubiquinone] 1 alpha subcomplex subunit 4	9.00E-17	gi|221116401|ref|XP_002164791.1|	PREDICTED: NADH dehydrogenase ubiquinone 1 alpha subcomplex subunit 4-like	6.00E-35
	ENTRYcomp38311_c0_seq1	-1.00	Q02375	NADH dehydrogenase [ubiquinone] iron-sulfur protein 4, mitochondrial	9.00E-46	gi|221120275|ref|XP_002157726.1|	PREDICTED: NADH dehydrogenase ubiquinone iron-sulfur protein 4, mitochondrial-like	8.00E-82
	ENTRYcomp26723_c0_seq1	-0.80	P52505	Acyl carrier protein, mitochondrial	1.00E-21	gi|449688855|ref|XP_002170625.2|	PREDICTED: acyl carrier protein, mitochondrial-like	9.00E-60
	ENTRYcomp8093_c0_seq1	-0.90	P42029	NADH dehydrogenase [ubiquinone] 1 alpha subcomplex subunit 8	2.00E-24	gi|221128469|ref|XP_002157365.1|	PREDICTED: NADH dehydrogenase ubiquinone 1 alpha subcomplex subunit 8-like	2.00E-76
	ENTRYcomp8078_c0_seq1	-0.70	Q9CR61	NADH dehydrogenase [ubiquinone] 1 beta subcomplex subunit 7	1.00E-17	gi|449669778|ref|XP_002159029.2|	PREDICTED: NADH dehydrogenase ubiquinone 1 beta subcomplex subunit 7-like	6.00E-53
	ENTRYcomp35898_c0_seq1	-0.70	P52503	NADH dehydrogenase [ubiquinone] iron-sulfur protein 6, mitochondrial	6.00E-31	gi|221120828|ref|XP_002155877.1|	PREDICTED: NADH dehydrogenase ubiquinone iron-sulfur protein 6, mitochondrial-like	4.00E-62
	ENTRYcomp18684_c0_seq1	-0.60	P0CB84	NADH dehydrogenase [ubiquinone] iron-sulfur protein 7, mitochondrial	9.00E-91	gi|449673668|ref|XP_002170450.2|	PREDICTED: NADH dehydrogenase ubiquinone iron-sulfur protein 7, mitochondrial-like, partial	1.00E-116
	ENTRYcomp19044_c0_seq1	-0.60	P0CB86	NADH dehydrogenase [ubiquinone] 1 beta subcomplex subunit 8, mitochondrial	6.00E-15	gi|221112960|ref|XP_002163865.1|	PREDICTED: NADH dehydrogenase ubiquinone 1 beta subcomplex subunit 8, mitochondrial-like	2.00E-98
	ENTRYcomp38022_c0_seq1	-0.60	P04394	NADH dehydrogenase [ubiquinone] flavoprotein 2, mitochondrial	0	gi|221127644|ref|XP_002160547.1|	PREDICTED: NADH dehydrogenase ubiquinone flavoprotein 2, mitochondrial-like	3.00E-158
	ENTRYcomp7722_c0_seq1	-0.40	Q0MQG8	NADH dehydrogenase [ubiquinone] iron-sulfur protein 3, mitochondrial	0	gi|449679475|ref|XP_002163056.2|	PREDICTED: NADH dehydrogenase ubiquinone iron-sulfur protein 3, mitochondrial-like	1.00E-174
	ENTRYcomp44257_c0_seq1	-0.20	Q9VA11	Probable complex I intermediate-associated protein 30, mitochondrial	1.00E-29	gi|221126604|ref|XP_002154845.1|	PREDICTED: probable complex I intermediate-associated protein 30, mitochondrial-like	1.00E-135
Complex II	ENTRYcomp7907_c0_seq1	-0.90	Q9CXV1	Succinate dehydrogenase [ubiquinone] cytochrome b small subunit, mitochondrial	2.00E-18	gi|221132919|ref|XP_002160472.1|	PREDICTED: succinate dehydrogenase ubiquinone cytochrome b small subunit, mitochondrial-like	1.00E-84
	ENTRYcomp35911_c0_seq1	-0.70	P70097	Succinate dehydrogenase cytochrome b560 subunit, mitochondrial	5.00E-35	gi|221129025|ref|XP_002164804.1|	PREDICTED: succinate dehydrogenase cytochrome b560 subunit, mitochondrial-like	7.00E-97
	ENTRYcomp10620_c0_seq1	-0.60	Q9YHT2	Succinate dehydrogenase [ubiquinone] iron-sulfur subunit, mitochondrial	0	gi|221128855|ref|XP_002165357.1|	PREDICTED: succinate dehydrogenase ubiquinone iron-sulfur subunit, mitochondrial-like	5.00E-180
Complex III	ENTRYcomp24492_c0_seq1	-2.10	Q5M9I5	Cytochrome b-c1 complex subunit 6, mitochondrial	3.00E-17	gi|169657226|gb|ACA62955.1|	mitochondrial ubiquinol-cytochrome c reductase complex 11 kDa protein	1.00E-37
	ENTRYcomp23831_c0_seq1	-0.70	Q9D855	Cytochrome b-c1 complex subunit 7	8.00E-28	gi|221129750|ref|XP_002160238.1|	PREDICTED: cytochrome b-c1 complex subunit 7-like	5.00E-60
	ENTRYcomp8116_c0_seq1	-0.60	P23004	Cytochrome b-c1 complex subunit 2, mitochondrial	1.00E-82	gi|449672203|ref|XP_004207658.1|	PREDICTED: cytochrome b-c1 complex subunit 2, mitochondrial-like	0
	ENTRYcomp134233_c0_seq1	-1.60	Q8R1I1	Cytochrome b-c1 complex subunit 9	6.00E-18	gi|675384101|gb|KFM76998.1|	Cytochrome b-c1 complex subunit 9, partial	2.00E-18
Complex IV	ENTRYcomp35554_c0_seq1	-5.00	Q6PBH5	NADH dehydrogenase [ubiquinone] 1 alpha subcomplex subunit 4	2.00E-07	gi|449688913|ref|XP_002156075.2|	PREDICTED: NADH dehydrogenase ubiquinone 1 alpha subcomplex subunit 4-like 2-like	1.00E-34
	ENTRYcomp8420_c0_seq1	-1.00	Q62425	NADH dehydrogenase [ubiquinone] 1 alpha subcomplex subunit 4	9.00E-17	gi|221116401|ref|XP_002164791.1|	PREDICTED: NADH dehydrogenase ubiquinone 1 alpha subcomplex subunit 4-like	6.00E-35
	ENTRYcomp26856_c0_seq1	-0.80	O94581	Cytochrome c oxidase subunit 6B	1.00E-25	gi|221113796|ref|XP_002165950.1|	PREDICTED: cytochrome c oxidase subunit 6B-like	1.00E-43
	ENTRYcomp7892_c0_seq1	-0.30	Q9TTT7	Cytochrome c oxidase subunit 6A1, mitochondrial	3.00E-22	gi|221102584|ref|XP_002153881.1|	PREDICTED: cytochrome c oxidase subunit 6A1, mitochondrial-like	7.00E-63
ATP synthase complex	ENTRYcomp35727_c0_seq1	-1.00	Q96253	ATP synthase subunit epsilon, mitochondrial	7.00E-11	gi|221125157|ref|XP_002159727.1|	PREDICTED: ATP synthase subunit epsilon, mitochondrial	3.00E-30
	ENTRYcomp23780_c0_seq1	-1.10	Q9CPQ8	ATP synthase subunit g, mitochondrial	8.00E-12	gi|221101640|ref|XP_002161310.1|	PREDICTED: ATP synthase subunit g, mitochondrial-like isoform 1	2.00E-67
	ENTRYcomp23074_c0_seq2	-1.00	P31399	ATP synthase subunit d, mitochondrial	8.00E-12	gi|221116237|ref|XP_002153970.1|	PREDICTED: ATP synthase subunit d, mitochondrial-like	4.00E-51
	ENTRYcomp35811_c0_seq1	-1.00	P21571	ATP synthase-coupling factor 6, mitochondrial	3.00E-10	gi|221107089|ref|XP_002156219.1|	PREDICTED: ATP synthase-coupling factor 6, mitochondrial-like	2.00E-46
	ENTRYcomp7968_c0_seq1	-0.90	Q06055	ATP synthase lipid-binding protein, mitochondrial	8.00E-34	gi|221130316|ref|XP_002162613.1|	PREDICTED: ATP synthase lipid-binding protein, mitochondrial-like	3.00E-59
	ENTRYcomp8355_c0_seq1	-0.80	Q9D3D9	ATP synthase subunit delta, mitochondrial	1.00E-35	gi|221115652|ref|XP_002167886.1|	PREDICTED: ATP synthase subunit delta, mitochondrial-like	4.00E-86
	ENTRYcomp29209_c0_seq1	-1.90	Q06055	ATP synthase lipid-binding protein, mitochondrial	2.00E-20	gi|197260868|gb|ACH56931.1|	mitochondrial F1F0-ATP synthase subunit c/ATP9/proteolipid	9.00E-27
	ENTRYcomp7878_c0_seq1	-0.60	P05631	ATP synthase subunit gamma, mitochondrial	0	gi|221122232|ref|XP_002167247.1|	PREDICTED: ATP synthase subunit gamma, mitochondrial-like	0
	ENTRYcomp35752_c0_seq1	-0.50	P13619	ATP synthase subunit b, mitochondrial	2.00E-30	gi|449668088|ref|XP_002155042.2|	PREDICTED: ATP synthase subunit b, mitochondrial-like	4.00E-127
	ENTRYcomp8533_c0_seq1	-0.20	Q5R546	ATP synthase subunit alpha, mitochondrial	0	gi|221131162|ref|XP_002163780.1|	PREDICTED: ATP synthase subunit alpha, mitochondrial	0

Blue; significantly (FDR ≤ 0.1) down-regulated in symbiotic state; light blue; down-regulated but not significant; orange, up-regultated but not significant. We selected the genes which are annotated as respiratory chain related both in Uniprot and NCBI-NR (E-value <=1e-5).

Table 3.7. Polycystin related contigs.

Contig ID	Fold change	Uniprot			NCBI-NR		
	(log2 sym/apo)	ID	Name	E-value	ID	Name	E-value
H. viridissima							
ENTRYcomp31703_c4_seq1	-0.44	O35245	PKD2 MOUSE Polycystin-2	3.00E-27	gi|449672554|ref|XP_002166908.2|	PREDICTED: polycystin-2-like	4.00E-49
ENTRYcomp31703_c2_seq1	-0.09	O35245	PKD2 MOUSE Polycystin-2	4.00E-20	gi|449672554|ref|XP_002166908.2|	PREDICTED: polycystin-2-like	3.00E-49
ENTRYcomp31703_c1_seq1	-0.73	O35245	PKD2 MOUSE Polycystin-2	1.00E-11	gi|449672554|ref|XP_002166908.2|	PREDICTED: polycystin-2-like	6.00E-18
ENTRYcomp28838_c0_seq1	0.51	Q13563	PKD2 HUMAN Polycystin-2	1.00E-09	gi|449677155|ref|XP_002160618.2|	PREDICTED: polycystic kidney disease protein 1-like 2-like	3.00E-49
ENTRYcomp32200_c0_seq10	0.25	Q4GZT3	PKD2 BOVIN Polycystin-2	0	gi|449672554|ref|XP_002166908.2|	PREDICTED: polycystin-2-like	0
ENTRYcomp35061_c0_seq2	0.5	Q4GZT3	PKD2 BOVIN Polycystin-2	1.00E-43	gi|449686628|ref|XP_002168699.2|	PREDICTED: polycystic kidney disease protein 1-like 2-like	2.00E-175
ENTRYcomp34688_c0_seq2	0.55	Q4GZT3	PKD2 BOVIN Polycystin-2	1.00E-14	gi|449686628|ref|XP_002168699.2|	PREDICTED: polycystic kidney disease protein 1-like 2-like	1.00E-60
ENTRYcomp32064_c2_seq1	-0.3	Q7TN88	PK1L2 MOUSE Polycystic kidney disease protein 1-like 2	9.00E-67	gi|449678409|ref|XP_002166423.2|	PREDICTED: polycystic kidney disease protein 1-like 2-like	0
ENTRYcomp34786_c1_seq24	1.43	Q7TN88	PK1L2 MOUSE Polycystic kidney disease protein 1-like 2	1.00E-64	gi|449685473|ref|XP_004210903.1|	PREDICTED: uncharacterized protein LOC101241810	0
ENTRYcomp35135_c0_seq20	1.54	Q7TN88	PK1L2 MOUSE Polycystic kidney disease protein 1-like 2	2.00E-59	gi|449677155|ref|XP_002160618.2|	PREDICTED: polycystic kidney disease protein 1-like 2-like	0
ENTRYcomp35374_c0_seq8	0.91	Q7TN88	PK1L2 MOUSE Polycystic kidney disease protein 1-like 2	1.00E-56	gi|449677155|ref|XP_002160618.2|	PREDICTED: polycystic kidney disease protein 1-like 2-like	0
ENTRYcomp31811_c0_seq1	1.05	Q7Z442	PK1L2 HUMAN Polycystic kidney disease protein 1-like 2	3.00E-70	gi|449663418|ref|XP_002155453.2|	PREDICTED: polycystic kidney disease protein 1-like 2-like	2.00E-165
ENTRYcomp25885_c1_seq1	1.16	Q7Z442	PK1L2 HUMAN Polycystic kidney disease protein 1-like 2	3.00E-45	gi|449680581|ref|XP_002153790.2|	PREDICTED: polycystic kidney disease protein 1-like 2-like	0
H. vulgaris							
ENTRYcomp58735_c5_seq1	-0.22	O35245	Polycystin-2	5.00E-07	gi|449674915|ref|XP_002166482.2|	PREDICTED: polycystic kidney disease protein 1-like 2-like	1.00E-130
ENTRYcomp61166_c0_seq2	-0.32	Q13563	Polycystin-2	5.00E-30	gi|449691116|ref|XP_002162996.2|	PREDICTED: polycystic kidney disease protein 1-like 2-like, partial	8.00E-155
ENTRYcomp59373_c4_seq10	-0.3	Q13563	Polycystin-2	4.00E-37	gi|449679575|ref|XP_002154072.2|	PREDICTED: polycystic kidney disease protein 1-like 2-like	6.00E-139
ENTRYcomp45557_c0_seq2	-0.13	Q13563	Polycystin-2	1.00E-18	gi|449672554|ref|XP_002166908.2|	PREDICTED: polycystin-2-like	4.00E-50
ENTRYcomp59373_c7_seq1	-0.51	Q13563	Polycystin-2	1.00E-15	gi|449686628|ref|XP_002168699.2|	PREDICTED: polycystic kidney disease protein 1-like 2-like	2.00E-70
ENTRYcomp50584_c0_seq1	-0.64	Q2EG98	Polycystic kidney disease protein 1-like 3	3.00E-11	gi|449680581|ref|XP_002153790.2|	PREDICTED: polycystic kidney disease protein 1-like 2-like	4.00E-61
ENTRYcomp56996_c2_seq1	0.9	Q2EG98	Polycystic kidney disease protein 1-like 3	5.00E-11	gi|449671291|ref|XP_004207464.1|	PREDICTED: polycystic kidney disease protein 1-like 2-like	2.00E-33
ENTRYcomp44572_c0_seq1	-0.56	Q4GZT3	Polycystin-2	7.00E-14	gi|449680581|ref|XP_002153790.2|	PREDICTED: polycystic kidney disease protein 1-like 2-like	2.00E-98
ENTRYcomp53544_c0_seq3	-0.13	Q4GZT3	Polycystin-2	0	gi|449672554|ref|XP_002166908.2|	PREDICTED: polycystin-2-like	0
ENTRYcomp61253_c1_seq16	-0.11	Q4GZT3	Polycystin-2	6.00E-40	gi|449680581|ref|XP_002153790.2|	PREDICTED: polycystic kidney disease protein 1-like 2-like	2.00E-177
ENTRYcomp58009_c1_seq1	-0.5	Q4GZT3	Polycystin-2	8.00E-27	gi|449663935|ref|XP_002163133.2|	PREDICTED: polycystic kidney disease 2-like 1 protein-like	5.00E-66
ENTRYcomp59803_c1_seq1	0	Q4GZT3	Polycystin-2	1.00E-26	gi|449680581|ref|XP_002153790.2|	PREDICTED: polycystic kidney disease protein 1-like 2-like	6.00E-123
ENTRYcomp58735_c3_seq1	-0.68	Q7TN88	Polycystic kidney disease protein 1-like 2	1.00E-30	gi|449677305|ref|XP_002169574.2|	PREDICTED: polycystic kidney disease protein 1-like 2-like	2.00E-126
ENTRYcomp56996_c0_seq1	1.23	Q7TN88	Polycystic kidney disease protein 1-like 2	3.00E-07	gi|449680581|ref|XP_002153790.2|	PREDICTED: polycystic kidney disease protein 1-like 2-like	1.00E-33
ENTRYcomp60486_c0_seq2	-0.22	Q7TN88	Polycystic kidney disease protein 1-like 2	4.00E-58	gi|449677155|ref|XP_002160618.2|	PREDICTED: polycystic kidney disease protein 1-like 2-like	0
ENTRYcomp58751_c3_seq1	-0.46	Q7TN88	Polycystic kidney disease protein 1-like 2	1.00E-24	gi|449691715|ref|XP_004212772.1|	PREDICTED: polycystic kidney disease protein 1-like 2-like, partial	1.00E-71
ENTRYcomp59373_c1_seq2	-0.35	Q7TN88	Polycystic kidney disease protein 1-like 2	8.00E-23	gi|449671291|ref|XP_004207464.1|	PREDICTED: polycystic kidney disease protein 1-like 2-like	6.00E-142
ENTRYcomp58735_c2_seq1	-0.2	Q7TN88	Polycystic kidney disease protein 1-like 2	4.00E-07	gi|449674915|ref|XP_002166482.2|	PREDICTED: polycystic kidney disease protein 1-like 2-like	6.00E-93
ENTRYcomp61253_c2_seq1	0.25	Q7TN88	Polycystic kidney disease protein 1-like 2	8.00E-06	gi|449671291|ref|XP_004207464.1|	PREDICTED: polycystic kidney disease protein 1-like 2-like	6.00E-44
ENTRYcomp62057_c0_seq1	-0.48	Q7Z442	Polycystic kidney disease protein 1-like 2	2.00E-60	gi|449685473|ref|XP_004210903.1|	PREDICTED: uncharacterized protein LOC101241810	0
ENTRYcomp61735_c0_seq4	-0.24	Q7Z442	Polycystic kidney disease protein 1-like 2	8.00E-77	gi|449663418|ref|XP_002155453.2|	PREDICTED: polycystic kidney disease protein 1-like 2-like	0
ENTRYcomp60748_c2_seq1	-0.46	Q7Z442	Polycystic kidney disease protein 1-like 2	3.00E-54	gi|449678409|ref|XP_002166423.2|	PREDICTED: polycystic kidney disease protein 1-like 2-like	0
ENTRYcomp61253_c0_seq1	-0.32	Q7Z442	Polycystic kidney disease protein 1-like 2	3.00E-11	gi|449672980|ref|XP_002158569.2|	PREDICTED: polycystic kidney disease protein 1-like 2-like, partial	2.00E-151
ENTRYcomp59373_c5_seq1	0.02	Q7Z443	Polycystic kidney disease protein 1-like 3	2.00E-18	gi|449671291|ref|XP_004207464.1|	PREDICTED: polycystic kidney disease protein 1-like 2-like	3.00E-70
ENTRYcomp58009_c0_seq2	-0.55	Q9P0L9	Polycystic kidney disease 2-like 1 protein	1.00E-161	gi|449663933|ref|XP_002159199.2|	PREDICTED: polycystin-2-like	0
ENTRYcomp58009_c2_seq1	-0.64	Q9P0L9	Polycystic kidney disease 2-like 1 protein	8.00E-23	gi|449663935|ref|XP_002163133.2|	PREDICTED: polycystic kidney disease 2-like 1 protein-like	2.00E-39
ENTRYcomp45557_c3_seq1	0.01	Q9P0L9	Polycystic kidney disease 2-like 1 protein	1.00E-80	gi|449663931|ref|XP_004205835.1|	PREDICTED: polycystic kidney disease 2-like 1 protein-like	1.00E-178
ENTRYcomp45557_c1_seq1	0.04	Q9P0L9	Polycystic kidney disease 2-like 1 protein	5.00E-71	gi|449663931|ref|XP_004205835.1|	PREDICTED: polycystic kidney disease 2-like 1 protein-like	5.00E-131
ENTRYcomp45557_c2_seq1	-0.35	Q9P0L9	Polycystic kidney disease 2-like 1 protein	3.00E-16	gi|449672554|ref|XP_002166908.2|	PREDICTED: polycystin-2-like	5.00E-24
ENTRYcomp59373_c2_seq1	-0.31	Q9P0L9	Polycystic kidney disease 2-like 1 protein	8.00E-07	gi|449680581|ref|XP_002153790.2|	PREDICTED: polycystic kidney disease protein 1-like 2-like	2.00E-39
ENTRYcomp59803_c0_seq1	-0.04	Q9U1S7	Polycystin-2	1.00E-07	gi|449674915|ref|XP_002166482.2|	PREDICTED: polycystic kidney disease protein 1-like 2-like	8.00E-39

Blue; significantly (FDR ≤ 0.1) down-regulated in symbiotic state; light blue; down-regulated but not significant; orange, up-regulated but not significant. We selected the genes which are annotated as polycystin related both in uniprot and NCBI-NR with E-value <=1e-5

Table 3.8. Cadherin related contigs.

Contig ID	fold change (log2 sym/apo)	Uniprot			NCBI-NR		
		ID	Name	E-value	ID	Name	E-value
H. viridissima							
ENTRYcomp33485_c0_seq1	1.30	O15943	Neural-cadherin	0	gi|449691455|ref|XP_004212679.1|	PREDICTED: fat-like cadherin-related tumor suppressor homolog, partial	0
ENTRYcomp23103_c1_seq1	1.40	Q9HCU4	Cadherin EGF LAG seven-pass G-type receptor 2	0	gi|386118337|gb|AFI99116.1|	seven transmembrane protocadherin flamingo	0
ENTRYcomp31845_c0_seq2	1.30	Q9HCU4	Cadherin EGF LAG seven-pass G-type receptor 2	3.00E-63	gi|449667390|ref|XP_004206556.1|	PREDICTED: protocadherin Fat 1-like	1.00E-96
ENTRYcomp33798_c0_seq1	0.40	Q9HCU4	Cadherin EGF LAG seven-pass G-type receptor 2	4.00E-69	gi|449671473|ref|XP_002161598.2|	PREDICTED: protocadherin Fat 3-like	0
ENTRYcomp34179_c0_seq1	0.40	Q14517	Protocadherin Fat 1	0	gi|449676476|ref|XP_002167194.2|	PREDICTED: protocadherin Fat 3-like	0
ENTRYcomp32654_c0_seq1	-0.10	Q9VW71	Fat-like cadherin-related tumor suppressor homolog	3.00E-39	gi|449669313|ref|XP_004206990.1|	PREDICTED: cadherin-related tumor suppressor-like	0
ENTRYcomp20341_c0_seq1	0.20	Q6V0I7	Protocadherin Fat 4	0	gi|449679036|ref|XP_002161856.2|	PREDICTED: protocadherin Fat 4-like	0
ENTRYcomp34652_c0_seq3	1.00	Q2PZL6	Protocadherin Fat 4	2.00E-43	gi|449672938|ref|XP_002154309.2|	PREDICTED: protocadherin Fat 4-like, partial	0
ENTRYcomp34762_c0_seq1	0.50	Q2PZL6	Protocadherin Fat 4	0	gi|449691444|ref|XP_004212674.1|	PREDICTED: protocadherin Fat 4-like, partial	0
ENTRYcomp32926_c4_seq1	0.80	Q6V1P9	Protocadherin-23	8.00E-140	gi|386118331|gb|AFI99113.1|	dachsous protocadherin	0
H. vulgaris							
ENTRYcomp51174_c0_seq1	-0.80	P33450	Cadherin-related tumor suppressor	0	gi|449691444|ref|XP_004212674.1|	PREDICTED: protocadherin Fat 4-like, partial	0
ENTRYcomp59247_c1_seq2	0.00	Q2PZL6	Protocadherin Fat 4	5.00E-160	gi|449679036|ref|XP_002161856.2|	PREDICTED: protocadherin Fat 4-like	0
ENTRYcomp61537_c2_seq3	0.20	Q2PZL6	Protocadherin Fat 4	1.00E-76	gi|449672938|ref|XP_002154309.2|	PREDICTED: protocadherin Fat 4-like, partial	0
ENTRYcomp61674_c0_seq1	-0.30	Q8BNA6	Protocadherin Fat 3	0	gi|449676476|ref|XP_002167194.2|	PREDICTED: protocadherin Fat 3-like	0
ENTRYcomp63679_c0_seq1	-0.40	Q8BNA6	Protocadherin Fat 3	5.00E-59	gi|449671473|ref|XP_002161598.2|	PREDICTED: protocadherin Fat 3-like	0
ENTRYcomp45180_c0_seq1	-0.60	Q8R508	Protocadherin Fat 3	0	gi|449677345|ref|XP_002162352.2|	PREDICTED: protocadherin Fat 1-like	0
ENTRYcomp56690_c0_seq1	-0.40	Q8R508	Protocadherin Fat 3	5.00E-16	gi|449667390|ref|XP_004206556.1|	PREDICTED: protocadherin Fat 1-like	0
ENTRYcomp44500_c0_seq1	-0.60	Q9HCU4	Cadherin EGF LAG seven-pass G-type receptor 2	6.00E-51	gi|449663411|ref|XP_004205742.1|	PREDICTED: protocadherin Fat 3-like	0
ENTRYcomp64062_c0_seq1	-0.40	Q9HCU4	Cadherin EGF LAG seven-pass G-type receptor 2	5.00E-39	gi|449663411|ref|XP_004205742.1|	PREDICTED: protocadherin Fat 3-like	2.00E-83
ENTRYcomp62511_c0_seq1	-0.50	Q9HCU4	Cadherin EGF LAG seven-pass G-type receptor 2	4.00E-10	gi|449667390|ref|XP_004206556.1|	PREDICTED: protocadherin Fat 1-like	3.00E-132
ENTRYcomp59247_c0_seq1	0.00	Q9HCU4	Cadherin EGF LAG seven-pass G-type receptor 2	2.00E-87	gi|449679036|ref|XP_002161856.2|	PREDICTED: protocadherin Fat 4-like	0
ENTRYcomp53617_c0_seq1	0.20	Q9NYQ6	Cadherin EGF LAG seven-pass G-type receptor 1	2.00E-12	gi|449683117|ref|XP_002170720.2|	PREDICTED: cadherin EGF LAG seven-pass G-type receptor 1-like	0
ENTRYcomp55131_c0_seq1	-0.10	Q9VW71	Fat-like cadherin-related tumor suppressor homolog	5.00E-44	gi|449669313|ref|XP_004206990.1|	PREDICTED: cadherin-related tumor suppressor-like	0

Blue; significantly (FDR ≤ 0.1) down-regulated in symbiotic state; light blue; down-regulated but not significant; orange, up-regultated but not significant; red, significantly (FDR ≤ 0.1) up-regulated in symbiotic state. We selected the genes which are annotated as cadherin related both in uniprot and NCBI-NR with E-value <=1e-5

Table 3.9. Caspase 3 and metalloproteinase related contigs.

Contig ID	Fold change (log2 sym/apo)	Uniprot			NCBI-NR		
		ID	Name	E-value	ID	Name	E-value
				H. viridissima			
Caspase							
ENTRYcomp33819_c1_seq2	0.87	Q95ND5	Caspase-3	#######	gi|567757471|ref|NP_001274721.1|	caspase-3-like__Hydra_vulgaris	3.00E-109
ENTRYcomp29937_c0_seq1	-0.06	Q8MKI5	Caspase-3	#######	gi|449679433|ref|XP_002159783.2|	PREDICTED:_caspase-3-like__Hydra_vulgaris	6.00E-150
ENTRYcomp32332_c0_seq1	0.29	Q5IS99	Caspase-3	#######	gi|449672311|ref|XP_002165630.2|	PREDICTED:_caspase-3-like__Hydra_vulgaris	3.00E-177
Metalloproteinase							
ENTRYcomp32506_c0_seq9	1.17	P51512	Matrix metalloproteinase-16	#######	gi|449664771|ref|XP_002168334.2|	PREDICTED:_matrix_metalloproteinase-19-like__Hydra_vulgaris	4.00E-77
ENTRYcomp17324_c0_seq1	-0.56	O13065	Matrix metalloproteinase-18	#######	gi|449671383|ref|XP_004207480.1|	PREDICTED:_matrix_metalloproteinase-24-like__Hydra_vulgaris	0
ENTRYcomp20374_c0_seq1	-1.01	Q99542	Matrix metalloproteinase-19	#######	gi|5616492|gb|AAD45804.1|AF162688_1	matrix_metalloproteinase__Hydra_vulgaris	7.00E-47
ENTRYcomp36671_c0_seq1	-0.68	Q9NPA2	Matrix metalloproteinase-25	#######	gi|5616492|gb|AAD45804.1|AF162688_1	matrix_metalloproteinase__Hydra_vulgaris	0
ENTRYcomp7185_c0_seq1	-0.49	Q9NPA2	Matrix metalloproteinase-25	#######	gi|449686980|ref|XP_004211314.1|	PREDICTED:_matrix_metalloproteinase-24-like__Hydra_vulgaris	2.00E-108
				H. vulgaris			
Caspase							
ENTRYcomp49733_c0_seq1	0.07	Q60431	Caspase-3	#######	gi|449679433|ref|XP_002159783.2|	PREDICTED:_caspase-3-like__Hydra_vulgaris	0
ENTRYcomp67559_c0_seq1	-0.34	P70677	Caspase-3	#######	gi|567757471|ref|NP_001274721.1|	caspase-3-like__Hydra_vulgaris	0
ENTRYcomp23875_c0_seq1	-0.30	Q8MJC3	Caspase-3	#######	gi|449687876|ref|XP_002169866.2|	PREDICTED:_caspase-3-like__Hydra_vulgaris	4.00E-55
ENTRYcomp36793_c0_seq1	0.33	Q5IS99	Caspase-3	#######	gi|221118431|ref|XP_002158718.1|	PREDICTED:_caspase-3-like__Hydra_vulgaris	0
ENTRYcomp58730_c0_seq1	0.31	Q5IS99	Caspase-3	#######	gi|449687876|ref|XP_002169866.2|	PREDICTED:_caspase-3-like__Hydra_vulgaris	0
ENTRYcomp64314_c0_seq1	-0.29	Q5IS99	Caspase-3	#######	gi|449672311|ref|XP_002165630.2|	PREDICTED:_caspase-3-like__Hydra_vulgaris	0
Metalloproteinase							
ENTRYcomp60007_c0_seq1	0.47	P51512	Matrix metalloproteinase-16	#######	gi|391330624|ref|XP_003739756.1|	PREDICTED:_matrix_metalloproteinase-16-like__Metaseiulus_occidentalis	3.00E-59
ENTRYcomp48054_c0_seq1	-0.45	Q99542	Matrix metalloproteinase-19	#######	gi|221115658|ref|XP_002168462.1|	PREDICTED:_matrix_metalloproteinase-25-like__Hydra_vulgaris	1.00E-176
ENTRYcomp49371_c0_seq3	-0.18	Q9Y5R2	Matrix metalloproteinase-24	#######	gi|449692030|ref|XP_002155089.2|	PREDICTED:_matrix_metalloproteinase-24-like,_partial__Hydra_vulgaris	0
ENTRYcomp54811_c0_seq1	0.39	Q9R0S2	Matrix metalloproteinase-24	#######	gi|449664773|ref|XP_004205997.1|	PREDICTED:_matrix_metalloproteinase-24-like__Hydra_vulgaris	4.00E-176
ENTRYcomp62865_c0_seq1	0.67	Q99PW6	Matrix metalloproteinase-24	#######	gi|5616492|gb|AAD45804.1|AF162688_1	matrix_metalloproteinase__Hydra_vulgaris	0
ENTRYcomp23775_c0_seq1	-0.15	Q9H306	Matrix metalloproteinase-27	#######	gi|449682739|ref|XP_002164557.2|	PREDICTED:_matrix_metalloproteinase-27-like__Hydra_vulgaris	0

Blue; significantly (FDR ≤ 0.1) down-regulated in symbiotic state; Red, significantly (FDR ≤ 0.1) up-regulated in symbiotic state. We selected the genes which are annotated as polycystin related both in uniprot and NCBI-NR with E-value <=1e-5

Table 3.10. Bicarbonate related contigs

Contig ID	Fold change (log2 sym/ap	Uniprot			NCBI-NR		
		ID	Name	E-value	ID	Name	E-value
				H. viridissima			
ENTRYcomp315 93_c0_seq1	0.75	O88343	Electrogenic sodium bicarbonate cotransporter 1	######	gi|449677655|ref|X P_002158749.2|	PREDICTED: electrogenic sodium bicarbonate cotransporter 1-like	0
ENTRYcomp205 39_c0_seq1	0.65	P43166	Carbonic anhydrase 7	######	gi|449680380|ref|X P_002162005.2|	PREDICTED: carbonic anhydrase 13-like, partial	######
				H. vulgaris			
ENTRYcomp575 79_c1_seq2	-1.18	P23280	Carbonic anhydrase 6	######	gi|449688943|ref|X P_002167592.2|	PREDICTED: carbonic anhydrase-like, partial	######
ENTRYcomp597 07_c1_seq1	0.22	Q02094	Ammonium transporter Rh type A	######	gi|221114395|ref|X P_002166094.1|	PREDICTED: ammonium transporter Rh type C-like 2-like	######
ENTRYcomp554 04_c0_seq1	0.41	P43166	Carbonic anhydrase 7	######	gi|449676974|ref|X P_002168775.2|	PREDICTED: putative carbonic anhydrase 5-like	######
ENTRYcomp598 91_c0_seq2	0.01	Q02094	Ammonium transporter Rh type A	0	gi|449669287|ref|X P_002167946.2|	PREDICTED: ammonium transporter Rh type A-like	0

Blue; significantly (FDR ≤ 0.1) down-regulated in symbiotic state; light blue; down-regulated but not significant; orange, up-regultated but not significant; red, significantly (FDR ≤ 0.1) up-regulated in symbiotic state. We selected the genes which are annotated as bicarbonate transport

Table 3.11. Cathepsin related contigs

Contig ID	Fold change (log2 sym/apo)	Uniprot			NCBI-NR		
		ID	Name	E-value	ID	Name	E-value
				H. viridissima			
ENTRYcomp7886_c0_seq1	-0.37	Q95029	Cathepsin L	3.00E-131	gi|449673497|ref|XP_002169904.2|	PREDICTED: cathepsin L-like	0
ENTRYcomp7953_c0_seq1	-0.22	Q26636	Cathepsin L	8.00E-127	gi|221090861|ref|XP_002167224.1|	PREDICTED: cathepsin L-like	0
ENTRYcomp23095_c0_seq1	0.14	P07858	Cathepsin B	5.00E-127	gi|449667614|ref|XP_002166962.2|	PREDICTED: cathepsin B-like	0
ENTRYcomp28005_c1_seq1	-0.12	Q26636	Cathepsin L	1.00E-118	gi|449681105|ref|XP_002158608.2|	PREDICTED: cathepsin L-like	0
ENTRYcomp19450_c0_seq1	-0.14	Q9R1T3	Cathepsin Z	1.00E-128	gi|449671115|ref|XP_002154535.2|	PREDICTED: cathepsin Z-like	0
ENTRYcomp23151_c0_seq1	-0.12	P00787	Cathepsin B	1.00E-120	gi|221107055|ref|XP_002166984.1|	PREDICTED: cathepsin B-like	0
ENTRYcomp29001_c0_seq1	-0.04	Q9R1T3	Cathepsin Z	1.00E-124	gi|449671113|ref|XP_002154692.2|	PREDICTED: cathepsin Z-like	0
ENTRYcomp19260_c0_seq1	-0.03	P43234	Cathepsin O	5.00E-61	gi|449668436|ref|XP_002162416.2|	PREDICTED: cathepsin O-like	6.00E-170
				H. vulgaris			
ENTRYcomp57356_c0_seq1	0.81	Q95029	Cathepsin L	5.00E-134	gi|221090861|ref|XP_002167224.1|	PREDICTED: cathepsin L-like	0
ENTRYcomp62387_c0_seq1	0.78	P07688	Cathepsin B	5.00E-116	gi|221107055|ref|XP_002166984.1|	PREDICTED: cathepsin B-like	0
ENTRYcomp62470_c0_seq1	0.65	Q9R1T3	Cathepsin Z	8.00E-126	gi|449671115|ref|XP_002154535.2|	PREDICTED: cathepsin Z-like	0
ENTRYcomp23657_c0_seq1	0.56	Q26636	Cathepsin L	5.00E-115	gi|449681105|ref|XP_002158608.2|	PREDICTED: cathepsin L-like	0
ENTRYcomp62403_c0_seq1	0.57	Q9R1T3	Cathepsin Z	2.00E-124	gi|449671113|ref|XP_002154692.2|	PREDICTED: cathepsin Z-like	0
ENTRYcomp23363_c0_seq1	1.39	P43509	Cathepsin B-like cysteine proteinase	2.00E-88	gi|585112317|gb|EWM29737.1|	cathepsin b	1.00E-110
ENTRYcomp62116_c0_seq1	0.40	Q95029	Cathepsin L	4.00E-133	gi|449673497|ref|XP_002169904.2|	PREDICTED: cathepsin L-like	0
ENTRYcomp49428_c0_seq1	0.39	P00787	Cathepsin B	6.00E-126	gi|449667614|ref|XP_002166962.2|	PREDICTED: cathepsin B-like	0
ENTRYcomp57444_c0_seq1	0.36	Q26636	Cathepsin L	8.00E-106	gi|221117518|ref|XP_002157675.1|	PREDICTED: cathepsin L-like	0
ENTRYcomp23300_c0_seq1	0.24	P43234	Cathepsin O	3.00E-62	gi|449668436|ref|XP_002162416.2|	PREDICTED: cathepsin O-like	0
ENTRYcomp101169_c0_seq1	0.82	P05689	Cathepsin Z	6.00E-51	gi|585107161|gb|EWM25400.1|	cathepsin z	2.00E-90
ENTRYcomp56144_c1_seq1	0.33	Q26636	Cathepsin L	1.00E-47	gi|449679414|ref|XP_002161570.2|	PREDICTED: cathepsin L-like	1.00E-93

Blue; significantly (FDR≤0.1) down-regulated in symbiotic state; light blue; down-regulated but not significant; orange, up-regulated but not significant; red, significantly (FDR≤0.1) up-regulated in symbiotic state. We selected the genes which are annotated as cathepsin t related both in uniprot and NCBI-NR with E-value <=1e-5

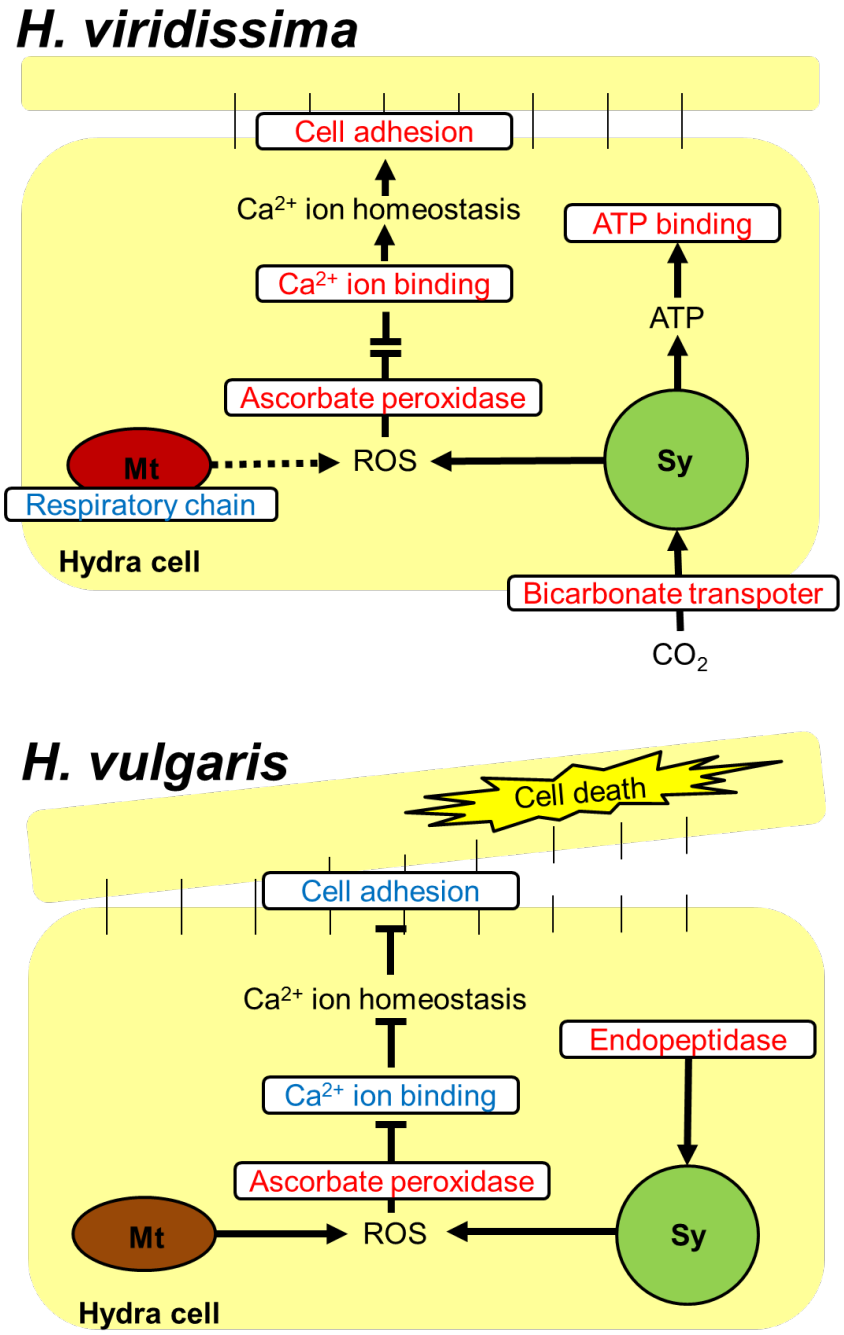

Figure 3.9. A proposed model of the endosymbiotic interaction between the two *Hydra* species and algae. The endosymbiotic hydra is exposed to reactive oxygen species (ROS) extracted from both mitochondria (Mt) and the symbiont (Sy). ROS cause oxidative stress in the hydra cell, and both species respond to the stress by up-regulating ascorbate peroxidase. However, *H. vulgaris* still suffers the oxidative stress, and the stress induces disruption of the Ca_2^+ homeostasis, which contributes to the cell death. In addition, *H. vulgaris* tries to remove the algae by up-regulation of the endopeptidase genes. On the other hand, *H. viridissima* represses ROS by down-regulation of respiratory chain genes of mitochondria, and the disruption of Ca_2^+ homeostasis is repressed by the up-regulation of Ca_2^+ binding and cell adhesion genes. *H. viridissima* supplies CO_2 to the algae by up-regulation of bicarbonate transporter and receive ATP from the symbiont. The Genes/systems are shown as up-regulated (red), down-regulated (blue).

4 Chapter 4

General discussion

In my doctoral thesis, I have aimed to provide an insight into the endosymbiosis between hydra and green algae in terms of both evolutionary (Chapter 2) and physiological (Chapter 3) aspects. As a result of investigating the endosymbiosis of *H. vulgaris* and *H. viridissima* groups, I have reached the following conclusions:

1) Many *H. vulgaris* group strains survive without harboring the algae, even though they have the potential to harbor them.

2) The evolution of endosymbiosis in *H. vulgaris* group is more recent than those in other cnidarian cases.

3) The interaction with algae is extensively different between *H. vulgaris* and *H. viridissima* groups; the endosymbiosis is advantageous for *H. viridissima* group on starvation tolerance and growth, whereas it is not advantageous or may even be disadvantageous to the survival of *H. vulgaris* group.

4) The differential gene expression pattern of *H. viridissima* group is more similar to those of other endosymbiotic hosts, such as *Paramecium* and *Ciona* than that of *H. vulgaris* group.

I discuss about my studies based on these conclusions. In the culture collection of hydra species, all six of the *H. viridissima* group strains harbor the algae. On the other hand, only two among twenty-five *H. vulgaris* group strains harbor the algae. However, it was unknown whether other twenty-three aposymbiotic *H. vulgaris* group strains have the potential to harbor the algae. In Chapter 2, I examined the endosymbiotic potential of the aposymbiotic strains by artificially introducing the endosymbiotic algae and found that 12 among 23 aposymbiotic strains are able to harbor them. Based on the result, I conclude that the strategies for the endosymbiosis are different between both hydra species. *H. viridissima* group have the endosymbiotic potential, and all of them actually harbor the algae. On the other hand, many *H. vulgaris* group strains have the

potential to harbor the algae, but most of them survive without harboring the algae (**conclusion No. 1**).

In addition to my experiment of artificial introduction of the endosymbiotic algae into non-symbiotic *H. vulgaris* group strains as well as my phylogenetic analysis, I showed that the evolution of the endosymbiotic potential occurred only once during the radiation of the *H. vulgaris* group strains, which is estimated to be 3.1 - 11 million years ago. On the other hand, a previous study suggested that the endosymbiosis in *H. viridissima* group took place before radiation of the *H. viridissima* group strains, which is estimated to have occurred 27 - 36 million years ago (Martínez et al., 2010). In another study, the fossil record suggests that the evolution of the coral zooxanthellae symbiosis has occurred in the Triassic period (201 - 252 million years ago, Stanley and Swart, 2014). Taking into account these results, the evolution of the endosymbiosis in *H. vulgaris* group was more recent than that of other cnidarian species (**conclusion No. 2**).

In the experiment measuring growth and tolerance for starvation, symbiotic *H. viridissima* group shows a higher growth rate and greater tolerance for starvation than aposymbiotic *H. viridissima* group. On the other hand, the growth of the symbiotic *H. vulgaris* group were almost identical to the aposymbiotic *H. vulgaris* group, and the tolerance for starvation in the symbiotic *H. vulgaris* group was lower than that in aposymbiotic one. Moreover, the change of the gene expression pattern by the endosymbiosis was also extensively different between *H. vulgaris* and *H. viridissima* groups. *H. viridissima* group have the molecular mechanisms to repress oxidative stress and suppression apoptosis. On the other hand, *H. vulgaris* group does not have such systems to repress the oxidative stress caused by endosymbiotic algae and mitochondria, and genes that are related to calcium ion binding and cell adhesion were down-regulated by the endosymbiosis, which implies that intracellular calcium ion homeostasis was disrupted by the oxidative stress and induced apoptosis. Taking these facts into account, the

endosymbiosis was advantageous for the survival of *H. viridissima*, group and *H. viridissima* group has established the molecular mechanisms for forming stable endosymbiotic relationships with the algae. Consequently, the endosymbiosis was not advantageous for survival of *H. vulgaris* group, and *H. vulgaris* group might try to remove the endosymbiotic algae from the hydra's cell (**conclusion No. 3**).

Moreover, I compared the pattern of the gene expression changes among the hydras which were used in my study, and *Paramecium bursaria* and *Ciona varians*. *P. bursaria* harbors several dozens of green algae, which are identified as genus *Chlorella*, and *C. varians* harbors dinoflagellate called *Symbiodinium.* Both species are also able to survive without endosymbiosis (aposymbiotic), and the differential gene expression analysis of those species were conducted in the previous studies (Kodama et al., 2014; Riesgo et al., 2014). I conducted the differential gene expression analysis of these species, using the same methods as were used with the hydras, and compared the differential gene expression pattern among these species. The results showed that the differential gene expression pattern in *H. viridissima* group was more similar to *P. bursaria* and *C. varians* than *H. vulgaris* group (Figure 3.4). I therefore concluded that the molecular mechanisms of *H. viridissima* group are more similar to the other existing endosymbiotic organisms than that of *H. vulgaris* group (**conclusion No. 4**).

Here, the following questions are suggested by this research: It is possible for the endosymbiotic relationships between *H. vulgaris* group and the algae really proceed to a stable endosymbiotic relationship, such as the endosymbiosis between *H. viridissima* group and the algae? It is also possible that the endosymbiotic relationships between the two hydra species were totally distinct phenomena, and therefore, the endosymbiotic relationship with *H. vulgaris* group and the algae might never become stable such as *H. viridissima* group. Evolutionary theory predicts that the symbiotic relationships should be unstable owing to conflict of interest between the host and symbiont (Toft and Andersson, 2010). For this reason, many authors have

suggested that mutualism should eventually be evolved from parasitism (Ewald, 1987; Ishikawa, 1988). Recent genomic studies also support the idea that mutualism could evolve from parasitism (Sachs et al., 2011; Toft and Andersson, 2010). In order to reduce the burden on the host, Eward (1987) suggests that vertical transmission, defined as the direct transfer of a symbiont from a parent host to its offspring is a key factor. In *Hydra*, the transmission from a parent to its offspring easily occurs than sexual reproduction, because a parent produces its offspring mainly by budding (Figure 1.4). Moreover, growth of the symbiotic *H. vulgaris* group is equal to aposymbiotic *H. vulgaris* group when feeding three times per a week (Figure 3.1), suggesting that long-term endosymbiotic relationships can manage to be kept through generations. As a long-term endosymbiotic relationship has been established between *H. vulgaris* group and the algae, selection for functions that benefit the host could lead to mutualism (Toft and Andersson, 2010).

From my studies of the endosymbiosis of hydra, I showed that both *H. viridissima* and *H. vulgaris* groups show endosymbiosis with green algae, but the effects of the endosymbiosis at the phenotypic levels and molecular levels, and the strategy against the endosymbiosis are extensively different between the two species. These differences are due to the time after gaining the endosymbiotic potential. The evolution of the endosymbiosis in *H. vulgaris* group is more recent than in *H. viridissima* group and other cnidarian species. Thus, I suggest that the evolutionary stages of the endosymbiosis for two hydra species (Figure 4.1): The relationship between *H. vulgaris* group and the algae was immature; on the other hand, the relationship between *H. viridissima* group and the algae has already been established. As endosymbiosis is one of the major driving forces in evolution of life, it is quite important to understand how the stable endosymbiotic relationships between host and symbiont are established. As hydra is one of the model organisms, *H. vulgaris* group, which shows immature endosymbiosis, and *H. viridissima* group, which shows matured endosymbiosis, are among the best organisms to

elucidate the evolution of the endosymbiosis, both in terms of how endosymbiotic potential is acquired to how stable endosymbiotic relationships are formed.

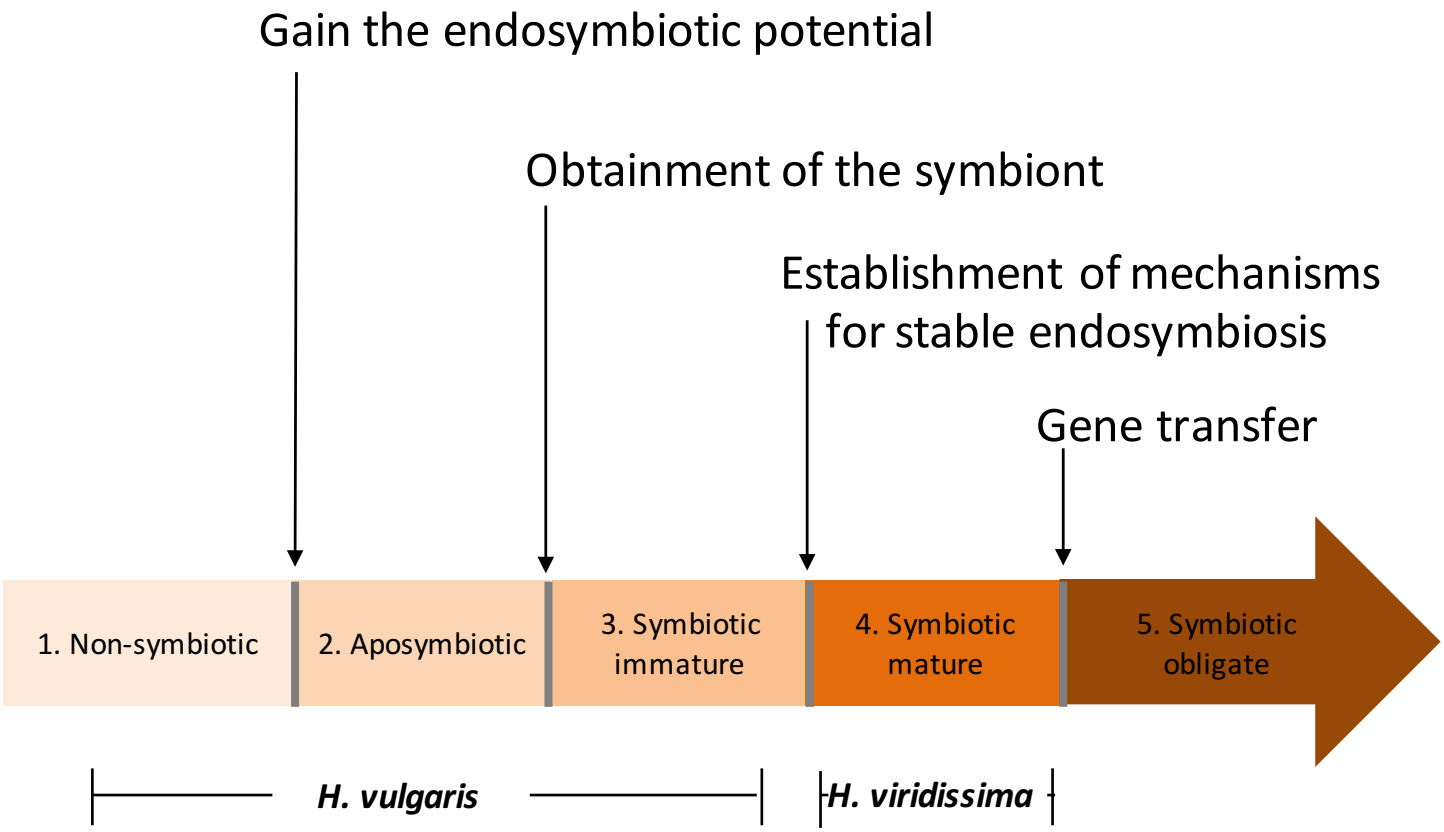

Figure 4.1. A plausible evolutionary stage of endosymbiosis in the two Hydra species.

5 References

Amimoto, Y., Kodama, R., Kobayakawa, Y., 2006. Foot formation in *Hydra*: a novel gene, anklet, is involved in basal disk formation. Mech. Dev. 123, 352–61. doi:10.1016/j.mod.2006.03.002

Apel, K., Hirt, H., 2004. Reactive oxygen species: metabolism, oxidative stress, and signal transduction. Annu. Rev. Plant Biol. 55, 373–399. doi:10.1146/annurev.arplant.55.031903.141701

Benson, D.A., 2004. GenBank. Nucleic Acids Res. 33, D34–D38. doi:10.1093/nar/gki063

Bhattacharya, D., Yoon, H.S., Hackett J.D., 2003. Photosynthetic eukaryotes unite: endosymbiosis connects the dots. BioEssays. 26, 50-60.

Byeon J.H., Seo, E.S., Lee, J.B., Lee, M.J., Kim, J.K, Yoo, J.W, Jung, Y., Lee, B.L., 2015. A specific cathepsin-L-like protease purified from an insect midgut shows antibacterial activity against gut symbiotic bacteria. Dev. Comp. Immunol. 53, 79-84.

Bullerwell, C.E., Gray, M.W., 2004. Evolution of the mitochondrial genome: Protist connections to animals, fungi and plants. Curr. Opin. Microbiol. 7: 528–34.

Camacho, C., Coulouris, G., Avagyan, V., Ma, N., Papadopoulos, J., Bealer, K., Madden, T.L., 2009. BLAST+: architecture and applications. BMC Bioinformatics 10, 421. doi:10.1186/1471-2105-10-421

Champbell, R.D., Bode, H.R., 1983. Teminology for morphology and cell types. Hydra: Research method. H. M. Lenhoff. New York, Plenum Press, 5-14.

Chapman, J.A., Kirkness, E.F., Simakov, O., Hampson, S.E., Mitros, T., Weinmaier, T., Rattei, T., Balasubramanian, P.G., Borman, J., Busam, D., Disbennett, K., Pfannkoch, C., Sumin, N., Sutton, G.G., Viswanathan, L.D., Walenz, B., Goodstein, D.M., Hellsten, U., Kawashima, T., Prochnik, S.E., Putnam, N.H., Shu, S., Blumberg, B., Dana, C.E., Gee, L.,

Kibler, D.F., Law, L., Lindgens, D., Martinez, D.E., Peng, J., Wigge, P.A., Bertulat, B., Guder, C., Nakamura, Y., Ozbek, S., Watanabe, H., Khalturin, K., Hemmrich, G., Salvenmoser, W., Heimberg, A.M., Wheeler, B.M., Peterson, K.J., Bo, A., Tischler, P., Wolf, A., Gojobori, T., Remington, K.A., Strausberg, R.L., Venter, J.C., Technau, U., Hobmayer, B., Bosch, T.C.G., Holstein, T.W., Fujisawa, T., Bode, H.R., David, C.N., Rokhsar, D.S., Steele, R.E., 2010. The dynamic genome of Hydra. Nature. 464, 592-6. doi:10.1038/nature08830

Chwieralski, C.E., Welte, T., Bühling, F., 2006. Cathepsin-regulated apoptosis. Apoptosis 11, 143–149. doi:10.1007/s10495-006-3486-y

Crosnier, C., Bustamante, L.Y., Bartholdson, S.J., Bei, A.K., Theron, M., Uchikawa, M., Mboup, S., Ndir, O., Kwiatkowski, D.P., Duraisingh, M.T., Rayner, J.C., Wright, G.J., 2011. Basigin is a receptor essential for erythrocyte invasion by Plasmodium falciparum. Nature 480, 534–7. doi:10.1038/nature10606

Dennis, G. Jr, Sherman, B.T., Hosack, D.A., Yang, J., 2003. DAVID : Database for Annotation , Visualization , and Integrated discovery. Genome Biol. 4, 3.

Desalvo, M.K., Voolstra, C.R., Sunagawa, S., Schwarz, J.A., Stillman, J.H., Coffroth, M.A., Szmant, A.M., Medina, M., 2008. Differential gene expression during thermal stress and bleaching in the Caribbean coral *Montastraea faveolata*. Mol. Ecol. 17, 3952–3971. doi:10.1111/j.1365-294X.2008.03879.x

Douglas, A., Smith, D.C., 1984. The Green Hydra Symbiosis . VIII . Mechanisms in Symbiont Regulation. Proc. R. Soc. Lond. B. Biol. Sci. 221, 291-319. doi:10.1098/rspb.1984.0035

Dunn, S.R., Pernice, M., Green, K., Hoegh-Guldberg, O., Dove, S.G., 2012. Thermal stress promotes host mitochondrial degradation in symbiotic cnidarians: Are the batteries of the reef going to run out? PLoS One. 7. doi:10.1371/journal.pone.0039024

Ewald, P.W., 1987. Transmission modes and evolution of the parasite-mutualism continuum. Ann. N.Y. Acad. Sci. 503, 295-305.

Fujita, T., Matsushita, M., Endo, Y., 2004. The lectin-complement pathway - Its role in innate immunity and evolution. Immunol. Rev. 198, 185–202. doi:10.1111/j.0105-2896.2004.0123.x

Furla, P., Allemand, D., Orsenigo, M., Allemand, D., 2000. Involvement of H^+-ATPase and carbonic anhydrase in inorganic carbon uptake for endosymbiont photosynthesis. Am J Physiol Regulatory Integrative Comp Physiol. 278, 870–81.

Futahashi, R., Tanaka, K., Tanahashi, M., Nikoh, N., Kikuchi, Y., Lee, B.L., Fukatsu, T., 2013. Gene expression in gut symbiotic organ of stinkbug affected by extracellular bacterial symbiont. PLoS One 8, e64557. doi:10.1371/journal.pone.0064557

Grasso, L.C., Maindonald, J., Rudd, S., Hayward, D.C., Saint, R., Miller, D.J., Ball, E.E., 2008. Microarray analysis identifies candidate genes for key roles in coral development. BMC Genomics 9, 540. doi:10.1186/1471-2164-9-540

Haas, B.J., Papanicolaou, A., Yassour, M., Grabherr, M., Blood, P.D., Bowden, J., Couger, M.B., Eccles, D., Li, B., Lieber, M., Macmanes, M.D., Ott, M., Orvis, J., Pochet, N., Strozzi, F., Weeks, N., Westerman, R., William, T., Dewey, C.N., Henschel, R., Leduc, R.D., Friedman, N., Regev, A., 2013 De novo transcript sequence reconstruction from RNA-seq using the Trinity platform for reference generation and analysis. Nat. Protoc. 8, 1494-512. doi:10.1038/nprot.2013.084

Habetha, M., Bosch, T.C.G., 2005. Symbiotic Hydra express a plant-like peroxidase gene during oogenesis. J. Exp. Biol. 208, 2157–2164. doi:10.1242/jeb.01571

Heck, K.L., Carruthers, T.J.B., Duarte, C.M., Hughes, A.R., Kendrick, G., Orth, R.J., Williams, S.W., 2008. Trophic transfers from seagrass meadows subsidize diverse marine and terrestrial consumers. Ecosystems 11, 1198–1210. doi:10.1007/s10021-008-9155-y

Hemmrich, G., Anokhin, B., Zacharias, H., Bosch, T.C.G., 2007. Molecular phylogenetics in Hydra , a classical model in evolutionary developmental biology 44, 281–290. doi:10.1016/j.ympev.2006.10.031

Hill, M.S., 1996. Symbiotic zooxanthellae enhance boring and growth rates of the tropical sponge Anthosigmella varians forma varians. Mar. Biol. 125, 649–654. doi:10.1007/BF00349246

Hirano, S., Nose, A., Hatta, K., Kawakami, A., Takeichi, M., 1987. Calcium-dependent cell-cell adhesion molecules (cadherins): Subclass specificities and possible involvement of actin bundles. J. Cell Biol. 105, 2501–2510. doi:10.1083/jcb.105.6.2501

Hofmann, D.K., Fitt, W.K., Fleck, J., 1996. Checkpoints in the life-cycle of Cassiopea spp.: Control of metagenesis and metamorphosis in a tropical jellyfish. Int. J. Dev. Biol. 40, 331–338.

Hofmann, D.K., Kremer, B.P., 1981. Carbon metabolism and strobilation in Cassiopea andromedea (Cnidaria: Scyphozoa): Significance of endosymbiotic dinoflagellates. Mar. Biol. 65, 25–33. doi:10.1007/BF00397064

Holland, B.S., Dawson, M.N., Crow, G.L., Hofmann, D.K., 2004. Global phylogeography of Cassiopea (Scyphozoa: Rhizostomeae): molecular evidence for cryptic species and multiple invasions of the Hawaiian Islands. Mar. Biol. 145, 1119–1128. doi:10.1007/s00227-004-1409-4

Holstein, T.W., Hobmayer, E., Technau, U., 2003. Cnidarins: an evolutionary conserved model system for regeneration? Dev. Dyn. 226, 257-67.

Ishikawa, H., 1988. Symbiosis and Evolution. Baifukan, Tokyo.

Jimbo, M., Yanohara, T., Koike, K., Koike, K., Sakai, R., Muramoto, K., Kamiya, H., 2000. The D-galactose-binding lectin of the octocoral Sinularia lochmodes: Characterization and possible relationship to the symbiotic dinoflagellates. Comp. Biochem. Physiol. - B Biochem. Mol. Biol. 125, 227–236. doi:10.1016/S0305-0491(99)00173-X

Kamako, S., Imamura, N., 2006. Effect of Japanese *Paramecium bursaria* extract on photosynthetic carbon fixation of symbiotic algae. J. Eukaryot. Microbiol. 53, 136–41. doi:10.1111/j.1550-7408.2005.00084.x

Kaminuma, E., Mashima, J., Kodama, Y., Gojobori, T., Ogasawara, O., Okubo, K., Takagi, T., Nakamura, Y., 2010. DDBJ launches a new archive database with analytical tools for next-generation sequence data. Nucl. Acids Res. 38, 33–38. doi:10.1093/nar/gkp847

Kawaida, H., Ohba, K., Koutake, Y., Shimizu, H., Tachida, H., Kobayakawa, Y., 2013. Symbiosis between hydra and chlorella: Molecular phylogenetic analysis and experimental study provide insight into its origin and evolution. Mol. Phylogenet. Evol. doi:10.1016/j.ympev.2012.11.018

Kawaida, H., Shimizu, H., Fujisawa, T., Tachida, H., Kobayakawa, Y., 2010. Molecular phylogenetic study in genus Hydra 468, 30–40. doi:10.1016/j.gene.2010.08.002

Kayal, E., Bentlage, B., Collins, A.G., Kayal, M., Pirro, S., Lavrov, D. V, 2012. Evolution of linear mitochondrial genomes in medusozoan cnidarians. Genome Biol. Evol. 4, 1–12. doi:10.1093/gbe/evr123

Kodama, Y., Suzuki, H., Dohra, H., Sugii, M., Kitazume, T., Yamaguchi, K., Shigenobu, S., Fujishima, M., 2014. Comparison of gene expression of Paramecium bursaria with and without *Chlorella variabilis* symbionts. BMC Genomics 15, 183. doi:10.1186/1471-2164-15-183

Koulen, P., Cai, Y., Geng, L., Maeda, Y., Nishimura, S., Witzgall, R., Ehrlich, B.E., Somlo, S., 2002. Polycystin-2 is an intracellular calcium release channel. Nat. Cell Biol. 4, 191–197. doi:10.1038/ncb754

Kovacević, G., Kalafatić, M., Ljubesić, N., 2005. Endosymbiotic alga from green hydra under the influence of cinoxacin. Folia Microbiol. (Praha). 50, 205–208. doi:10.1007/BF02931567

Kovacevic, G., 2012. Value of the *Hydra* model system for studying symbiosis. Int. J. Dev. Biol. 56, 627-635.

Langmead, B., Salzberg, S.L., 2012. Fast gapped-read alignment with Bowtie 2. Nat. Methods 9, 357–9. doi:10.1038/nmeth.1923

Lee, S., Tak, E., Lee, J., Rashid, M. a, Murphy, M.P., Ha, J., Kim, S.S., 2011. Mitochondrial H_2O_2 generated from electron transport chain complex I stimulates muscle differentiation. Cell Res. 21, 817–834. doi:10.1038/cr.2011.55

Lenhoff, H.M., 1983. Culturing large numbers of Hydra. In: Lenhoff, H.M. (Ed.), Hydra Research Methods. Plenum, New York, 53–62.

Lesser, M.P., 2006. Oxidative stress in marine environment: Biochemistry and physiological ecology. Annu. Rev. Physiol. 68, 253–278. doi:10.1146/annurev.physiol.68.040104.110001

Li, H., Durbin, R., 2010. Fast and accurate long-read alignment with Burrows-Wheeler transform. Bioinformatics 26, 589–595. doi:10.1093/bioinformatics/btp698

Mack, R.N., Lonsdale, W.M., 2001. Humans as global plant dispersers: Getting more than we bargained for. Bioscience 51, 95. doi:10.1641/0006-3568(2001)051[0095:HAGPDG]2.0.CO;2

Magrane, M., Consortium, U.P., 2011. UniProt Knowledgebase: A hub of integrated protein data. Database 2011, 1–13. doi:10.1093/database/bar009

Marchi, S., Giorgi, C., Suski, J.M., Agnoletto, C., Bononi, A., Bonora, M., De Marchi, E., Missiroli, S., Patergnani, S., Poletti, F., Rimessi, A., Duszynski, J., Wieckowski, M.R., Pinton, P., 2012. Mitochondria-Ros crosstalk in the control of cell death and aging. J. Signal Transduct. 2012, 1–17. doi:10.1155/2012/329635

Margulis, L., 1971. Origin of eukaryotic cells. Yale University Press.

Margulis, L., Sagan, D., 2002. Acquiring genomes: A theory of the origin of species. Basic Books, New York.

Martínez, D.E., Iñiguez, A.R., Percell, K.M., Willner, J.B., Signorovitch, J., Campbell, R.D., 2010. Molecular phylogenetics and evolution phylogeny and biogeography of Hydra (Cnidaria : Hydridae) using mitochondrial and nuclear DNA sequences 57, 403–410. doi:10.1016/j.ympev.2010.06.016

McDadden, G.I., 2001. Primary and secondaty endosymbiosis and the origin of plastids. J. Phycol. 37, 951-59.

Meyer, E.L.I., Weis, V.M., 2012. Study of cnidarian-algal symbiosis in the " Omics " age. Biol. Bull. 223, 44–65.

Montalbetti, N., Cantero, M.R., Dalghi, M.G., Cantiello, H.F., 2008. Reactive oxygen species inhibit polycystin-2 (TRPP2) cation channel activity in term human syncytiotropphoblast. Placenta. 29, 510-8.

Moreno-Hagelsieb, G., Latimer, K., 2008. Choosing BLAST options for better detection of orthologs as reciprocal best hits. Bioinformatics 24, 319–324. doi:10.1093/bioinformatics/btm585

Muscatine, L., Lenhoff, H.M., 1963. Symbiosis: On the role of algae symbiotic with Hydra. Science, 142, 956–958. doi:10.1126/science.142.3594.956

Muller-Parker, G., D'Elia, C.F., 1997. Interactions between corals and their symbiotic algae. In Birkeland C (Ed) Life and Death of Coral Reefs. Chapman & Hall, New York, 96-113.

Muller-Parker, G., Pardy R.L., 1987. The Green Hydra Symbiosis: Analysis of a field population. Biol. Bull. 173, 367-76.

Muscatine, L., Lenhoff, H.M., 1963. Symbiosis of hydra and algae II. Effects of limited Food and starvation on growth of symbiotic and aposymbiotic hydra. Biol. Bull. 123, 316-28.

Muscatine, L., Porter, J.W., 1977. Reef Corals : Mutualistic symbioses adapted to nutrient-poor environments. Bioscience 27, 454–460. doi:10.2307/1297526

Nagasaki, H., Mochizuki, T., Kodama, Y., Saruhashi, S., Morizaki, S., Sugawara, H., Ohyanagi, H., Kurata, N., Okubo, K., Takagi, T., Kaminuma, E., Nakamura, Y., 2013. DDBJ read annotation pipeline: A cloud computing-based pipeline for high-throughput analysis of next-generation sequencing data. DNA Res. An Int. J. Rapid Publ. Reports Genes Genomes 20, 383–390. doi:10.1093/dnares/dst017

Odum, H.T., Odum, E.P., 1955. Trophic structure and productivity of a windward coral reef community on eniwetok atoll. Ecol. Monogr. 25, 291–320.

Orrenius, S., Zhivotovsky, B., Nicotera, P., 2003. Calcium: Regulation of cell death: the calcium–apoptosis link. Nat. Rev. Mol. Cell Biol. 4, 552–565. doi:10.1038/nrm1150

Rahat, M., Adar, O., 1980. Effect of symbiotic zooxanthellae and temperature on budding and strobilation in cassiopeia andromeda. Biol. Bull. 159, 394-401.

Riesgo, A., Peterson, K., Richardson, C., Heist, T., Strehlow, B., Mccauley, M., Cotman, C., Hill, M., Hill, A., 2014. Transcriptomic analysis of differential host gene expression upon uptake of symbionts : a case study with Symbiodinium and the major bioeroding sponge Cliona varians.

Roberts, A., Pachter, L., 2013. Streaming fragment assignment for real-time analysis of sequencing experiments. Nat. Methods 10, 71–3. doi:10.1038/nmeth.2251

Ronquist, F., Huelsenbeck, J.P., 2003. MrBayes 3: Bayesian phylogenetic inference under mixed models. Bioinformatics 19, 1572–1574. doi:10.1093/bioinformatics/btg180

Sachs, J.L., Essenberg, C.J., Turcotte, M.M., 2011. New paradigms for the evolution of beneficial infections. Trends Ecol. Evol. 26, 202–209. doi:10.1016/j.tree.2011.01.010

Schimper, A.F.W., 1883. Über die Entwicklung der chorophyllkörner und farbkörper. Bot. Zeitung. 41:105–14. [Title translation: On the development of chloroplasts and chromoplasts.]

Shigenobu, S., Watanabe, H., Hattori, M., Sakaki, Y., Ishikawa, H., 2000. Genome sequence of the endocellular bacterial symbiont of aphids Buchnera sp. APS. Nature 407, 81–6. doi:10.1038/35024074

Sievers, F., Wilm, A., Dineen, D., Gibson, T.J., Karplus, K., Li, W., Lopez, R., McWilliam, H., Remmert, M., Söding, J., Thompson, J.D., Higgins, D.G., 2011. Fast, scalable generation of high-quality protein multiple sequence alignments using Clustal Omega. Mol. Syst. Biol. 7, 539. doi:10.1038/msb.2011.75

Stamatakis, A., 2006. RAxML-VI-HPC: Maximum likelihood-based phylogenetic analyses with thousands of taxa and mixed models. Bioinformatics 22, 2688–90. doi:10.1093/bioinformatics/btl446

Stanley, G.D., Swart, P.K., 1995. Paleontological society evolution of the coral-zooxanthenllae symbiosis during the triassic : A geochemical approach evolution of the coral-zooxanthellae symbiosis during the Triassic : a geochemical approach 21, 179–199.

Steihusen, U., Weiske, J., Badock, V., Tauber, R., Bommert, K., Huber, O., 2001. Cleavage and shedding of E-cadherin after induction of apoptosis. J. Biol. Chem. 276, 4972–4980. doi:10.1074/jbc.M006102200

Sun, J., Nishiyama, T., Shimizu, K., Kadota, K., 2013. TCC : Differential expression analysis for tag count data with robust normalization strategies. BMC Bioinformatics. 14, 219.

Takano, J., Sugiyama, T., 1983. Genetic analysis of developmental mechanisms in hydra. VIII. Head-activation and head-inhibition potentials of a slow-budding strain (L4). J. Embryol. exp. Morph. 78, 141-68.

Tamura, K., Battistuzzi, F.U., Billing-Ross, P., Murillo, O., Filipski, A., Kumar, S., 2012. Estimating divergence times in large molecular phylogenies. Proc. Natl. Acad. Sci. U. S. A. 109, 19333–8. doi:10.1073/pnas.1213199109

Tamura, K., Stecher, G., Peterson, D., Filipski, A., Kumar, S., 2013. MEGA6: Molecular Evolutionary Genetics Analysis version 6.0. Mol. Biol. Evol. 30, 2725–9. doi:10.1093/molbev/mst197

Timmis, J.N., Ayliffe M.A., Huang, C.Y., Martin, W., 2004. Endosymbiotic gene transfer: organelle genomes forge eukaryotic chromosomes. Nat. Rev. Genet. 5, 123-35.

Toft, C., Andersson, S.G.E., 2010. Evolutionary microbial genomics: insights into bacterial host adaptation. Nat. Rev. Genet. 11, 465–475. doi:10.1038/nrg2798

Voigt, O., Erpenbeck, D., Wörheide, G., 2008. A fragmented metazoan organellar genome: the two mitochondrial chromosomes of Hydra magnipapillata. BMC Genomics 9, 350. doi:10.1186/1471-2164-9-350

Wang, Z., Gerstein, M., Snyder, M., 2009. RNA-Seq: a revolutionary tool for transcriptomics. Nat. Rev. Genet. 10, 57–63. doi:10.1038/nrg2484

Waring, J.F., Ciurlionis, R., Jolly, R. a., Heindel, M., Ulrich, R.G., 2001. Microarray analysis of hepatotoxins in vitro reveals a correlation between gene expression profiles and mechanisms of toxicity. Toxicol. Lett. 120, 359–368. doi:10.1016/S0378-4274(01)00267-3

Weis, V.M., 2008. Cellular mechanisms of Cnidarian bleaching: stress causes the collapse of symbiosis. J. Exp. Biol. 211, 3059–66. doi:10.1242/jeb.009597

Weis, V.M., Levine, R.P., Station, H.M., Grove, P., 1996. Differential protein profiles reflect the different lifestyles of symbiotic and aposymbiotic *Anthopleura elegantissima*, a sea anemone from temperature waters. J. Exp. Biol. 892, 883–892.

Weis, V.M., Smith, G.J., Muscatine, L., 1989. A "CO2 supply" mechanisms in zooxanthellate cnidarians: role of carbonic anhydrase. Mar. Biol. 100, 195–202. doi:10.1007/BF00391958

Weis, W.I., Taylor, M.E., Drickamer, K., 1998. The c-type lectin superfamily in the immune-system. Immunol. Rev. 163, 19–34.

Wood-Charlson, E.M., Hollingsworth, L.L., Krupp, D. a., Weis, V.M., 2006. Lectin/glycan interactions play a role in recognition in a coral/dinoflagellate symbiosis. Cell. Microbiol. 8, 1985–1993. doi:10.1111/j.1462-5822.2006.00765.x

6 Acknowledgement

First of all, I would like to express my deepest respect and gratitude to my supervisors, Dr. Takashi Gojobori and Dr. Kazuho Ikeo for his intensive guidance and generous support.

I would like to express my sincere gratitude to Dr. Hiroshi Shimizu and the members of his laboratory for their expert advice and continuing collaboration.

I would like to appreciate the fruitful discussion with Dr. Masafumi Nozawa and the members of Laboratory for DNA Data Analysis.

I am thankful to my colleagues and friends at NIG for the warm companionship.

At the very end of this thesis, I express special thanks to my mother, aunt, and grandmother for their unconditional support through my life. I hoped to see them with this Ph.D. thesis.